2001

Traffic grooming and wavelength conversion in optical networks

Sashisekaran Thiagarajan
Iowa State University

INFORMATION TO USERS

This manuscript has been reproduced from the microfilm master. UMI films the text directly from the original or copy submitted. Thus, some thesis and dissertation copies are in typewriter face, while others may be from any type of computer printer.

The quality of this reproduction is dependent upon the quality of the copy submitted. Broken or indistinct print, colored or poor quality illustrations and photographs, print bleedthrough, substandard margins, and improper alignment can adversely affect reproduction.

In the unlikely event that the author did not send UMI a complete manuscript and there are missing pages, these will be noted. Also, if unauthorized copyright material had to be removed, a note will indicate the deletion.

Oversize materials (e.g., maps, drawings, charts) are reproduced by sectioning the original, beginning at the upper left-hand corner and continuing from left to right in equal sections with small overlaps.

Photographs included in the original manuscript have been reproduced xerographically in this copy. Higher quality 6" x 9" black and white photographic prints are available for any photographs or illustrations appearing in this copy for an additional charge. Contact UMI directly to order.

ProQuest Information and Learning
300 North Zeeb Road, Ann Arbor, MI 48106-1346 USA
800-521-0600

Traffic grooming and wavelength conversion in optical networks

by

Sashisekaran Thiagarajan

A dissertation submitted to the graduate faculty

in partial fulfillment of the requirements for the degree of

DOCTOR OF PHILOSOPHY

Major: Computer Engineering

Program of Study Committee:
Arun K. Somani, Major Professor
Robert J. Weber
Ahmed E. Kamal
Manimaran Govindarasu
Soma Chaudhuri

Iowa State University

Ames, Iowa

2001

UMI Number: 3034229

UMI Microform 3034229

ProQuest Information and Learning Company
300 North Zeeb Road
P.O. Box 1346
Ann Arbor, MI 48106-1346

Graduate College
Iowa State University

This is to certify that the doctoral dissertation of

Sashisekaran Thiagarajan

has met the dissertation requirements of Iowa State University

Signature was redacted for privacy.

Major Professor

Signature was redacted for privacy.

For the Major Program

DEDICATION

I would like to dedicate this thesis to my parents without whose support I would not have been able to complete this work.

TABLE OF CONTENTS

LIST OF TABLES

LIST OF FIGURES

ABSTRACT

Wavelength Division Multiplexing (WDM) using wavelength-routing has emerged as the dominant technology for use in wide area and metropolitan area networks. Traffic demands in wide area and metropolitan area networks today are characterized by dynamic, heterogeneous flows. While each wavelength in optical fiber links has transmission capacity at gigabit per second rates, users typically require connections at rates that are lower than the full wavelength capacity. Therefore, future wavelength routing networks will employ a layered architecture, employing the best of optical and electronic switching. In this thesis, we explore network design and operation methodologies to improve the network utilization and blocking performance of such optical transport networks. First we provide an introduction to optical networks from first generation networks such as SONET/SDH to second generation networks such as wavelength routing network which employ optical add-drop multiplexers and optical crossconnects at the nodes. We describe the network node architecture, the principles of routing and wavelength assignment and explain the need and role of wavelength conversion in such optical networks. We present an algorithm to optimally place wavelength conversion devices at the network nodes so as to optimize blocking performance. Depending on the topology, our algorithm offers savings in computation time of up to 95 percent when compared to the exhaustive method.

Next, to make the network viable and cost-effective, it must be able to offer sub-wavelength services and must be able to pack these services efficiently onto the wavelengths. The act of multiplexing, demultiplexing and switching of sub-wavelength services or low-rate traffic streams onto wavelengths is defined as traffic grooming. Constrained grooming networks are those which perform traffic aggregation and deaggregation at the network edge. Sparse grooming networks are those which perform grooming at the edge and perform traffic switching in the

core of the network. We study the effect of traffic grooming on the blocking performance in these networks through simulations and analyses. Compared to constrained grooming, sparse grooming offers an order of magnitude decrease in blocking probability for high line-speed connections and multiple orders of magnitude decrease in blocking for low line-speed connections. We also study the issue of capacity fairness in such traffic grooming WDM networks and develop a connection admission control (CAC) algorithm to improve the fairness among traffic connections with different capacities. The CAC algorithm provides good capacity fairness while at the same time does not penalize the overall blocking performance significantly. We finally address the issues involved in dynamic routing and wavelength assignment in survivable WDM grooming networks. We develop two schemes for grooming primary and backup traffic streams onto wavelengths: Mixed Primary-Backup Grooming Policy (MGP) and Segregated Primary-Backup Grooming Policy (SGP). We use simulation results to evaluate the effectiveness of our schemes on different network topologies using different routing and wavelength assignment scenarios. We show that MGP is useful in network topologies such as the ring, characterised by low connectivity and high load correlation and SGP is useful in network topologies, such as the mesh-torus, characterized by good connectivity and a significant amount of traffic switching and mixing at the nodes.

CHAPTER 1. Optical Networking - A Gentle Introduction

1.1 Optical Networks - The story thus far

An optical network is one in which the dominant physical layer technology for data transport is optical fiber. Optical fiber offers low-loss transmission over an enormous frequency range of about 25 THz, which is orders of magnitude more than the bandwidth available in copper cables. In addition, optical fiber offers lower bit error rates than any other transmission media and is less susceptible to various kinds of electromagnetic interferences and other undesirable effects. This makes it the medium of choice for transmission of data at rates greater than a few megabits per second over distances more than a kilometer.

Initially, optical networks used fiber solely as a transmission medium, with all the switching and data processing handled by the electronics at the network nodes. Such *first-generation optical networks* were widely deployed in public telecommunications networks as well as private enterprise networks and carried a single digital signal per fiber per propagation direction at wavelengths of either 1310 nm or 1550 nm. Examples of such networks are Enterprise Serial Connection (ESCON), Fiber Channel, high-performance parallel interface (HIPPI) [1], fiber distributed data interface (FDDI) [2] and Synchronous Optical Network/ Synchronous Digital Hierarchy (SONET/SDH) [3]. Of these, the most successful and widely spread technology is SONET/SDH. While the public telecommunications infrastructure in North America is dominated by SONET, Europe and Asia follow SDH, a similar standard.

SONET/SDH was designed in the late 1980s as a common standard for high bit rate fiber optic transmission. It was specifically introduced to alleviate the multiplexing and interoperability problems that existed in the telecommunications infrastructure, which at that time, was based on the *plesiochronous digital hierarchy*. SONET/SDH has since evolved to incor-

porate extensive management information to monitor network performance and offer network protection, through Automatic Protection Switching (APS) in ring topologies, to offer a high degree of reliability.

However as the demand for bandwidth increased due to the emergence of Internet, the immediate solution to increase the capacity on fiber was to increase the bit rate using higher-speed electronics. However this form of traditional time division multiplexing came under pressure from the *electronic TDM bottleneck*. This demands that each port in the TDM network not only be able to handle its own bits, but also traffic belonging to other nodes in the network which passes through the port. Hence the bit rate of the electronic equipment at the ports needs to scale as the product of number of ports and the per port bit rate. As the network evolves to higher values of this port-bit rate product, it quickly exceeds the speed of the fastest available digital logic technology. In addition, as TDM technology is pushed beyond 40 Gbps, impairments due to amplifier cascades, dispersion, nonlinearities and crosstalk become more significant for such high capacity systems. There has been significant research work done in all-optical TDM and soliton propagation, in which dispersion effects are cancelled out by dispersion management and using dispersion shifted fiber. Although rates of around 250 Gbps have been demonstrated in such cases, all-optical TDM technologies are still not ready for commercial implementation.

Wavelength Division Multiplexing (WDM) has thus emerged as the most promising technology for taking the full advantage of the bandwidth potential of fiber and thereby satisfying the increasing demand for bandwidth. WDM divides the huge bandwidth of a fiber into many nonoverlapping channels to simultaneously transmit different data streams at multiple carrier wavelengths. Each of these channels operate at moderate data rates of around 2.5 Gbps to 10 Gbps which are well within the capacity of conventional electronic information processing devices in use today. The data rate is likely to extend to 40 Gbps in the future. The emergence of WDM can be attributed to a host of advances in optical component technologies. The introduction of single-mode fibers (SMF) allowed for elimination of intermodal dispersion effects and increased transmission distances and enabled dramatic increases in the bit rates.

These single-mode fibers initially used commercially available lasers operating at 1310 nm, the zero dispersion point of the fiber. As 1550 nm lasers, corresponding to the lowest loss region of silica fiber, became available, dispersion-shifted fiber was developed to have zero chromatic dispersion in the 1550 nm window. The development of the single-longitudinal mode (SLM) distributed feedback (DFB) laser increased the bit rates of WDM signals to more than a Gb/s. But the most significant advancement that revolutionized the industry was the invention of the erbium-doped fiber amplifier (EDFA). These amplifiers permitted, for the first time, the direct amplification of optical signals over a wide spectrum of wavelengths without conversion to the electronic domain. The link capacity could now also be increased by adding more wavelengths rather than increasing the bit-rate. To deal with chromatic dispersion, dispersion compensating fiber was developed which helped accommodate the broad range of wavelengths at high bit rates. Further advances in fiber optics have lead to the development of the non-zero dispersion fiber (TrueWave [4]) which permits WDM signals to travel in a single fiber without crosstalk and the development of AllWave [4] fiber which eliminates the *water-peak* at 1390 nm and enabled the use of that part of the spectral region of the fiber. By 1998, more than 90 percent of the networks of major long-haul carriers were employing WDM technology for *point-to-point transmission* links. Current state-of-the-art in WDM technology can achieve up to 320 wavelengths per fiber with each wavelength carrying 10 Gb/s, for a total transmission capacity of up to 3.2 Tb/s [5].

Most of the early research and experimental efforts were focussed on *broadcast-and-select networks* [6]. Such networks were initially considered as an attractive way to build Local Area Networks (LANs) and Metropolitan Area Networks (MANs) and were usually configured as star or bus topologies. In such networks, all the transmitted signals are merged and broadcast to the receivers in the nodes. Information exchange is achieved by wavelength selection which is implemented using a suitable media access protocol (MAC) and a combination of fixed transmitters and receivers, and tunable transmitters and receivers. Although a number of broadcast and select testbeds (Lambdanet [7], NTT [8], Rainbow [9]) demonstrating circuit switching have been developed by various research labs, these networks are not widely de-

ployed commercially. This is due to the fact that these networks are more expensive to deploy and cannot compete commercially with the low costs of other technologies such as switched Ethernet.

Recent advancements in optical systems technology such as all-optical add-drop multiplexers (OADMs) and all-optical crossconnects (OXCs) have further enabled the evolution of WDM from simple point-to-point networks to full circuit-switched *wavelength-routed networks* suitable for Wide Area Networks (WANs). The key optical component in such OADMs and OXCs is the optical switch. This device is capable of switching signals from a given input port to a given output port. These optical systems can selectively process (add, drop or switch) different wavelengths without *opto-electronic-optic* (O-E-O) conversion requirements and establish cut-through channels called *lightpaths* between non-adjacent nodes. This allows for a *virtual topology* to be overlaid on the physical topology where the lightpaths represent the virtual links. While certain parameters such as the maximum bit rate or bandwidth and some parameters related to the link power budget may be specified, the circuit-switched lightpath service is essentially transparent to the protocol and bit rate of the data signal. Due to this, existing protocols can be supported and newer protocols can be easily introduced without disturbing the older protocol data streams.

Using OADMs and OXCs, wavelength-routing networks are usually configured as either ring or mesh topology networks. WDM ring networks are usually used to support legacy SONET traffic. The wavelength switching capabilities in the ring can also be used to provide traffic protection features similar to APS in SONET rings. WDM mesh networks are likely to be used as backbone infrastructures connecting WDM rings together or as *all-optical islands* connecting multiple access networks. Hence this network can be looked upon as an *optical layer* providing lightpath services to the higher layers. A number of experimental testbeds to demonstrate the feasibility of WDM mesh networks have been built or are currently under development. Multiwavelength Optical Network (MONET) program [10] funded by DARPA and undertaken by Bellcore is a wavelength routing testbed with eight wavelengths spaced by 200 GHz and modulated at 2.5 Gb/s. This testbed used OADMs in rings interconnected to a

long-distance backbone network of OXCs. In Europe, a pan-European optical network is being deployed under the Advanced Communication Technologies and Services (ACTS) program [11]. Today reconfigurable dynamic OADMs are commercially available and OXCs are just beginning to be shipped out to carriers for field installation and testing.

In the following three sections, we will give brief overview of the various optical networking technologies that are being deployed or are already a part of the public and private optical communications infrastructure today. In section 1.6, we will discuss the research issues and factors motivating our thesis and this will be followed by the outline and contributions of our thesis in section 1.7.

1.2 First Generation Optical Networks - SONET/SDH

SONET is an ANSI standard for optical communication providing framing and defines a hierarchy of interface rates that allow data streams at different rates to be multiplexed. SONET defines optical carrier levels and electrically equivalent synchronous transport signals (STSs) ranging from 51.84 Mb/s (OC-1) up to 9.8 Gb/s (OC-192). The international equivalent of SONET is SDH, standardized by the International Telecommunications Union - Telecommunications Standardization Sector (ITU-T). Since SONET and SDH are functionally similar, we will only provide a brief of SONET below.

In SONET, the base signal is the synchronous transport signal level 1 (STS-1). The basic frame structure is 90 bytes × 9 rows. SONET employs a multiplexing scheme in which a client signal is mapped into a synchronous payload envelope (SPE) consisting of 87 bytes × 9 rows. In addition, a set of overhead of bytes called the path overhead, consisting of 3 bytes/row is also added. This path overhead is used for operations, administration and maintenance. The SPE container along with its path overhead is called a *virtual tributary* (VT) in SONET. The resulting frame is put out every $125\mu sec$ and frames are emitted into the fiber regardless of whether there are any useful data to send. This gives a rate of 51.84 Mb/s for STS-1 line speed. By multiplexing multiple frames in the $125\mu sec$ period, higher-rate SONET signals are obtained. These higher-rate signals (STS-N) are obtained by interleaving the bytes of N

STS-1s. This hierarchical multiplexing is shown in Figure 1.1. A *concatenated* higher-rate frame (STS-Nc) can also be formed by grouping all overhead bytes of the various N STS-1 frames in consecutive columns and then adding the payload columns of each frame afterward. The concatenated frame can also be used to transport higher-speed non-SONET signals. For example, a 150 Mb/s ATM signal is mapped to a STS-3c signal.

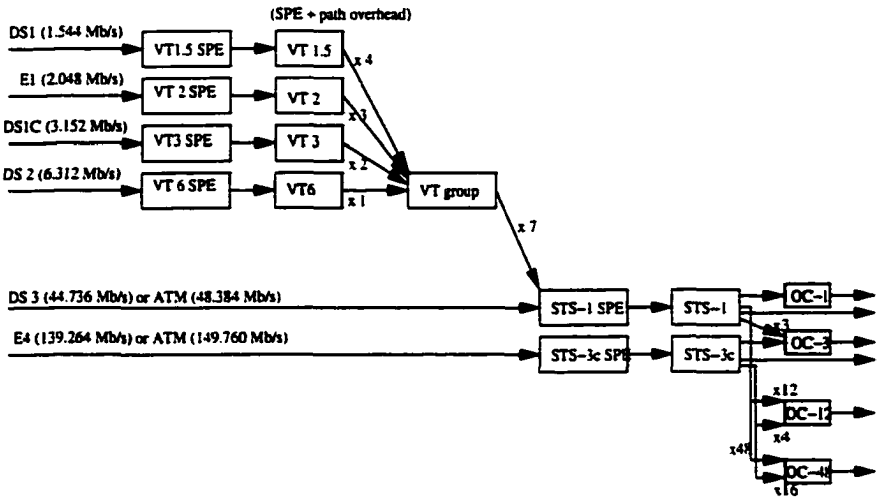

Figure 1.1 SONET Virtual Tributary Hierarchy

SONET networks are typically deployed as either point-to-point links, linear networks or multiple interconnected rings. Rings are more commonly used since they provide service protection in the presence of failures through the Automatic Protection Switching (APS) feature of SONET. Figure 1.2 illustrates the various elements of a SONET infrastructure. Point-to-point links consists of line terminating equipment (LTE) at the ends of the link. In linear networks, linear add-drop multiplexers (ADMs) are used to add or drop lower-rate traffic streams from a high-rate stream. Rings are also composed of ADMs which, in addition to performing the add/drop function, incorporate the APS mechanism to handle failures. Depending on the APS provided, these rings can be configured as unidirectional path-switched rings (UPSRs) or bidirectional line-switched rings (BLSRs) with either two (BLSR/2) or four (BLSR/4) fiber link spans. To connect two rings together, we make use of a digital cross-connect (DCS). The DCS provides switching functions and is used to crossconnect traffic streams across rings. The DCSs

and ADMs groom the low-rate traffic streams by switching and packing them into higher-rate streams.

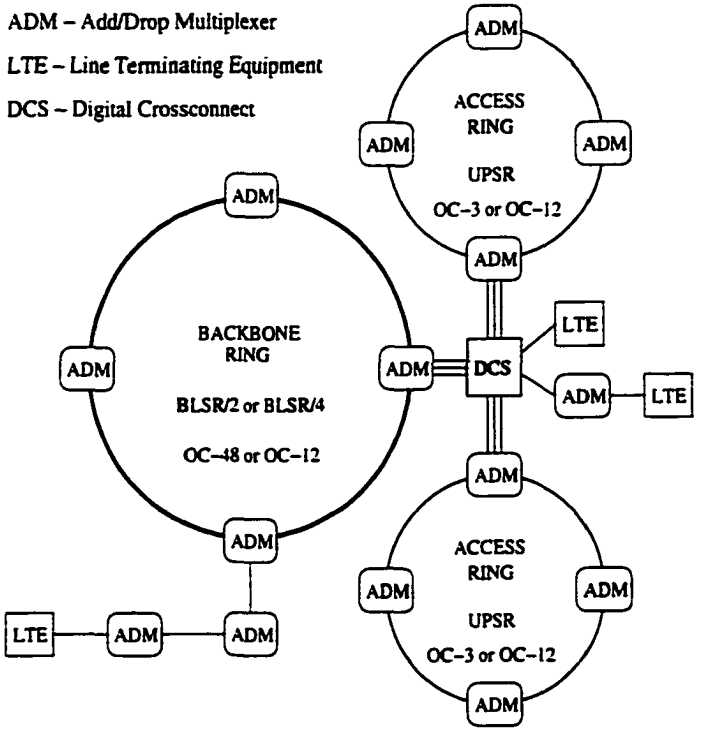

Figure 1.2 SONET Network Infrastructure

The APS feature of SONET provides protection for fiber cuts by automatically redirecting traffic affected by the failure to alternative routes. This protection switching feature typically occurs in approximately 50 ms. Two types of mechanisms are currently supported: 1+1 and 1:1. In 1+1 protection, the traffic stream is transmitted simultaneously along two paths. The destination decides which path to receive based on failure conditions. In 1:1 protection, two paths are also allocated, but the traffic stream is only transmitted only on one path called the working path and the other path is called the protected path. In the event of the failure of the working path, the protected path takes over its function.

SONET consists of four sublayers: path, line, section and physical. The lowest physical layer is concerned with actual transmission of bits across the fiber, the physical properties of light and the fiber to be used. This layer uses scrambling to prevent long runs of 1s and 0s

in the data. The session layer is present at each regenerator in the network and handles a single point-to-point fiber run. This layer is responsible for generating the standard frame at one end and processing it at the other. The line layer is responsible for multiplexing multiple tributaries onto a single line. It also performs protection switching to restore service in the event of a failure. The path layer deals with end-to-end issues and is responsible for monitoring and tracking the status of a connection.

Although SONET can efficiently support constant bit rate applications directly through VTs and STS-N frame signals, for variable bit rate, packet-based clients such as Internet Protocol (IP) or Asynchronous Transfer Mode (ATM), the use of constant rate SONET signals is wasteful. To solve this, protocols for transport of IP and ATM networking technologies over SONET have been defined. The ATM Forum has defined SONET interfaces which involve the mapping of ATM cells into SPEs. ATM cells are directly and continuously mapped into the SONET payload because an integral number of its 53-byte cells will not fit into a single frame. At the receiver side, the Cyclic Redundancy Check (CRC) field of the ATM cell headers is used to delineate the cells from the SONET payload. To run IP over SONET, ATM was initially used as an intermediate layer. Each IP datagram was encapsulated into an ATM adaptation layer type 5 (AAL-5) frame using multi-protocol logical link control (LLC) and subnetwork attachment point (SNAP) encapsulation. The resulting AAL-5 protocol data unit (PDU) is then segmented into 48-byte payloads for ATM cells. The ATM cells are then mapped into SONET frames. However, this results in an overhead of 18 to 25 percent in addition to the 4 percent SONET overhead. Therefore, mapping of IP into SONET using point-to-point protocol (PPP) and high-level data link control (HDLC) have been defined. IP datagrams are initially encapsulated into PPP packets. The PPP-encapsulated IP datagrams are then framed using HDLC protocol. The HDLC framed datagrams are then scrambled and placed back to back in the SONET SPE. This mapping brings down the overhead to approximately 2 percent.

1.3 Point-to-point WDM Systems

Figure 1.3 depicts a point-to-point WDM system with w wavelengths. In this figure, only half-duplex channels are depicted. A duplicate system is typically used in the opposite direction to realize full-duplex communication. The standard transmitter element here consists of a semiconductor laser diode and a laser modulator and converts the electrical signal to an optical signal. The optical output power of the laser is usually up to +10 dBm and has a modulation bandwidth of 10 GHz. Transmitter modules are commercially available for 10 Gbps transmission and in research labs, lasers with modulation bandwidths of 100 GHz have been demonstrated. Optical multiplexers and demultiplexers are constructed using fiber Bragg grating [12] or arrayed waveguide gratings [13]. Optical receivers terminate the optical signal and convert to an electrical signal. They are usually comprised of a photodetector and an optical filter for filtering out all but the required wavelength. State-of-the-art receivers today have sensitivities around -30 dBm for 2.5 Gbps and close to -20 dBm for 10 Gbps. EDFAs can be used as power amplifiers, line amplifiers and pre-amplifiers. The power amplifier which is used in front of the transmitter, is used to provide the maximum possible output power. The pre-amplifier which is used before the receiver is designed to provide high gain with the highest sensitivity. Specifically, it is designed to add the least amount of additional noise. The line amplifier, which is used in-line with the fiber is used to compensate for fiber link attenuation losses, combines the characteristics of both the pre-amplifier and the power amplifier.

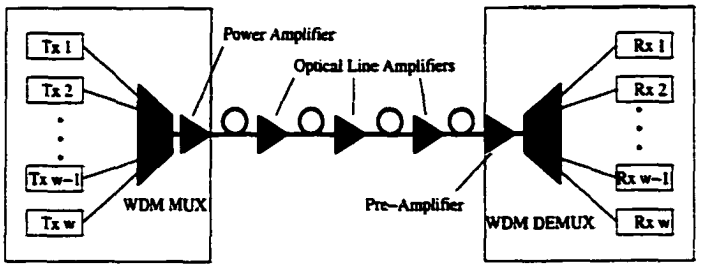

Figure 1.3 A Point to Point WDM Link

1.4 Second Generation Optical Networks

1.4.1 Broadcast-and-Select WDM Networks

A WDM broadcast-and-select networks is one in which all the input signals from the network nodes are combined, and broadcast back to all the nodes in the network. Typically the network is configured by connecting the nodes via bi-directional fiber links to a passive star coupler device, as shown in Figure 1.4. Although bus configurations have been proposed, the star coupler network is more popular, as it has a superior power budget compared to the bus and ring. The star coupler is either a single piece of glass that splits the signal it receives on any of its ports to all the ports or it can be made out of optical couplers. In Figure 1.5, we show a 8×8 star coupler network configured using 2×2 star coupler.

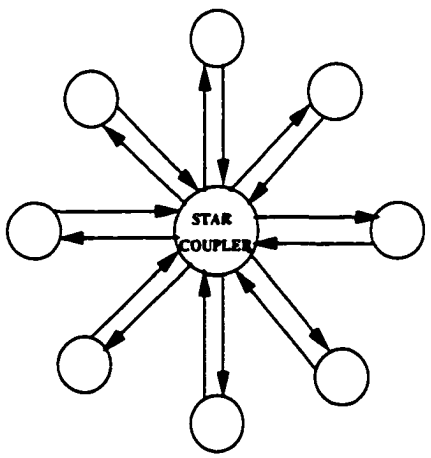

Figure 1.4 Broadcast Star Topology

Since the star coupler is passive and unpowered, it is reliable and requires no control and management. Hence, the main networking issue that needs to be addressed is the coordination between nodes that have to tune their wavelengths to transmit and receive information from each other. The network nodes can have 1) fixed transmitters and fixed receivers, 2) have fixed transmitters and tunable receivers, 3) have fixed receivers and tunable transmitters, or 4) have tuning capabilities for both receivers and transmitters. In the first case, a node will be able to communicate with only a fixed subset of the nodes in the network. In this case, a

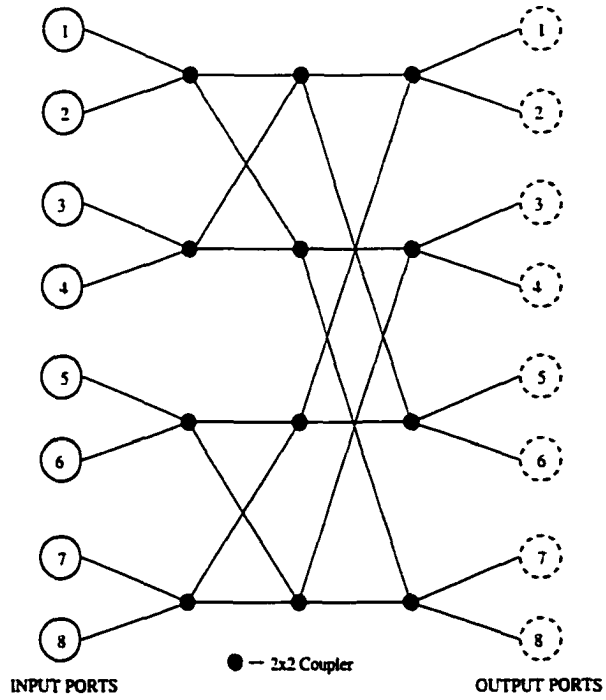

Figure 1.5 Internal Structure of a star coupler

regular virtual topology (such as Shufflenets, GEMNET, Kautz graphs or de Bruijn graphs) is implemented on the broadcast-and-select passive star network. The information from a source would have to traverse multiple hops through intermediate nodes to get to its destination. Due to the regular virtual topology, there may be different shortest-path routes for a given source to destination pair. Hence appropriate routing algorithms need to be implemented to balance the traffic load on the links in the network. If the network uses some form of tuning at either or both the source and destination, then these networks are referred to as single-hop networks. In a single-hop network, once the data stream is transmitted as light, it continues without conversion into electronic form until it reaches its destination. In this case, both the transmitter at the source and the receiver at the destination should be tuned to the same wavelength for the duration of the packet transmission time. In addition, if two transmitters of different nodes transmit on the same wavelength, the signal collides and is lost or corrupted. Moreover, two transmitters can send information to a single receiver at the same time. Hence efficient medium-access control (MAC) protocols should be designed to resolve

these contentions and to avoid or minimize collisions so as to allocate wavelength channels for different connections in an efficient manner. If these networks support packet switching, then the finite amount of time that the transmitter or receiver takes to switch between wavelengths assumes more significance. Hence, the tunable transmitter or receiver should be capable of fast tuning between wavelengths. However, such optical components are still being developed today and are still not commercially available. In addition, these networks are limited in their scalability and network size is limited by the number of wavelengths. This limits their use to high-speed local area networks (LANs) and metropolitan area networks (MANs). However, compared to electronic technologies such as switched Ethernet, the cost of optical components for the broadcast-and-select network is relatively high. This has prevented the commercial deployment of the broadcast-and-select network.

1.5 Wavelength-Routing Networks

Wavelength-routing networks are networks in which information is routed and switched based on wavelength. These networks consist of wavelength-routing nodes or optical add/drop multiplexers interconnected by fiber optic links. Unlike broadcast-and-select networks, wavelength routing networks do not suffer from splitting losses and offer advantages of wavelength reuse and scalability. In addition, these networks offer a high degree of reliability as the virtual topology can be reconfigured to provide alternate paths in the event of failures. Another advantage of wavelength-routed networks is the protocol-transparent nature of the lightpaths. This enables the optical network to act as an optical layer and be able to support a variety of data traffic irrespective of their protocol and bit rates.

In such networks, information is exchanged between nodes by establishing lightpaths. The lightpath is basically an all-optical circuit-switched connection between two nodes and can span over multiple fiber links in the network. The lightpath is set up by reserving the same wavelength channel throughout its path in the network. This requirement is referred to as the *wavelength continuity constraint*. Specifically, each fiber link will have multiple lightpaths traversing its wavelengths. Each of the lightpaths traversing the fiber must be on a different

wavelength. In addition, the intermediate wavelength-routing nodes which the lightpath passes through, should configure their switches so that the signal is passed through the appropriate ports in the optical domain. Due to limitations in hardware and the number of wavelengths, it is not possible to set up lightpaths between every pair of source and destination nodes. Hence, the set of limited lightpaths between the nodes forms a virtual topology over the physical network.

1.5.1 Routing and Wavelength Assignment

In WDM networks, the problem of assignment of network resources to satisfy one or more connection requests is referred to as the Routing and Wavelength Assignment (RWA) problem. Since the problem is NP-complete, the conventional approach is to consider the two aspects of routing and wavelength assignment disjointly by first finding a route along which the connection can be established and then search for an appropriate assignment of wavelengths to the links of the selected path. A number of different routing and wavelength assignment approaches have been investigated in the literature. With respect to the traffic demand, there are two variations of the problem: (a) *static* or off-line traffic in which the set of traffic stream requests are given and the problem is cast as an optimization problem with the objective of minimizing the number of wavelengths used [14], [15] and (b) *dynamic* or online in which traffic stream requests arrive and depart randomly [16], [17], [25]. Routing algorithms can be classified as either static or adaptive. Fixed-routing [18] is a static routing technique where a single fixed route is predetermined for each source-destination (s-d) pair. Performance of fixed-path routing has been studied in [19], [20]. Adaptive routing approaches [21], [17], [22] typically depend on network state information to make decisions for connection establishment. These methods are more efficient than fixed-path routing but have longer connection setup delays and higher control overheads. Alternate routing, [23] [24], is a constrained but adaptive routing approach in which each s-d pair is assigned a set of paths. When a connection for a traffic stream is requested, one path is selected from the set of predetermined routes according to a policy. Adaptive unconstrained routing in [17] considered all paths between the source and destination to make

the routing decision. Jue and Xiao [21] also considered an adaptive routing technique called alternate-link routing. In this method, routing decisions are made adaptively on a hop-by-hop basis in a distributed manner by the network nodes. Fixed-paths least-congestion routing has been analyzed in [22]. Dynamic Wavelength Assignment (D-WA) algorithms, such as first-fit (FF) [15], random assignment (R) [19], most-used (MU) [17], Max-Sum (MS) [16] and Relative Capacity Loss (RCL) [25] have also been proposed. For a review of routing and wavelength assignment approaches in WDM networks, refer to [26].

1.5.2 Node Architecture

Figure 1.6 shows a fully reconfigurable OADM having input, output, add and drop ports. To let a wavelength pass through undisturbed, the corresponding optical switch is set in the *bar* state. If the wavelength needs to be added/dropped, then the optical switch is set to the cross state. In a fully reconfigurable OADMs, any wavelength can be added or dropped at any time without affecting the other wavelengths. The key elements required to implement reconfigurable wavelength crossconnect nodes are passive wavelength multiplexers, demultiplexers and switches. Figure 1.7 shows an all-optical crossconnect (OXC) with F incoming and outgoing fibers and W wavelengths on each fiber. The incoming wavelengths on a fiber are demultiplexed by a passive wavelength demultiplexer and the wavelengths are separated. Each of these wavelengths from each fiber are then sent to an $F \times F$ optical switch which is dedicated solely for switching the signals of only one wavelength. The outgoing wavelength from the optical switch are then redistributed to a wavelength multiplexer which multiplexes the different wavelengths and sends them out onto an outgoing fiber.

The key component in the OXC is the optical switch. An important characteristic of optical switches is the switching time. Since wavelength routed networks are circuit-switched networks, switches with millisecond switching times are acceptable. However, if network needs to support protection switching, then switching times of the order of microseconds is required. Switching technologies can be grouped into three categories:

- Electro-optic switches - lithium niobate waveguide switch and semiconductor optical

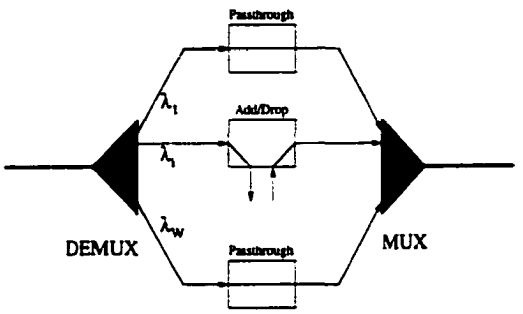

Figure 1.6 An Optical Add/Drop Multiplexer

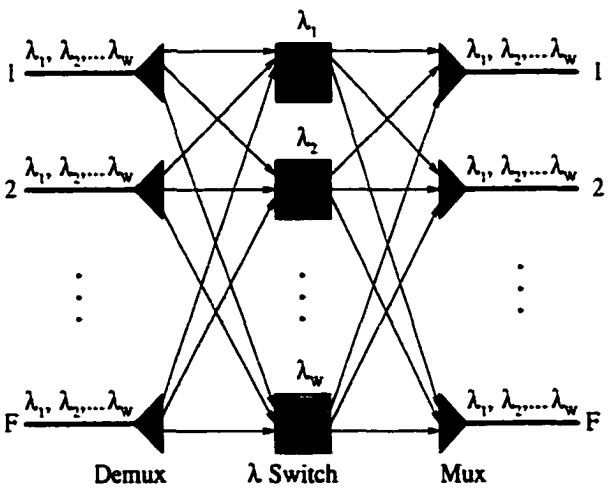

Figure 1.7 An optical crossconnect with no wavelength conversion

amplifiers.

- Thermo-optic switches - integrated-optic Mach-Zehnder interferometers.
- Mechanical switches - Micro-electro-mechanical systems (MEMS).

Of the above three, MEMS-based switches have generated the most excitement. Using MEMS-based switches, large all-optical crossconnects with hundreds of ports are feasible today and the vision of protocol-independent networking is one-step closer to reality. MEMS devices are miniature structures fabricated typically using silicon using a process called micro machining. The switching concept is based on a system of freely moving mirrors rotating around micromachined hinges. These mirrors are controlled by either electrostatic or electromagnetic drive mechanisms and can be used to direct the signal to the required output.

1.5.3 Wavelength Conversion

Figure 1.8 shows a wavelength-routed network with five OXC nodes interconnected by bi-directional links with two fibers per link, one fiber for each direction and two wavelengths per fiber. A lighpath for a traffic session from node B to node E have to obey the wavelength continuity constraint and is routed on the wavelength λ_1 on fiber links B-C and C-E. Assume that there are two other traffic sessions that are in progress from nodes D to A and A to B respectively. Further assume that traffic session from D to A is routed on wavelength λ_1 and traffic session from A to B is routed on wavelength λ_2.

Now when the demand for a traffic session from D to B arrives, a lightpath cannot be setup from D to B because both wavelengths are not free on both the fiber links D-A and A-B. Hence this traffic demand is now said to be blocked on the path D-A-B. On the other hand, if node A is equipped with wavelength conversion devices that sift the lightpath's signal on one wavelength to another, then this traffic demand can be supported and will not be blocked. This ability to convert a signal from one wavelength to another without the help of electronics is referred to as *all-optical wavelength conversion*. If the signal is converted to the electrical domain using a photodetector and subsequently used to modulate a laser at a

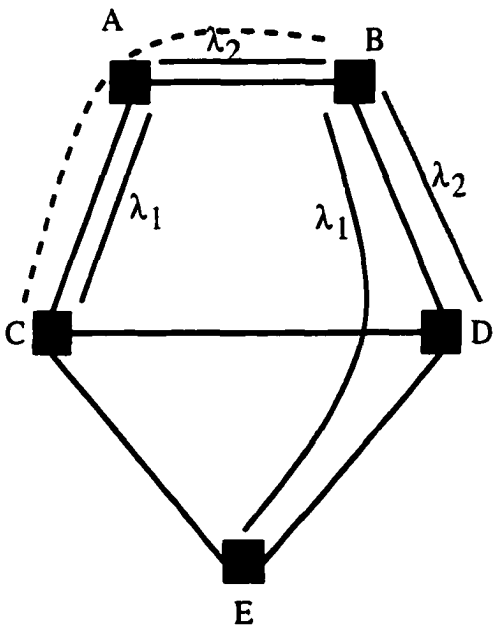

Figure 1.8 A wavelength-routed network with two wavelengths per fiber and OXCs at the nodes

different compliant output wavelength, then this is referred to as *opto-electronic wavelength conversion.* The disadvantage of opto-electronic wavelength conversion is that the protocol transparency of the optical signal is lost and requires the optical data to be in the specified modulation format and bit rate. All-optical wavelength conversion maintains the protocol transparency of the optical network. All-optical wavelength conversion technologies can be grouped into three categories:

- *Optical gating* such as cross-gain modulation (XGM) in Semiconductor Optical Amplifiers (SOAs)
- *Wave-mixing effects* such as four-wave mixing and difference frequency generation in passive waveguides and SOAs.
- *Interferometric effects* such as cross-phase modulation (XPM) in SOAs, Mach-Zehnder and Michelson interferometers, and nonlinear optical loop mirrors (NOLMs).

All-optical wavelength converters are still being prototyped in research laboratories and

such devices are still not commercially available. They are likely to remain costly devices in the near future. Henceforth, we will refer to all-optical wavelength conversion simply as wavelength conversion and a wavelength converter is assumed to be an optical device that employs one of the all-optical wavelength conversion technologies described above.

As we have illustrated in the network example above, wavelength conversion can play an important role in improving the utilization of wavelengths in the fiber links and help in reducing the blocking rate for traffic demands. Wavelength converters can be either full-range or limited-range with respect to their ability to convert the incoming wavelengths to outgoing wavelengths. Full-range wavelength converters (FWCs) can convert any input wavelength to any output wavelength. Limited-rage wavelength converters (LWCs) can convert an incoming wavelength to only a subset of outgoing wavelengths. The different types of wavelength conversion is illustrated in Figure 1.9.

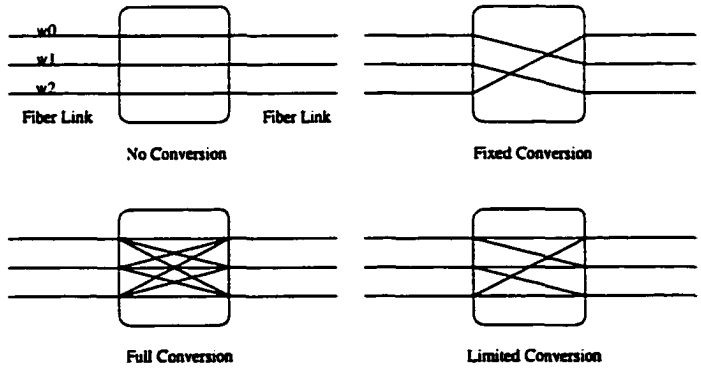

Figure 1.9 Types of Wavelength Conversion

When a crossconnect node is equipped with as many FWCs as the number of outgoing wavelengths, it is said to possess *full wavelength conversion* capability. A node equipped with LWCs is said to have *limited wavelength conversion* capability [27]. Since WCs are likely to remain costly devices, the cost of equipping all the nodes in the network with *full conversion* capability is high. Hence, a network in which *some* nodes are equipped with full conversion capability is more practical. Such a network is referred to as a *sparse wavelength conversion* network. Other wavelength conversion scenarios such as having a fewer number of FWCs

per node [28] or equipping some (or all) of the networks nodes with LWCs are also viable alternatives [29], [30], and [31]. In Figures 1.10, 1.11 and 1.12, we illustrate the different types of wavelength crossconnects with wavelength conversion capabilities.

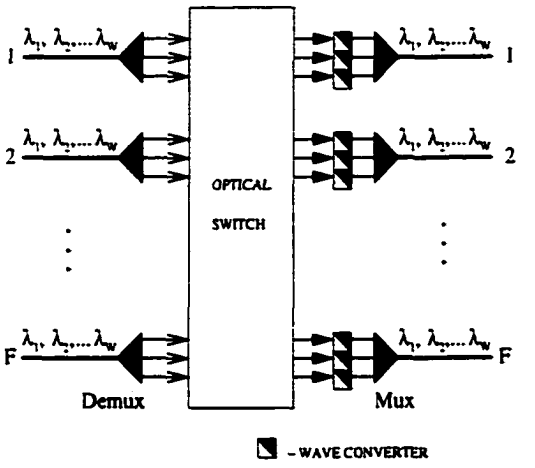

Figure 1.10 Optical crossconnect with a dedicated full wavelength converter at each output port for each wavelength.

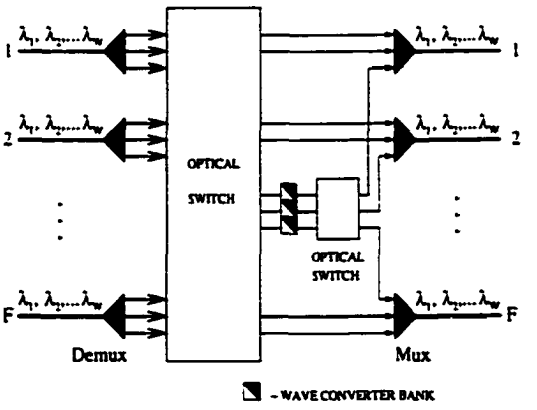

Figure 1.11 Optical crossconnect with a share-per-node architecture having a common wavelength converter bank.

Figure 1.10 shows an optical OXC, where a dedicated FWC is used for each wavelength for every output port. In this case, for a $F \times F$ OXC with F ports and W wavelengths, we need a total of $F \times W$ FWCs. Alternative architectures to save on the wavelength conversion cost have also been proposed. Figure 1.11 illustrates the use of a common wavelength converter

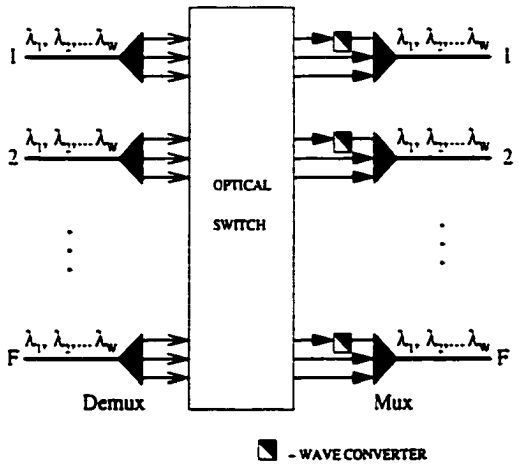

Figure 1.12 Optical crossconnect with a share-per-link architecture having a wavelength converter bank for each output port.

bank with FWCs which can be accessed by any of the incoming wavelengths by configuring the large optical switch. Only wavelengths needing conversion are routed to the conversion bank. The decrease in the number of FWCs is at the expense of increase in the optical switch complexity. Figure 1.12 illustrates a share-per-link approach in which a dedicated wavelength converter bank is used for each outgoing fiber port.

1.6 Issues and Motivation

With the emergence of the Internet, it is expected that the Internet Protocol (IP) will become the common data traffic convergence layer. WDM can effectively meet the exponential increase in demand for bandwidth today. Hence, a large amount of research is currently being carried out to develop new protocols, standards and network systems that eliminate the intermediate network layers such as SONET/SDH and ATM, and run IP directly over the WDM layer. An example of this convergence is the emergence of IP terabit routers with WDM wavelength interfaces. This vision of a two-layer communication infrastructure in which terabit IP routers are connected to an optical wavelength routing network is shown in figure 1.13.

In this case, the traffic engineering functions of ATM such as Quality of Service are assumed

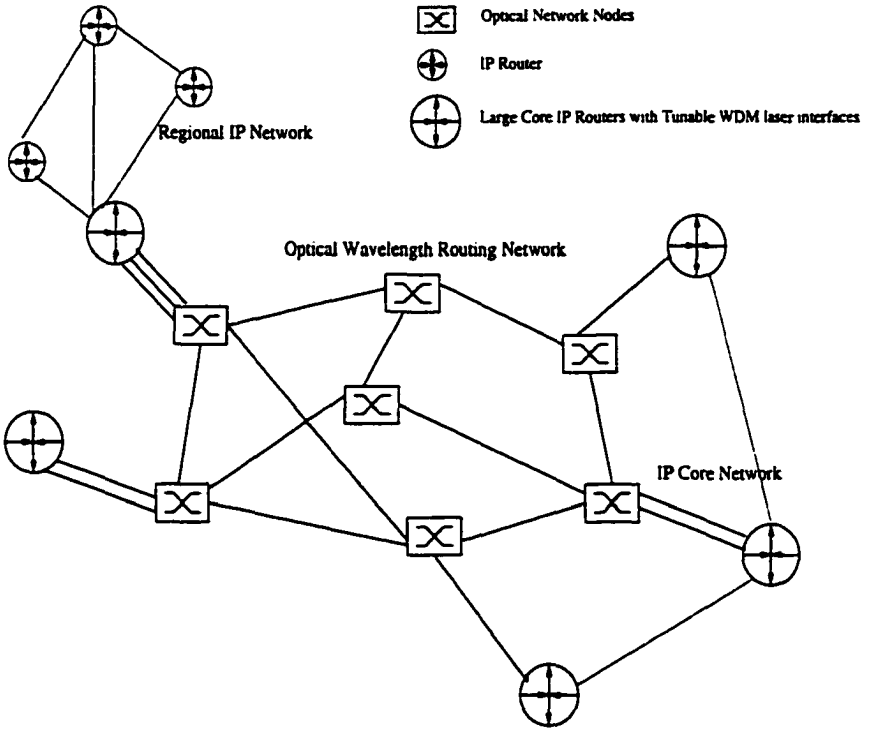

Figure 1.13 An wavelength-routed mesh network connecting IP routers

to be incorporated into IP and the transport functions of SONET/SDH such as APS and traffic aggregation are assumed to be provided by the wavelength-routing network. However, many corporations, telecommunication carriers and service providers have already invested heavily in voice and data transport infrastructures and it is quite unlikely they will embrace any new technology that does not support their existing legacy traffic. Hence, despite the elegance of the two-layer protocol stack model, a gradual migration for legacy services to IP-over-WDM -based networking is necessary. One of the ways to hasten this migration is to study and address the performance limitations and cost inefficiencies that exist in the existing legacy protocol layers, and eliminate them by applying and extending the functionality of the IP or WDM layers. Today, issues that enable such a method of migration are attracting the most attention in the research community.

In such a two-layer IP over WDM scenario, proponents of all-optical networks have predicted that all-optical switching, in conjunction with wavelength-routing and wavelength conversion, will eventually replace electronic switching in the core networks. Indeed, the availability of reconfigurable OADMs and large all-optical crossconnects, built using 2-D and 3-D MEMS, have certainly brought the all-optical network (AON) vision closer to reality. AONs allow nodes to exchange information by setting up lightpaths and establish a virtual topology over the physical fiber network. Lightpaths are set up by reserving the same wavelength channel throughout its path. This wavelength continuity constraint increases the probability of a call being blocked. All-optical wavelength converters (henceforth referred to as wavelength converters) play an important role in improving the utilization of the wavelengths in the fiber links and help in reducing the blocking rate by decreasing the effect of the wavelength continuity constraint. [28]. Today, such wavelength converters are still being prototyped in research laboratories and they are likely to remain costly devices for the near future. The benefits of using wavelength converters in wavelength-routed networks has been extensively studied [14], [19], [32], [20], [33], [34].

In [33], sparse wavelength conversion was studied and its effects on the blocking performance was illustrated. It was shown that although the performance of the network improved with

more conversion capability at the network nodes, the rate of improvement decreased with increasing conversion capability at the network nodes. This led to the conclusion that to obtain sufficiently high performance, it may not be necessary for all the nodes in the network to have wavelength conversion. On the other hand, it is more important to perform a detailed analysis of a given network topology in determining the number and node placement of the wavelength converters so as to obtain optimal blocking performance. This leads us to the first research problem in this thesis namely: *Which of the nodes in an arbitrary network topology should be equipped with wavelength conversion capabilities so as to optimize the blocking performance.*

At first glance, the all-optical approach appears to offer potential cost savings by limiting the electrical equipment at the nodes. Yet, OXCs today are capable of switching whole wavelengths and managing bandwidth only at the wavelength level. Also, optical processing and switching technologies at packet processing speeds are still being prototyped in research laboratories and are not yet commercially available. On the other hand, user traffic requirements today largely consists of traffic varying in range from STS-1 (51.84 Mbps) up to the full wavelength capacity (at around 2.5 Gbps or 10 Gbps). Any traffic request that does not require the full wavelength capacity will inefficiently pack the wavelength and leads to under-utilization of the network capacity. Therefore, the all-optical solution with sparse wavelength conversion may only be cost-effective for the case where the bandwidth demand between the node pairs in the network fully utilizes the lightpaths being provisioned between them and in the case of ultra-long haul transmission where an all-optical approach minimizes the cost by eliminating the need for intermediate electrical regenerators. Any cost saving achieved through elimination of electrical equipment in core networks might be offset by the extra WDM interface line cards that we need to add to support the under-utilized wavelengths. Addition of extra wavelengths at the nodes will result in a corresponding increase in the switch size of the OXC at each network node which will further add to the network cost.

To improve cost savings in terms of wavelength utilization and the amount of electrical equipment, we can employ a hybrid network architecture which utilizes both wavelength-routing and electronic switching and packs sub-wavelength traffic streams efficiently into the

wavelengths. This sub-wavelength traffic stream packing is referred to as *traffic grooming* and can be performed at the core and the edge of the network. WDM networks offering such sub-wavelength low-rate services are referred to as *WDM grooming networks.* A detailed introduction to traffic grooming is provided in Chapter 3. Efficient traffic grooming helps maximize the utilization of each wavelength and achieves cost reductions by improving optical passthrough and reducing the electronic equipment at the nodes. In this thesis, we will address fundamental issues related to the design and operation of WDM grooming networks. Specifically we will answer the following important questions:

- What is the role and classification of traffic grooming in WDM networks? How can we groom traffic streams onto a lighpath? How is the lightpath establishment procedure different from that of conventional wavelength routing networks which switch whole wavelengths? How does traffic grooming affect the blocking performance in the network?

- Can we develop an analytical framework to study the blocking performance of grooming networks? What is the difference in network performance when traffic grooming is performed at the core and when it is restricted to the edge? What is the amount of traffic grooming needed in a network so as to provide good performance?

- How do conventional routing and wavelength assignment algorithms perform in a WDM network with traffic grooming capabilities? In such networks, call requests that arrive at a node pair can ask for a lower-rate traffic connection to be established between them. In this case, what is the difference in network performance for call requests of different sub-wavelength capacities?

- Is the network system, that provides the low-rate connection services, fair to all sets of connection requests? If the network system is not fair, what kind of control mechanisms need to be incorporated to bring about fairness? Even if the control mechanism achieves fairness, what is its impact on the overall network performance?

- In WDM grooming networks, due to the high bandwidths involved, any link failure in the form of a fiber cut will have calamitous results unless network survivability is

included as an integral part of the network design and operation strategies. In a dynamic traffic grooming scenario, path protection schemes are likely to be more useful than path restoration schemes since the timescale for path restoration is difficult to specify and can be on the order of hundreds of milliseconds. In such a case, how can we offer path protection in a traffic grooming network? How can we efficiently groom multiple working and protection paths in the network? How does the topology, and the routing and wavelength assignment algorithm affect our choice of grooming?

1.7 Contributions and Outline of the Dissertation

The rest of the dissertation is organized as follows.

Optimal Wavelength Converter Placement: In Chapter 2, we discuss the role of wavelength conversion and develop an algorithm for optimally placing a given number of wavelength converters in all-optical networks with arbitrary topologies. We first introduce the simple network model upon which the algorithm is based. We then provide a formulation of the overall network blocking probability when a given number of nodes in the network is provided with full wavelength conversion capability. We then present our optimal converter placement algorithm and illustrate its operation using a simple network example. The savings offered by our algorithm is analyzed and compared with the exhaustive case. The benefits of our optimal algorithm is studied through network examples such as the path, mesh-torus and the NSFNET. It is found that the algorithm works better (offering efficiencies of more than 95 percent) than the exhaustive method on networks with high connectivity and when the number of nodes on which need to be equipped with converters is about half that of the number of nodes in the network. Finally we present four heuristics which can be used in lieu of the optimal algorithm to obtain solutions close to the optimal solution.

Traffic Grooming in Optical Networks: We define the concept of traffic grooming in Chapter 3. We provide a brief description of the WDM grooming network model and introduce the notations and terms that are used in the following chapters. We introduce two different types of WDM grooming networks: Constrained Grooming Networks and Sparse Grooming

Networks. We then describe the procedure for the set up and release of low-rate connections between node-pairs in mesh WDM grooming networks and illustrate the usefulness of traffic grooming through simple examples. The chapter concludes with a brief survey of the current research in traffic grooming in WDM ring networks.

Performance Analysis of WDM Grooming Networks: In Chapter 4, we develop approximate analytical models to calculate the blocking performance of constrained and sparse grooming networks. The analytical models take into account the capacity distribution on a wavelength and the correlation on neighboring links given that incoming call requests are of varying capacities. Previous research has concentrated on the case where the wavelength or a single time slot in a wavelength is the basic unit of bandwidth. Our analytical models provide the blocking performance for calls of different capacities and can be applied to networks with arbitrary topologies. We use analytical and simulation results to compare the performance of constrained and sparse grooming networks. Our results provided fairly good estimates of blocking for well-connected networks. We show that sparse grooming networks can offer a significant performance improvement in terms of reduction in blocking probability. Compared to constrained grooming, sparse grooming offers at least an order of magnitude decrease in blocking probability for high capacity connections and multiple orders of magnitude decrease in blocking for low capacity connections.

Capacity Fairness of WDM Grooming Networks: We address the concept of capacity fairness in WDM grooming networks in Chapter 5. In such networks, call request can ask for a low-rate connection to be established between a node pair. In this scenario, call requests that ask for capacity nearer to the full wavelength capacity are likely to experience higher blocking than those that ask for a smaller fraction. We address this capacity unfairness and provide a qualitative and quantitative definition for the same. We also provide study the capacity fairness of existing dynamic wavelength assignment algorithms. A connection admission control algorithm which can be used along with any wavelength scheme, is then proposed to achieve capacity fairness. The algorithm provides good capacity fairness while at the same time does not over-penalize the overall blocking performance.

Survivable WDM Grooming Networks: In Chapter 6, we address the issues of establishing dependable traffic stream connections in WDM grooming networks. To establish a dependable connection, we setup link-disjoint primary and backup traffic stream paths between the source and destination and use backup multiplexing to reduce the overhead of backup traffic streams. We present a dynamic algorithm to obtain the optimal spare capacity on a wavelength on a link when a number of backup traffic streams are multiplexed onto it. We propose two schemes for grooming traffic streams onto wavelengths: Mixed Primary-Backup Grooming Policy (MGP) and Segregated Primary-Backup Grooming Policy (SGP). We illustrate how these schemes can be applied in a WDM mesh network scenario along with a routing and wavelength assignment algorithm. We then present simulation results to evaluate the effectiveness of the proposed schemes on different network topologies using different routing and wavelength assignment methods. The effect of change in granularity and change in the number of alternate paths on the grooming policies are presented.

Summary and directions for future research are presented in Chapter 7.

CHAPTER 2. Wavelength Conversion and Optical Converter Placement in Arbitrary-Topology Wavelength-Routed Networks

2.1 Introduction

In a network without wavelength converter nodes, it is required that data for a call arriving at the input port of a node on one wavelength has to be switched to an output port of the node at the same wavelength. To satisfy such a connection request for a call, it is necessary that the connection path which is set up from the source to the destination, has a free wavelength on all its links. This requirement, called the *wavelength continuity constraint*, results in increasing the probability of a call being blocked. On the other hand, it has been shown in [28] that wavelength converters improve the performance of wavelength-routed networks in terms of blocking probability. The benefits of using wavelength converters in wavelength-routed networks has been studied in [14], [19], [32], [20], [33], [34].

Ramaswami and Sivarajan in [14] showed that use of wavelength converters resulted in a 10 to 40 percent increase in the amount of wavelength reuse. In addition, they also established lower bounds on the blocking probability for a network using any routing and wavelength assignment algorithm. In [19], it was shown that wavelength conversion can improve performance in large mesh networks where a path consists of many hops. Barry and Humblet in [20] studied the effects of path length, switch size and the hop number on the blocking probability in networks with and without wavelength converters. Subramanian et al.[33] studied sparse wavelength conversion and its effects on the blocking performance. They showed that the performance of the network improved as the conversion density (probability that a node in the network is capable of full wavelength conversion) was increased from 0 to 1. But, they also

found that the rate of improvement decreased with increasing conversion density. This meant that it may not be necessary for all the nodes to have wavelength converters for obtaining sufficiently high performance. On the other hand, they pointed out that it was more important to perform a detailed analysis of a given network topology in determining the number and node placement of the wavelength converters.

Realizing that wavelength conversion is expensive and may not be required at each wavelength, in the next section, we are concerned about deciding which of the nodes in a sparse conversion network should be equipped with full wavelength conversion capabilities so as to optimize the blocking performance. Specifically, given the number of nodes with full wavelength conversion capability, the traffic demand, the network topology and the number of available wavelengths, the goal is to find the node locations which can be equipped with full wavelength conversion so as to obtain optimum blocking performance. Henceforth, the phrase "placing a wavelength converter at a node" is defined as providing the node with full wavelength conversion capability. Such a node is referred to as a *wavelength converter node.*

2.1.1 Converter Placement

The problem of wavelength converter placement at the network nodes in sparse wavelength conversion networks was first considered in [35]. Optimal solutions (based on dynamic programming) for the path, bus and ring topologies were proposed for both uniform and non-uniform traffics. It was shown that considerable gains in blocking performance could be obtained when optimal placement was used compared to a random placement. In [36], a wavelength converter placement heuristic was presented which places wavelength converters at nodes with highest average output link congestion. While the heuristic gives almost-optimal results for the NSFNET example, due to the sequential placement of wavelength converters, it will not give near-optimal results for the simple case of a path topology with uniform traffic. In [37], three algorithms of linear complexity were presented to obtain near-optimal solutions for a path topology. They proved that optimal placement for end-to-end blocking probability is

obtained when the segments on the path have equal blocking probabilities. However, optimal placement was not always obtained since it was not always possible to divide the path into segments with equal blocking probability. Venugopal et al. [38] proposed a heuristic to place limited-range wavelength converters based on node congestion, length of the lightpaths and nodes where conversion is high. Reference [39] proposed a solution for obtaining the best placement of converters on a path. Reference[40] also dealt with heuristics for full-range wavelength converter placement in networks of arbitrary topology and with arbitrary traffic patterns. In this chapter, we develop an optimal solution to the converter placement problem for arbitrary network topologies by using the traffic model of [35]. The optimal solution provides the best performance so that the overall network blocking probability is minimized. Though computationally intensive, we show that the algorithm is more efficient than exhaustively searching all combinations of wavelength converter placements. We use the wavelength independence model given in [20] to evaluate the end-to-end blocking probability of a call. The algorithm, however, is independent of the performance model and can also be used to solve for the case of non-uniform traffic loads in the network.

The organization of the chapter is as follows. In Section 2, we describe the network model on which our algorithm is based. In Section 3, we present the optimal converter placement algorithm. In Section 4, we analyze the performance and explain the improvement in performance over an exhaustive search algorithm. The benefits of our wavelength converter placement algorithm are studied by analyzing some network examples such as the path, NSFnet and the mesh-torus in Section 5. We also provide some simple heuristics for converter placement in Section 6. We provide our conclusions in Section 7.

2.2 Network Model

We model the network using a directed graph G = (V,L) where V, the vertices in the graph, represents the set of network nodes and L, the directed edges in the graph, represent the set

of unidirectional optic fiber links in the network. Let the nodes be numbered $1, 2, ..., N$ and let l_{ij} represent the directed link from node i to node j. There are F wavelengths on each link and each call requires a full wavelength on each link it traverses. Each call uses a prespecified path - in this case, the shortest path based upon hop count. All the shortest paths in the network are assumed to satisfy the *optimality principle*. This principle states that if a node x is on the optimal shortest path from node y to node z then the optimal shortest path from node x to node z follows the same route after node x as that followed by the path from y to z. If the prespecified path is available then a lightpath is established between the source and the destination nodes.If the prespecified path is not available then the call may not be routed through an alternate path and is assumed to be blocked.

Let $A = [\lambda_{ij}]$ be the traffic matrix where $\lambda_{ij}, i \neq j$ denotes the node-pair load from node i to node j, and $\lambda_{ii} = 0$. Let the link loads per wavelength be ρ_{ij} for link l_{ij}. Specifically, ρ_{ij} is the probability that a given wavelength is occupied by a lightpath on link l_{ij}. The link loads per wavelength per link can be obtained from the node-pair loads by

$$\rho_{ij} = \frac{\sum \lambda_{sd}}{F} \; \forall \textit{ nodes } s, d \textit{ whose paths include link } l_{ij} \tag{2.1}$$

such that the path from s to d includes link l_{ij} provided λ_{sd} is small such that $\rho_{ij} < 1$. We assume that the load on a given wavelength on a link is statistically independent of the link loads of other wavelengths on that link and the loads on other links.

2.2.1 Blocking Probability Analysis of a Single Path

Let the number of converter nodes to be placed be K. Let $C = \{c(1), c(2), ..., c(K)\}$ be the *converter placement vector* such that $1 \leq c(i) < c(i+1) \leq N, 1 \leq i < K$. The entries of C denote the placement of converters among the nodes $1, 2, ..., N$. Now consider the path p of an end-to-end call from a source node s to a destination node d in the network. We define a *segment* to be the set of links on the path between two consecutive converter nodes or between the source (or destination) and a converter node. If the path contains no converter nodes, then

it consists of a single segment between the source and destination. Then

$$f(i,j) = 1 - (1 - \{\overline{\rho}_{ii_1}\overline{\rho}_{i_1i_2}...\overline{\rho}_{i_nj}\})^F \tag{2.2}$$

is the success probability in the segment from node i to node j on the path, where $\overline{\rho}_{xy} = 1-\rho_{xy}$ for link l_{xy} and $i_1, i_2, ..., i_n$ are the nodes in the segment between nodes i and j. Let the number of converters placed on the nodes (not including the source and destination nodes) of the path p be k, where $0 \leq k \leq K$. Given the converter placement vector C for the network, we have $d_{sd} = (d(1), d(2), ...d(k))$ *and* $d_{sd} \subset C$, the converter placement vector for the *path* such that the entries of $d(i), 1 \leq i \leq k$ correspond only to the node numbers of the path p which have converters on them. This divides the path p into $k+1$ segments. Hence the success probability of the end-to-end call with the converter placement vector being C is given by

$$S_{sd}(C) = \prod_{i=0}^{k} f(s_i) \tag{2.3}$$

where $f(s_i) = f(d(i), d(i+1)), 1 \leq i \leq k-1$ corresponds to the success probability of the segment s_i between the converter nodes $d(i)$ and $d(i+1)$. $f(s_0)$ corresponds to the success probability of the segment between the source node and converter node $d(1)$ and $f(s_k)$ corresponds to the success probability of the segment between the converter node $d(k)$ and the destination node. The blocking probability for the path is then obtained as

$$P_{sd}(C) = 1 - S_{sd}(C) \tag{2.4}$$

Using the above formula, we can calculate the blocking probabilities for all the paths in the network. From this, we obtain the blocking performance $\Gamma(C)$ of the network for the converter placement vector C by

$$\Gamma(C) = \frac{\sum_{\forall s,d} \lambda_{sd} P_{sd}(C)}{\sum_{\forall s,d} \lambda_{sd}} \tag{2.5}$$

The above formula can now be used to calculate the blocking performance and select the best converter placement that gives the minimum blocking performance Γ in the network.

2.3 Converter Placement Algorithm

One obvious way to solving the optimal converter placement problem is to use the method of exhaustive placement and blocking performance computation. In this method, given the directed graph G with N nodes and the number of converters K to be placed, we initially obtain the set of all converter placement combinations $C_l^K, 1 \leq l \leq \binom{N}{K}$. Here $\binom{N}{K}$ corresponds to the number of combinations of K converters out of N nodes. C_l^K here is the K-converter placement vector and can be further expanded as $C_l^K = (c_l^K(1), c_l^K(2), ..., c_l^K(K))$ where $c_l^K(x), 1 \leq x \leq K$ corresponds to the placement entry on K of the nodes of the network. Next for each converter placement combination, we calculate the corresponding blocking performance according to Equation 2.5. We then select that converter placement combination which gives the minimum blocking performance value as the optimal placement. Evidently this method is not an efficient and fast way to solve the problem.

Many factors like the amount of transit traffic at a node, path lengths, distances between converters, distances from the converters to other nodes, and the amount of traffic that needs to be switched at a node affect the optimal solution which makes converter placement in an arbitrary network a hard problem in general. It is also not always possible to make a sequence of stepwise decisions by placing converters one by one on the nodes and ending up with an optimal placement. That is, the optimal placement combination for $K-1$ nodes in the network may not be a proper subset of the optimal placement combination for K nodes. This can be illustrated by considering the optimal placement of converters in a bidirectional path network of 10 nodes with uniform link loads. As shown in Table 2.5, the optimal placement for one converter is either node 5 or node 6. On the other hand, the optimal placement for two converters is at nodes 4 and 7. In the algorithm, we make use of the exhaustive search method. However, we develop a method to reduce the computational requirements and still be able to find the optimal solution. Our algorithm uses the procedure defined in the following two subsections.

2.3.1 Construction of Auxiliary Graphs

Our converter placement algorithm proceeds in phases. In the first phase, we first construct N auxiliary directed graphs, $G_j = (V, E_j)$ for each node $j \in V$ such that E_j consists of only those edges $e \in L$ which are on those paths from the remaining $N-1$ nodes to node j. The edges are directed towards the destination node j. We consider only the shortest paths to node j from each node $i, i \in V$ *and* $i \neq j$. The shortest paths, in addition, satisfy the optimality property. Therefore, each graph G_j is acyclic. The first phase results in a family of auxiliary directed acyclic graphs $G_1, G_2, G_3, ..., G_N$ for each node $1, 2, ..., N$ acting as the destination. In each auxiliary graph G_j, there exists at least one or more nodes which have indegree of zero. We refer to these nodes as *primary source* nodes. Only the destination node has outdegree of zero. We collectively refer to the destination node and the primary source nodes as *outer* nodes of the auxiliary graph. All other nodes are referred to as *inner* nodes of the auxiliary graph. Let the number of *inner* nodes be $|I|$ and the number of *outer* nodes be $|O|$ so that $|O|+|I| = N$

2.3.2 Blocking Performance for an Auxiliary Graph

The second phase of the algorithm uses the simple principle that the blocking probabilities of the paths are not affected if converters are placed on the *outer* nodes in the auxiliary graph. In this phase, we first obtain all placement combinations $C_l^K, 1 \leq l \leq \binom{N}{K}$, on the whole network of N nodes. Each placement combination has an associated overall blocking performance variable $\Gamma(C_l^K)$ which is initialized to zero. Next, for each graph G_j, we obtain the blocking probabilities of the paths to the destination node by placing a subset of converters on the *inner* nodes of the graph. The idea is that if m converters are placed on the *inner* nodes and $K-m$ converters are placed on the *outer* nodes in any placement combination then the blocking probability on paths to node j in the auxiliary graph G_j depends only on the m converters placed on the inner nodes. We exhaustively place all combinations of m converters, where m is varied from a *lower limit* to a *higher limit* (as given in Equation 2.7) and calculate the blocking performances, $\Gamma_j(E_i^m)$ for G_j where E_i^m is the ith combination of

placing m converters on the *inner* nodes of the graph G_j. The value of i varies from 1 to $\binom{|I|}{m}$, the number of combinations of m out of $|I|$ *inner* nodes. E_i^m, also known as the m-converter placement vector, can be further expanded as $E_i^m = (e_i^m(1), e_i^m(2), ..., e_i^m(m))$ where $e_i^m(x), 1 \leq x \leq m$ corresponds to the placement entry of an *inner* node of the graph. The blocking performance $\Gamma_j(E_i^m)$ for the auxiliary graphs is defined as

$$\Gamma_j(E_i^m) = \frac{\sum_{\forall s, s \neq j} \lambda_{sj} P_{sj}(E_i^m)}{\sum_{\forall s,d} \lambda_{sd}} \tag{2.6}$$

The division by the sum of *all* node-pair loads is done so that the blocking performances obtained from all the auxiliary graphs can be directly added together to obtain the overall blocking performance of the entire network. Note that blocking performance of each auxiliary graph is calculated by using the blocking probability of only $N-1$ paths all of which end at a single destination node. The *lower limit* and *higher limit* values for m are obtained as follows:

$$\begin{aligned} \textit{lower limit} &= max\{0, K - |O|\} \\ \textit{higher limit} &= min\{|I|, K\} \end{aligned} \tag{2.7}$$

Next we obtain all combinations D_n^{K-m} of $K-m$ (m varied from the *higher limit* to the *lower limit*) converters placed only on the *outer* nodes. Here n varies from 1 to $\binom{|O|}{K-m}$. Now to each combination E_i^m, we append each of the combinations D_n^{K-m} to get K-converter placement combinations C_l^K on the whole network. All the K-converter placement combinations which are obtained from appending each E_i^m to any D_n^{K-m} will have the same blocking performance of $\Gamma_j(E_i^m)$. Hence for each of the C_l^K obtained, the blocking performance $\Gamma_j(E_i^m)$ is simply added to the corresponding overall blocking performance variable of $\Gamma(C_l^K)$. Recall that this can be done because the only converter positions that vary in all these combinations are in the *outer* nodes which do not affect the blocking probability of these paths. The above procedure provides the blocking performances corresponding to the auxiliary graph G_j for all the $\binom{N}{K}$ converter placement combinations. However we calculate the blocking probability for only

$$Path_{calc}^{G_j} = \sum_{m=lower\ limit}^{higher\ limit} \binom{|I|}{m} \tag{2.8}$$

combinations. It is interesting to note that the above procedure partitions the $\binom{N}{K}$ converter combinations in to $Path_{calc}^{G_j}$ *equivalence classes* where all of the elements in each of the equivalence classes have the same blocking probability. This procedure is carried out on all auxiliary graphs $G_j, 1 \leq j \leq N$. The blocking performance values in each case are calculated and accumulated to the appropriate overall blocking performance variables. We have now obtained the overall blocking performances for all $\binom{N}{K}$ placement combinations.

The overall blocking performance variable corresponding to a single K-converter placement combination gives us a measure of the call-blocking for all $N(N-1)$ paths from all sources to all destinations for that particular placement combination. We now select that converter placement combination which results in the minimal blocking performance value as the optimal solution. The pseudocode for the algorithm is given in Table 2.1. The function **Get_All_Combinations**(I,m) obtains the set of all combinations of m converters on the set of I nodes. The function **Get_Blocking_Performance**(E_i^m) gives the blocking performance of the auxiliary graph G_j for the $N-1$ paths to the destination node j.

2.3.3 Example

We will illustrate the working of the algorithm using the following example. We consider five WDM crossconnect nodes interconnected by point-to-point bidirectional fiber links in an arbitrary mesh topology as shown in Fig. 2.1(a). We also assume that the node traffic is uniform and all the node-pair loads from each of the nodes to each other is equal to 0.1. The shortest paths information available is assumed to be as shown in Table 2.2. An auxiliary graph G_E formed with only those edges which are on the shortest paths from nodes A, B, C, and D to E, is shown in Fig. 2.1(f). Similar auxiliary graphs obtained for nodes A, B, C and D acting as the destination are also shown in Fig. 2.1.

In auxiliary graph G_E, nodes C and D are the *inner* nodes and nodes A, B, and E are

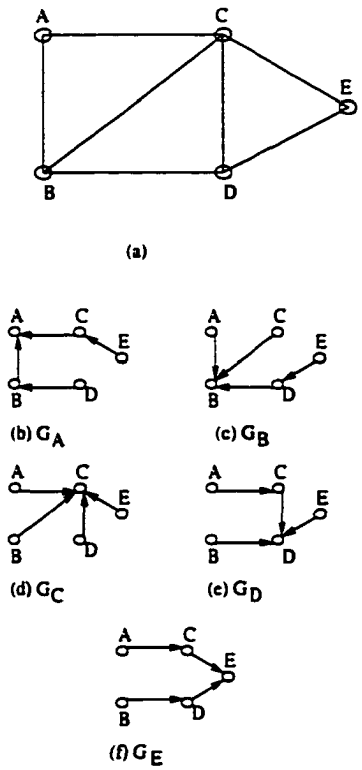

Figure 2.1 WDM network with five nodes and its auxiliary graphs G_A, G_B, G_C, G_D and G_E with destination nodes A, B, C, D and E respectively

the *outer* nodes. Let us assume that the number of converters to be placed is two. Hence the *lower* and *upper* limits for m are 0 and 2, respectively. The blocking performance values have to be calculated four times, once for $m = 0$, twice for $m = 1$(one converter placed on either node C or D), and once for $m = 2$. Thus $E^0 = \{(\phi)\}, E^1 = \{(C),(D)\}, and E^2 = \{(C,D)\}$ and $D^{K-2} = \{(\phi)\}$, $D^{K-1} = \{(A),(B),(E)\}$, and $D^{K-0} = \{(A,B),(A,E),(B,E)\}$. The blocking performance obtained when $m = 0$ is assigned to converter placement combinations (A,B), (A,E), and (B,E). The blocking performance obtained when $m = 1$ and node C has a converter is assigned to converter placement combinations (A,C), (B,C), and (E,C). The blocking performance value when $m = 1$ and node D has a converter is assigned to converter placement combinations (A,D), (B,D), and (E,D). When $m = 2$, there is only one placement combination of (C,D). The G_E column in Table 2.3 gives the blocking performance values for the auxiliary graph in Fig. 2.1(f). This procedure is also carried out for the remaining four auxiliary graphs corresponding to the nodes A, B, C, and D taken as the destinations, respectively. The total blocking performance for the whole network is calculated by adding up the values corresponding to a placement combination for all five graphs. Table 2.3 gives all the blocking performance values for each placement combination for all auxiliary graphs (G_A, G_B, G_C, G_D and G_E). The overall blocking performance for the network is also shown in Table 2.3. The placement combination which gives the minimum overall blocking performance value is taken as the optimal placement combination. In Table 2.3, we find the optimal placement combination of (C,D) gives the minimum overall blocking performance of 6.84e-04.

2.4 Algorithm Analysis

To show the correctness of our algorithm, note that to calculate the blocking performance for each auxiliary graph $G_j, 1 \leq j \leq N$, we calculate the path blocking probability for just $(N-1)$ paths. We can also easily see that for each auxiliary graph, we obtain $\binom{N}{K}$ placement combinations from the union of each and every one of the placement combinations of m converters on the *inner* nodes with each and every one of the placement combinations of

$K - m$ converters on the *outer* nodes where the value of m is as given in Eqn. 2.7. Hence our algorithm obtains the path blocking probability of $\binom{N}{K}\ N(N-1)$ paths. In the case of finding out the optimal placement and best blocking performance for all possible combinations using the method of exhaustive placement and blocking performance computation, the path blocking probability is also calculated for a total number of $\binom{N}{K}\ N(N-1)$ paths, where $\binom{N}{K}$ is the total number of placement combinations and $N(N-1)$ is the total number of paths in the graph. On the other hand, we save on the calculation of the blocking performance for many of the converter placements, since all converter placement combinations that differ only in the converter positions of outer nodes are assigned the same blocking performance value.

To quantify these savings, we first define the average number of *inner* nodes, N_I, for the network as $\frac{\sum_{j=1}^{j=N} N_I^j}{N}$, where N_I^j is the number of *inner* nodes of auxiliary graph G_j. Then the average number of *outer* nodes is N_O and $N_O = N - N_I$ where N is the total number of nodes in the graph. It must be mentioned that there are at least two *outer* nodes in every auxiliary graph. This is because each auxiliary graph is a directed acyclic graph and there is one node with outdegree zero i.e., the destination node and at least one node with indegree zero, a primary source node. Also as mentioned before, the blocking performance for each of the auxiliary graphs is calculated by computing the blocking probability of just $(N-1)$ paths. Hence the number of paths, P_{calc} for which the blocking probabilities need to be calculated are

$$P_{calc} = (N-1) \sum_{j=1}^{N} \sum_{m=lower\ limit}^{higher\ limit} \binom{N_I^j}{m} \tag{2.9}$$

where the *lower limit* and *higher limit* variables for varying m are obtained according to the conditions specified in Section 3.1. The first term, $(N-1)$, denotes the number of paths present in each auxiliary graph G_j for which the blocking probability has to be calculated, and the last summation term denotes the total number of placement combinations for which the blocking performance of the auxiliary graph needs to be calculated.

Assuming the following arbitrary values for a network: $N = 10$, $N_O^j = 4$, $N_I^j = 6$, for all G_j, and $K = 3$, an exhaustive search for the optimal placement needs $\binom{10}{3} \cdot 10(10-1) = 10800$ path calculations of the blocking probability. On the other hand, using the algorithm we need

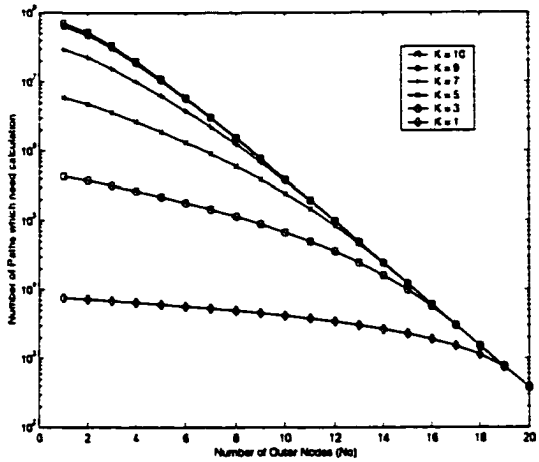

Figure 2.2 P_{calc} vs. N_O for $N = 20$ *and* $1 < K < 20$. Note: P_{calc} value for $N_O = 1$ corresponds to the case when the exhaustive algorithm is used. $N_O \geq 2$ corresponds to P_{calc} values when our algorithm is used.

$10(10-1) \cdot (1+7+21+35) = 5760$ path calculations of the blocking probability to get the optimal placement. We plot P_{calc} as a function of the number of *outer* nodes($N_O \geq 2$) for various K for in Fig. 2.2. The value for $N_O = 1$ corresponds to the case when the exhaustive algorithm is used. We find that, for all K, P_{calc} is lower than the total number of paths which need to be calculated for the exhaustive algorithm. As the number of *outer* nodes increases, the P_{calc} decreases rapidly. Hence the saving in calculation of blocking probability offered by the optimal algorithm increases as the number of *outer* nodes increases. In general, an increase in network connectivity or a decrease in the network diameter usually results in more number of outer nodes in the network and results in an increase in the improvement offered by the algorithm.

2.5 Numerical Results

We will first define the efficiency of our algorithm as the percentage of number of paths for which the blocking probability need not be calculated when our algorithm is used to the total

number of paths for all possible converter combinations when the exhaustive method is used:

$$\frac{P_{total} - P_{calc}}{P_{total}} \times 100 \tag{2.10}$$

where P_{calc} is as given in Equation 2.9 and $P_{total} = \binom{N}{K} N(N-1)$. As illustrated in the previous section, this efficiency depends on the average number of *outer* nodes of the network and the number of converters to be placed on the network.

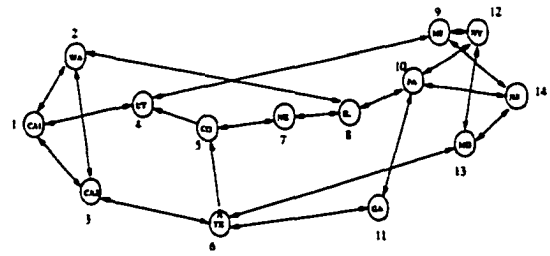

Figure 2.3 The NSFnet with 14 nodes and 21 edges

Although, we used the link-independence model in Section 2.2.1 to calculate the blocking probability of a source-destination path, the algorithm however is independent of the analytical model and more accurate models such as the link-correlation model specified in [33], can also be used to obtain optimal placement solutions. We implemented two versions of the algorithm, one using the independence model and the other using the correlation model specified in [33]. Although the correlation model does provide us with more accurate blocking probability values, as compared to the independence model, the optimal placement combinations obtained in both cases were almost similar as shown in Table 2.4. In addition, due to the complexity of calculations involved, the correlation model could be used in the algorithm only for networks of small size. Consequently, we will present the results of the algorithm using only the independence model in the remainder of this section.

Consider the optimal placement of converters in a bidirectional path network of $N = 10$ nodes. Table 2.5 gives the optimal placement solutions along with their blocking probability and the efficiency of the algorithm. The optimal placement column in the table indicates the nodes where a converter should be placed. It is obvious that the blocking probability decreases

as the number of converters K increases. However, the efficiency of the algorithm increases initially until $K = \lceil \frac{N}{2} \rceil$ and then decreases again. When $K = 5$, the blocking probability for 50% of the paths need not be calculated. We provide the optimal converter placement results and efficiency of the algorithm for 4×4 mesh-torus and the 14 node NSFNET shown in Fig. 2.3 in Table 2.6 and Table 2.7, respectively. The nodes in mesh-torus are numbered from 1 to 16, from left to right and from top to bottom. The node numbers of the NSFNET are shown in Fig. 2.3. It is observed that the algorithm works more efficiently with the mesh-torus and the NSFNET. Moreover the efficiency of the algorithm increases to a very high percentage when K increases to $\lceil \frac{N}{2} \rceil$. This confirms the fact that the algorithm works better than the exhaustive case for networks with high connectivity and high average number of *outer* nodes.

2.6 Heuristics

The optimal algorithm reduced the computations to achieve optimal wavelength converter placement. However, it is still expensive. Although converter placement is not optimal when attempted in a sequential manner, sometimes the solutions obtained can be close to the optimal placement. In this section, we provide four heuristics for placement of converters on the nodes of the network. All these heuristics are based on associating a weight to the nodes of the network. Converters are placed on the nodes in the order of increasing weight. The four heuristics vary in the manner the weight on the nodes are assigned.

1. The Path-based Index heuristic given in Fig.2.4 calculates the weight of the nodes by the number of the pre-specified paths passing through it.

2. The second heuristic, called the *Path-Length-based Index* (PLI) heuristic calculates the weight of the nodes as the sum of path lengths of all the source-destination pre-specified paths passing through it. The path length is an important parameter in determining the performance of the network. The effects of path length on the blocking probability of WDM networks has been studied in [20]. The blocking probability of a network with and without wavelength converters tends to increase as path length increases or as the number of hops from source

Path-based Index heuristic
$//P = \{p_1, p_2, ..., p_j\}$ be the set of paths, one for each s-d pair.
$//w_i$ is the weight of node v_i where $v_i \in V$, the set of nodes in the graph.
$//K$ is the number of converters.
$//l_j$ is the length of path p_j.
1. Initialize for all $v_i \in V, w_i = 0$
2. For each $p_j \in P$
3. For each node v_i that lies on path p_j, except the source and destination.
4. $w_i = w_i + 1$
5. EndFor
1 6. EndFor
7. Sort the nodes according to their weight and place converters on K nodes with the highest weights.

Figure 2.4 Path-based Index heuristic

to destination increases. Wavelength converters decrease the blocking probability by reducing the average hop lengths and minimizing the congestion on the links. Hence the PLI heuristic uses the path length as the selection parameter. This heuristic can be obtained by replacing line 4 in Fig.2.4 with $w_i = w_i + l_j$ where l_j is the length of the path p_j.

3. The third heuristic, called the *Traffic-Path-Length Product* (TPLP) heuristic calculates the index of a node by using the sum of the products of traffic rate and the path length of each source-destination path that passes through the node. This heuristic can again be obtained by replacing line 4 in Fig.2.4 with $w_i = w_i + l_j \times \lambda_{sd}$, where λ_{sd} is the traffic flowing on the path p_j corresponding to the source s and destination d.

4. The final heuristic, called the *Inner Node Index* (IN) is based on our optimal algorithm. After the first phase of creating the auxiliary graphs and separating the nodes of each auxiliary graph into *inner* and *outer* nodes, instead of calculating the blocking probabilities, we count the number of times each node is an inner node and assign that as the weight of the node. If the node has a count of zero, this means the node is an outer node in all the auxiliary graphs and can be completely excluded for converter placement. The steps of the heuristic are given in Fig. 2.5.

Inner Node Index heuristic
//w_i is the weight of node v_i where $v_i \in V$, the set of nodes in the graph.
//K is the number of converters.
1. For each node $v_j \in V$,
2. Construct_Auxiliary_Graph(G_j)
3. For each node $u_i \in G_j$,
4. If u_i is an *inner* node then $w_i = w_i + 1$
5. EndFor
6. Sort the nodes according to their weight and place converters on K nodes with highest weights.

Figure 2.5 Inner Node Index heuristic

The results of the four heuristics on the bidirectional path network, mesh-torus network and the NSFnet are tabulated in Tables 2.8, 2.9 and 2.10, respectively.

If we need to select K nodes for converter placement, a simple task would to select the best K nodes according to their weight. Assume $K = 4$, using the results in Table 2.8 for the bidirectional path, the best four node choices for converter placement in a 10 node path are (4,5,6,7) except in the case of IN heuristic, where all nodes with the same weight. For the mesh torus, in Table 2.9, the best four choices for converter placement are (6,7,10,11) in the first three heuristics and any four of (2,3,6,7,10,11,14,15) in the case of IN heuristic. For the NSFnet the best four choices are (4,6,8,10) for all four heuristics. Another solution would be to first select a set of nodes, say N_H, where $K < N_H$, as the best possible positions for converter placement. Now we can just calculate $\binom{N_H}{K}$ combinations and obtain the optimal placement positions. It should be noticed that the results obtained using the heuristics are consistent with what we obtained using the optimal algorithm. We also note that heuristic IN does not work well for regular topologies. We can also improve the performance of the heuristics for mesh networks by excluding nodes of degree two, which source or sink relatively low traffic compared to other nodes. The reason is that these nodes act more as passthrough nodes for wavelengths and are less likely to be a good choice for converter placement.

2.7 Conclusion

In this chapter, we reviewed the role and need for wavelength conversion and presented an algorithm for optimally placing a given number of converters in all-optical networks with arbitrary topologies. We also developed a network model to evaluate the blocking performance of such networks. The algorithm was divided into two phases. The first phase was the creation of auxiliary graphs using each node in the network as the destination node.In the second phase, we detailed the procedure for obtaining the blocking performance for all the converter placement combinations by calculating the blocking performance for only some combinations. We used the principle that all converter placement combinations that differ only in the outer nodes can be assigned the same blocking performance value. The algorithm was further explained using a simple network example. The savings in calculation was analyzed and compared with the exhaustive case. It was found that the savings in calculation introduced by our algorithm increases rapidly as the number of outer nodes increases. Since the number of outer nodes is directly dependent on the network connectivity, it was inferred that an increase in network connectivity results in an increase in the improvement offered by the algorithm. The benefits of our algorithm was further confirmed by studying the optimal converter placement on examples such as the path, mesh-torus and the NSFNET. The efficiency of the algorithm was defined and tabulated for each of the networks. It was found that the algorithm works very well (offering efficiency of more than 95%) than the exhaustive method on networks with high connectivity and when the number of converters to be placed is about half that of the number of nodes in the network. Finally we presented four heuristics which could be used in lieu of the optimal algorithm to obtain solutions close to the optimal solution.

Table 2.1 Algorithm

```
begin
  for each node j ∈ V,
    Construct_Auxiliary_Graph(G_j),
    //G_j = (V, E_j) is constructed such that E_j consists
    //of only those edges that are on those shortest paths
    //from all nodes i, i ∈ V and i ≠ j.
  end for
  C^K = Get_All_Combinations(N,K)
  //C^K = {C_1^K, C_2^K, ...} is the set of all combinations
  //of K converters on the set of N nodes.
  for each C_p^K in C^K
    Γ(C_p^K) = 0
  end for
  for each graph G_j,
    I ← φ, O ← φ
    // I and O denote the set of inner and outer nodes
    // respectively (initially null) for each node x in G_j,
      if (indegree(x) = 0) OR (outdegree(x) = 0) then
        O ← O ∪ {x}
      else
        I ← I ∪ {x}
      end if
    end for
    // |I| & |O| denote the no. of inner & outer nodes
    // respectively
    lower_limit = max{0, K − |O|}
    higher_limit = min{|I|, K}
    for m = lower_limit to higher_limit
      E^m = Get_All_Combinations(I,m)
      //E^m = {E_1^m, E_2^m, ...} is the set of all combinations
      // of m converters on the set of I nodes.
      D^{K−m} = Get_All_Combinations(O,K − m)
      //D^{K−m} = {D_1^{K−m}, D_2^{K−m}, ...} is the set
      //of all combinations of K − m converters
      //on the set of O nodes.
      for each E_i^m ∈ E^m
        Γ_j(E_i^m) = Get_Blocking_Performance(E^m,)
        for each D_n^{K−m} ∈ D^{K−m}
          C_temp^K =Combination(E_i^m, D_n^{K−m})
          //The above function denotes the union of the
          //combination of nodes in E_i^m and D_n^{K−m}
          Γ(C_temp^K) = Γ(C_temp^K) + Γ_j(E_i^m)
        end for
      end for
    end for
  end for
  C_opt = C_n^K such that Γ(C_n^K) is Min_∀p{Γ(C_p^K}
  // C_opt denotes the optimal placement combination.
end.
```

Table 2.2 Shortest Path Information for Network Shown in Fig. 2.1

From B to A : $B \rightarrow A$	From D to C : $D \rightarrow C$
From C to A : $C \rightarrow A$	From E to C : $E \rightarrow C$
From D to A : $D \rightarrow B \rightarrow A$	From A to D : $A \rightarrow C \rightarrow D$
From E to A : $E \rightarrow C \rightarrow A$	From B to D : $B \rightarrow D$
From A to B : $A \rightarrow B$	From C to D : $C \rightarrow D$
From C to B : $C \rightarrow B$	From E to D : $E \rightarrow D$
From D to B : $D \rightarrow B$	From A to E : $A \rightarrow C \rightarrow E$
From E to B : $E \rightarrow D \rightarrow B$	From B to E : $B \rightarrow D \rightarrow E$
From A to C : $A \rightarrow C$	From C to E : $C \rightarrow E$
From B to C : $B \rightarrow C$	From D to E : $D \rightarrow E$

Table 2.3 Blocking Performance for Different Auxiliary Graphs and Total Blocking Performance for the Network

Combi-nation	Blocking Performance					
	G_A	G_B	G_C	G_D	G_E	Overall Network
(A,B)	0.000201	0.000259	0.000069	0.000249	0.000341	0.001119
(A,C)	0.000264	0.000259	0.000069	0.000109	0.000201	0.000902
(A,D)	0.000341	0.000119	0.000069	0.000249	0.000264	0.001042
(A,E)	0.000341	0.000259	0.000069	0.000249	0.000341	0.001259
(B,C)	0.000124	0.000259	0.000069	0.000109	0.000201	0.000762
(B,D)	0.000201	0.000119	0.000069	0.000249	0.000264	0.000902
(B,E)	0.000201	0.000259	0.000069	0.000249	0.000341	0.001119
(C,D)	0.000264	0.000119	0.000069	0.000109	0.000124	**0.000684**
(C,E)	0.000264	0.000259	0.000069	0.000109	0.000201	0.000902
(D,E)	0.000341	0.000119	0.000069	0.000249	0.000264	0.001042

Table 2.4 Optimal Converter Placement for the Bi-directional Path(5 nodes) with uniform node-pair loads $\lambda = 0.1$ &$F = 3$. using correlation and independence models for path blocking

K	Correlation Model		Independence Model	
	Optimal Placement	Blocking Probability	Optimal Placement	Blocking Probability
1	3	4.563072e-05	3	2.696702e-05
2	(2,3) or (3,4)	4.382560e-05	(2,3) or (3,4)	1.923167e-05
3	(2,3,4)	4.201963e-05	(2,3,4)	1.149625e-05

Table 2.5 Optimal Placement in a Bi-directional Path of 10 nodes with uniform link loads $\rho = 0.05$ &$F = 3$.

K	Optimal Placement	Blocking Probability	Algorithm Efficiency (%)
1	(5) or (6)	0.002414	18
2	(4,7)	0.001490	32
3	(3,5,7) or (4,6,8)	0.001035	42
4	(3,5,6,8)	0.000789	48
5	(3,5,6,7,8) or (3,4,5,6,8)	0.000647	50
6	(3,4,5,6,7,8)	0.000505	48
7	(3,4,5,6,7,8,9) or (2,3,4,5,6,7,8)	0.000410	42
8	(2,3,4,5,6,7,8,9)	0.000315	32

Table 2.6 Optimal Placement in a 4 x 4 Mesh-Torus of 16 nodes with uniform node-pair loads $\lambda = 0.1$ &$F = 5$. (For $K = 6$ and $K = 7$ there are a total of 20 and 16 optimal placement combinations. Due to space constraints, we just list one for each)

K	Optimal Placement	Blocking Probability	Algorithm Efficiency (%)
1	(6,7,10,11)	0.010481	50
2	(6,11) or (7,10)	0.008345	75.83
3	(6,10,11) or (6,7,11) or (7,10,11) or (6,7,10)	0.007012	88.57
4	(6,7,10,11)	0.005678	94.56
5	(6,7,10,11) & any one of (2,3,5,8,9,12,14,15)	0.004916	97.25
6	(5,6,7,8,10,11),...	0.004154	98.41
7	(5,6,7,8,10,11,15), ...	0.003392	98.88
8	(2,6,7,8,9,10,11,15) or (3,5,6,7,10,11,12,14)	0.002630	99.01

Table 2.7 Optimal Converter Placement in the NSFNET(14 nodes) with uniform node-pair loads $\lambda = 0.1$ &$F = 5$.

K	Optimal Placement	Blocking Probability	Algorithm Efficiency (%)
1	(4)	0.014554	52.04
2	(4,6)	0.010329	77.70
3	(4,6,8)	0.007436	89.72
4	(4,6,8,10)	0.005742	95.05
5	(4,5,6,8,10)	0.004698	97.30
6	(4,5,6,8,9,10)	0.003722	98.17
7	(2,4,5,6,8,9,10)	0.002777	98.40

Table 2.8 Node weights obtained using heuristics in a Bidirectional Path of 10 nodes with uniform link loads $\rho = 0.05$

Node	PI	PLI	TPLP	IN
1	0	0	0.000000	0
2	16	88	0.655000	9
3	28	154	1.010000	9
4	36	198	1.215000	9
5	40	220	1.320000	9
6	40	220	1.320000	9
7	36	198	1.215000	9
8	28	154	1.010000	9
9	16	88	0.655000	9
10	0	0	0.000000	0

Table 2.9 Node weights obtained using heuristics in a 4×4 Mesh-Torus of 16 nodes with uniform node-pair loads $\lambda = 0.1$.

Node	PI	PLI	TPLP	IN
1	9	24	2.400000	3
2	17	48	4.800000	11
3	17	48	4.800000	11
4	9	24	2.400000	3
5	17	48	4.800000	3
6	25	72	7.200000	11
7	25	72	7.200000	11
8	17	48	4.800000	3
9	17	48	4.800000	3
10	25	72	7.200000	11
11	25	72	7.200000	11
12	17	48	4.800000	3
13	9	24	2.400000	3
14	17	48	4.800000	11
15	17	48	4.800000	11
16	9	24	2.400000	3

Table 2.10 Node weights obtained in the NSFNET(14 nodes) with uniform node-pair loads $\lambda = 0.1$

Node	PI	PLI	TPLP	IN
1	12	32	3.200000	6
2	14	38	3.800000	6
3	14	38	3.800000	6
4	25	69	6.900000	9
5	20	54	5.400000	6
6	34	90	9.000000	10
7	3	7	0.700000	3
8	21	57	5.700000	7
9	16	42	4.200000	6
10	24	62	6.200000	8
11	3	7	0.700000	3
12	14	36	3.600000	6
13	8	20	2.000000	4
14	0	0	0.000000	0

CHAPTER 3. Traffic Grooming in Optical Networks

3.1 Introduction

While data traffic in ultra-long-haul WDM networks is usually characterized by large, homogeneous data flows, wide-area and metropolitan area WDM networks have to deal with dynamic, heterogeneous service requirements. In such WAN and MAN networks, equipment costs increase if separate wavelengths are used for each individual service. Moreover while each wavelength still has transmission capacity at gigabit per second rates (eg. OC-48 or OC-192 and on to OC-768 in the future), users may require connections at rates that are lower than the full wavelength capacity. In addition, for networks of practical size, the number of available wavelengths is still lower by a few orders of magnitude than the number of source to destination connections that need to be made. Hence, to make the network viable and cost-effective, it must be able to offer sub-wavelength services and must be able to pack these services efficiently onto the wavelengths. These sub-wavelength services, henceforth referred to as *low-rate traffic streams*, can vary in range from say, STS-1 (51.84 Mbps) capacity up to the full wavelength capacity. Such an act of multiplexing, demultiplexing and switching of lower-rate traffic streams onto high capacity lightpaths is referred to as *traffic grooming*. WDM networks offering such sub-wavelength low-rate services are referred to as *WDM grooming networks*. Efficient traffic grooming improves the wavelength utilization and reduces equipment costs.

We illustrate the importance of efficient traffic grooming using a simple example, consider a WDM unidirectional path-switched ring (UPSR) with four nodes interconnected by fiber optic links with three wavelengths on each fiber. Each wavelength has capacity of 2.5 Gb/s (or OC-48 capacity). Suppose the traffic requirement is for 2 OC-12 circuits between each pair of nodes in the ring. Then the total traffic is 12 OC-12 circuits or 3 OC-48 rings (on 3

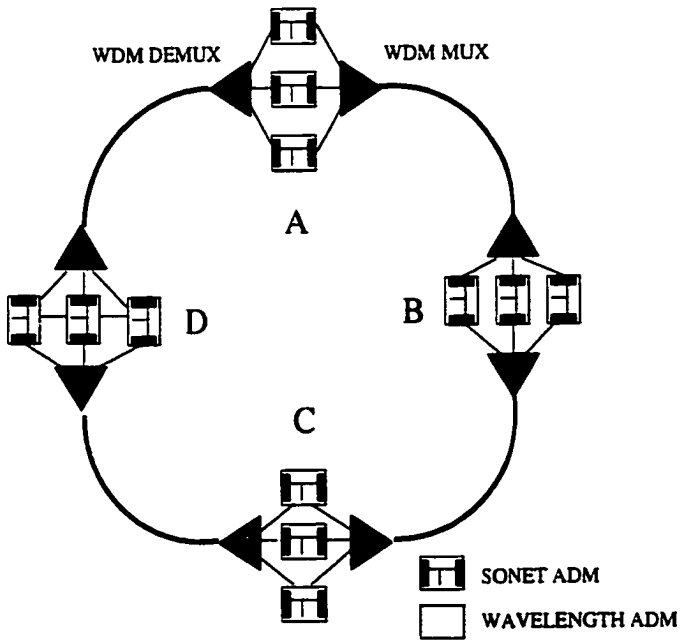

Figure 3.1 No Traffic Grooming

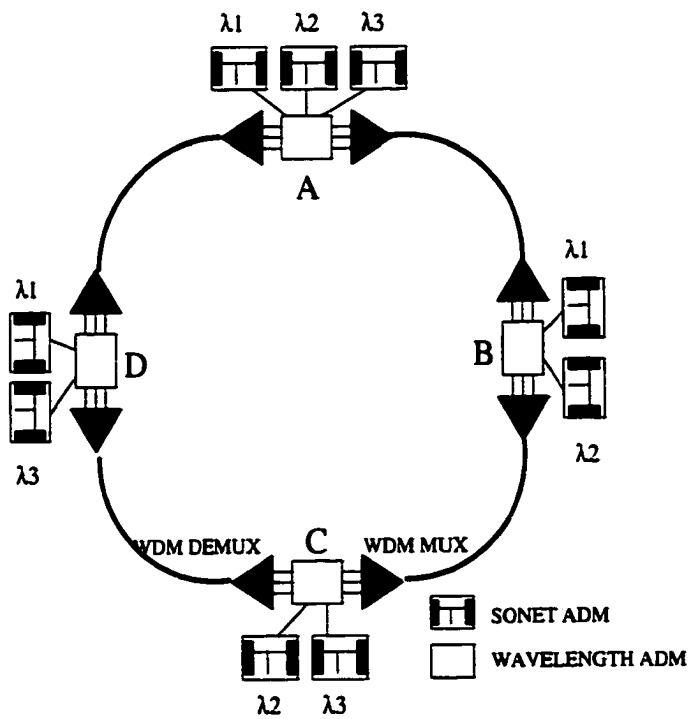

Figure 3.2 With Traffic Grooming

wavelengths). Consider the following two assignments of traffic on the wavelengths of the ring.

Assignment 1

$\lambda_1 = A \leftrightarrow D, C \leftrightarrow B$

$\lambda_2 = A \leftrightarrow B, C \leftrightarrow D$

$\lambda_3 = A \leftrightarrow C, D \leftrightarrow B$

Assignment 2

$\lambda_1 = A \leftrightarrow B, B \leftrightarrow D$

$\lambda_2 = A \leftrightarrow C, B \leftrightarrow C$

$\lambda_3 = A \leftrightarrow D, C \leftrightarrow D$

Assignment 1 of the traffic to wavelengths would result in each node in the ring requiring a SONET ADM for each wavelength requiring a total of 12 SONET ADMs. This is equivalent to that number of SONET ADMs required in a point-to-point WDM ring (Figure 3.1 to support the same traffic. On the other hand, in assignment 2, we groom the traffic efficiently so that only two SONET ADMs are needed at three nodes (with the fourth node having three SONET ADMs) in the ring, Figure 3.2 giving a total requirement of only 9 SONET ADMs. In addition, we can also show that the minimum number of ADMs is not necessarily achieved with the minimum number of wavelengths. Consider a 9-node WDM/SONET Bidirectional Line Switched Ring (BLSR) with nodes numbered A to I in which two different routing and wavelength assignment (RWA) algorithms have been used to route a common set of demands. Let the set of traffic demands be $A \leftrightarrow B, A \leftrightarrow C, B \leftrightarrow C, D \leftrightarrow E, E \leftrightarrow F, F \leftrightarrow D, G \leftrightarrow H, H \leftrightarrow I, I \leftrightarrow G$ Further assume each traffic demand asks for a full wavelength capacity.

RWA Algorithm 1

$\lambda_1 = A \leftrightarrow B, B \leftrightarrow C, C \leftrightarrow A$ (3 ADMs)

$\lambda_2 = D \leftrightarrow E, E \leftrightarrow F, F \leftrightarrow D$ (3 ADMs)

$\lambda_3 = G \leftrightarrow H, H \leftrightarrow I, I \leftrightarrow G$ (3 ADMs)

RWA Algorithm 2

$$\lambda_1 = B \leftrightarrow C, C \leftrightarrow A, E \leftrightarrow F, F \leftrightarrow D, G \leftrightarrow H \text{ (8 ADMs)}$$

$$\lambda_2 = A \leftrightarrow B, D \leftrightarrow E, H \leftrightarrow I, I \leftrightarrow G \text{ (7 ADMs)}$$

The first RWA algorithm uses 9 ADMs but 3 wavelengths to route the traffic demands but the second RWA algorithm uses 15 ADMs but only 2 wavelengths to route the traffic demands. This shows the RWA algorithm that uses additional capacity uses lesser number of ADMs while that which uses additional ADMs routes the traffic demands in lesser number of wavelengths. From this we can conclude that traditional RWA algorithms

In such WDM grooming networks, each lightpath typically carries many multiplexed lower-rate traffic streams. The act of multiplexing and demultiplexing of traffic streams is performed by the OADMs at the nodes. The OADMs add/drop the wavelength for which grooming is needed and electronic ADMs then multiplex or demultiplex the traffic streams onto the wavelength. The act of switching the traffic streams from one wavelength to another is performed by the crossconnect at the nodes. That is, a traffic stream occupying a set of time slots on a wavelength on a fiber can be switched to a different set of time slots on a different wavelength on another fiber. However, this *traffic stream switching* capability comes at the cost of increased crossconnect complexity. In addition to the space-switching of wavelengths, the crossconnect may have to be provided with wavelength conversion and time-slot interchange equipment. An example of a commercial grooming switch is CIENA's *Multiwave Coredirector* switch which offers non-blocking switching and grooming traffic streams from STS-1 up to STM - 64. Currently, all-optical wavelength conversion and all-optical time-slot interchange devices are still not commercially available and it is more attractive to use electronic methods of implementation to incorporate these features into the network. In the future, it may be possible to perform all-optical traffic grooming. Such all-optical traffic grooming networks may prove to be more cost-effective and manageable than their electronic counterparts.

3.2 Grooming Networks Model

We consider a WDM network with network nodes of two types: *Wavelength-Selective Crossconnect (WSXC)* nodes and *Wavelength-Grooming Crossconnect (WGXC)* nodes. Figures 3.3 and 3.4 show the node architecture of a WSXC and WGXC node respectively. These networks nodes are interconnected by fiber-optic links which can be either bi-directional or unidirectional. WSXC nodes have OXCs, which space-switch full wavelengths from an input port to an output port, and OADMs, which groom the traffic streams onto the added/dropped wavelengths. However, WSXC nodes cannot switch traffic streams between wavelengths. WGXC nodes, in addition to having the functionality of a WSXC, are capable of time-slot interchange and can switch lower-rate traffic streams from a set of time slots on one wavelength on an input port to a different set of time slots on another wavelength on an output port. We assume that this switching is fully non-blocking and can be performed for all wavelengths from any input port to any output port. Hence, full wavelength conversion capability is implicitly available at the WGXC node. Such a node is said to have *full grooming* capability. If switching of lower-rate traffic streams is performed only on a restricted number of wavelengths, then the node is said to have *limited grooming capability*. We assume that all the WGXC nodes in our network are provided with full grooming capability. A network in which only some of the nodes of the network are WGXC nodes is referred to as a *sparse grooming network*. On the other hand, a network with only WSXC nodes and no WGXC nodes is referred to as a *constrained grooming network*, since grooming is constrained to the ADMs at the nodes.

3.2.1 Connection Setup and Release

The connection setup and release procedure in traffic grooming networks is different from the lightpath establishment process of conventional wavelength routing networks. A low-rate traffic session is routed along a path traversing through intermediate WSXC and WGXC nodes between the source and destination. If the path traverses through one or more intermediate WGXC nodes then the traffic session involves more than one lightpath. Lightpaths between the source, destination or intermediate WGXC nodes satisfy the wavelength continuity constraint,

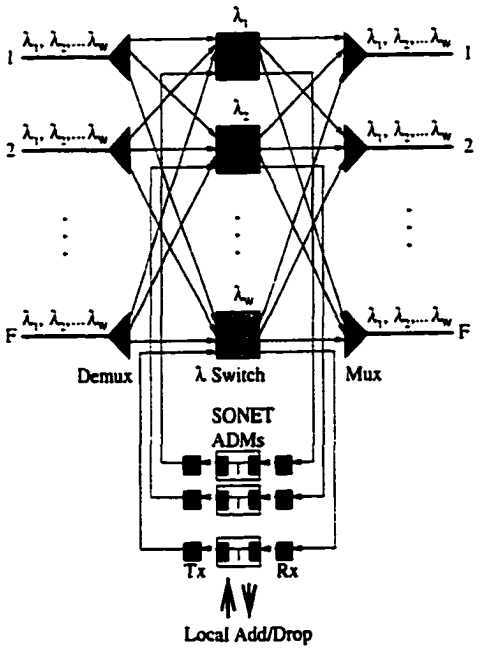

Figure 3.3 Wavelength Selective Crossconnect Node

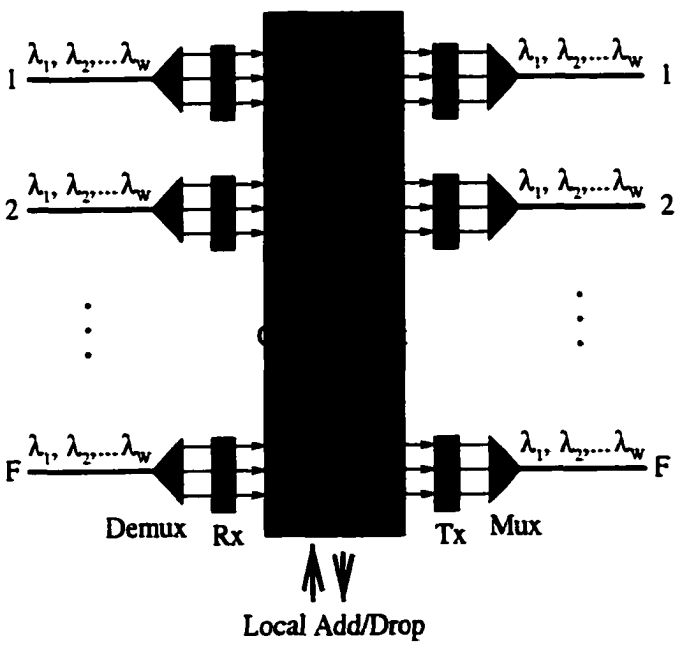

Figure 3.4 Wavelength Grooming Crossconnect Node

that is, the traffic stream occupies the same wavelength on all the links of the path between the source, destination or intermediate WGXC nodes. However lighpaths between WGXC nodes can be routed on different wavelengths. In this manner, each lightpath typically carries many multiplexed lower-speed traffic streams. During connection setup, it should be confirmed whether the lightpaths, that have been established earlier, have the required amount of capacity before they can be used to accommodate the new traffic session. Consider an example of a sub-network, shown in Figure 3.5, which can be a part of a bigger mesh network. Assume a single wavelength is currently available on the path from A to F. Let the capacity of the wavelength be C. Further assume that all the nodes on the path are WSXC nodes. Suppose a request arrives for a connection from node B to E for a line capacity of $C/4$. This is established immediately on the available wavelength by configuring the OADMs at nodes B and E, and by configuring the OXCs at nodes C and D. Note that we add/drop the wavelength only at nodes B and E, and not at nodes C and D. Let a second request arrive for a connection from node A to node F for a line capacity of $C/4$. This is also established on the same wavelength by setting up lightpaths from A to B and from E to F, and by using the same lightpath on the wavelength between B to E that was established for the first connection. In this process, the first traffic stream is not disturbed. The wavelength is now add/dropped at four nodes, namely, A, B, E and F. Let a third request arrive for a connection from A to G for line capacity $C/4$. However, this connection cannot be established on the wavelength and will be blocked. The reason is, the path for the third connection request from A to G deviates away from the path of the lightpath on the wavelength and node D is only a WSXC node.

Let a fourth request arrive for a connection from node C to D for a line capacity of $C/4$. At this point, we have two options. (a) We can assume any lightpath that has been established should not be disturbed. Therefore, the traffic stream cannot be established on the same wavelength and is blocked. (b) However, if a temporary disturbance to the lightpath is acceptable. We can establish the third call on the same wavelength by add/dropping the wavelength at node C and D. The lightpath is now split into three parts. This temporary disturbance can be made possible by the presence of fast OADMs and fast reconfigurable OXCs at the nodes.

For our network model, we assume the latter case (option *b*) and assume the nodes have fast OADMs and OXCs. On the other hand, if nodes C and D happen to be WGXC nodes, then it is possible to satisfy all the call requests.

When a call leaves the network, the lightpaths that are used to hold the traffic connection release the capacity used by the traffic stream. However, the lightpaths themselves might continue to operate over the wavelengths since they might have other traffic streams multiplexed over them. If the traffic stream was the sole one to have used the lighpath, then the lightpath itself can be released and the wavelengths on the links can be freed.

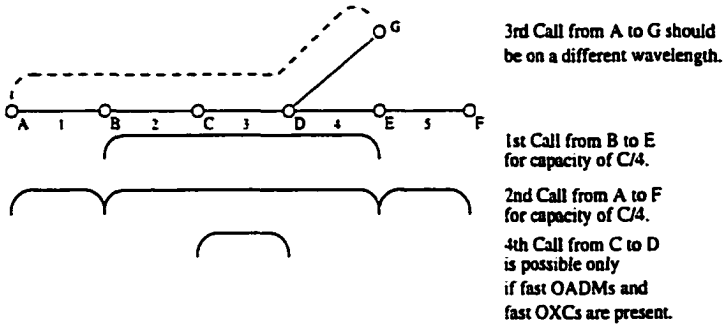

Figure 3.5 Network Example

3.3 Network Simulation and Traffic Assumptions

The following assumptions are used in our WDM grooming network simulation model:

1. The network consists of V nodes with L links. Each link is bidirectional and consists of a pair of fibers with W wavelengths each in each direction.

2. Each wavelength has capacity C and has a line-speed indicated by a parameter g (C is assumed to be divisible by g) referred to as the *granularity*. A lightpath that traverses a wavelength can support a maximum of g traffic streams. In other words, at most g low-rate traffic streams can be multiplexed onto the lightpath. The capacity of a traffic stream can vary from C/g(line-speed 1) to the full wavelength capacity C (line-speed g). We define a *line-speed* j traffic stream as a traffic stream occupying a capacity jC/g on the lightpath.

3. Calls arrive at a node according to a Poisson process with rate λ. Each call is equally likely to be destined to any of the remaining $V-1$ nodes. The arrival rate of calls λ_{sd} for a node pair (s,d) is then $\lambda/(V-1)$. Each call can request a line-speed j, where $1 \leq j \leq g$. The arrival rate of calls at a source-destination pair and requesting a line-speed j is $\lambda_{sd}(j)$. Each set of calls of line-speed j from a source to a destination requests equal total capacity of calls in its line speed class. In other words, if the combined capacity of calls to a node pair is say, Kg, then each line-speed class contributes a capacity of K through its call arrivals. For example, line-speed 1 traffic will have K call arrivals, line-speed 2 will have $K/2$ call arrivals and similarly line-speed j traffic will have K/j call arrivals. Therefore, the probability, r_j that a call is of line-speed j is

$$r_j = \frac{1/j}{\sum_{i=1}^{g} 1/i} \tag{3.1}$$

The expected value of j, $E\{j\}$ is then given by

$$E\{j\} = \sum_{j=1}^{g} j r_j = \frac{g}{\sum_{i=1}^{g} 1/i} \tag{3.2}$$

The *arrival rate per unit line-speed per s-d pair* is now defined as

$$\hat{\lambda_{sd}} = \lambda_{sd} E\{j\} \tag{3.3}$$

Here the term "unit line-speed" refers to the capacity of the lowest granularity traffic stream that can be groomed on to the lightpath. $\hat{\lambda_{sd}}$ is essentially the arrival rate of calls at s-d pairs in the network if all call requests are of the lowest granularity, i.e., of line-speed 1.

4. We assume fixed path routing i.e., each call uses a prespecified path. If the path cannot accommodate the call, then the call is assumed to be blocked and is lost.

5. Call requests cannot be split up among wavelengths on a link. Specifically, we assume that a traffic request can occupy only one wavelength on a link in the path. As explained in the previous section, we assume that fast OADMs and fast reconfigurable OXCs are

available in the nodes. Hence a lightpath can be disturbed to multiplex a traffic stream into it.

6. The duration of each call request is assumed to be exponentially distributed with unit mean.

7. We also assume that there are enough OADMs, i.e., receivers/transmitters at the nodes to handle the traffic that originates from the nodes. The traffic from a node is then limited by the degree of the node, the number of wavelengths on the fibers and the capacity of the wavelengths.

3.4 Traffic Grooming in WDM Rings - A Literature Review

Most of the work in the literature on traffic grooming has been concentrated on providing efficient networks designs in SONET/WDM rings for improving the overall network cost. In a SONET/WDM ring network, each lightpath carries several low-rate traffic streams. The nodes in the ring network are equipped with OADMs and SONET ADMs. These OADMs terminate only those lighpaths whose traffic streams need to source or sink at the node. The remaining lighpaths optically passthrough the node without any processing. The terminated lightpath are converted to electronic form and are each processed by a SONET ADM. The SONET ADM adds or drops low-rate traffic streams from the channel stream and sends the channel back to the OADM in the optical form. The OADM then multiplexes the wavelength with other wavelengths in the outgoing fiber. Current research studies have concentrated on reducing the higher-layer electronic processing equipment (SONET ADMs) whose cost dominates over the cost of the optical equipment (number of wavelengths) in the WDM ring network. Research studies on traffic grooming can be grouped based on whether they address static or dynamic traffic.

3.4.1 Static Traffic Grooming

The static traffic grooming problem can be defined as follows: Given the traffic demand set of low-rate connections needed between the node pairs on the ring, assign the traffic to wavelengths such that the number of SONET ADMs are minimized. Since we are establishing a set of lightpaths on the WDM network, this problem is a special instance of the virtual topology design problem for which, in certain circumstances, a solution can be found.

Gerstel, Ramaswami and Sasaki discuss traffic grooming for different ring architectures in [41]. They assume that electronic processing equipment at the nodes included SONET ADMs and digital crossconnect systems (DCS) for crossconnecting and switching traffic streams from one wavelength to another. In the worst cost scenario, all the nodes in the ring network are equipped with DCSs and each link has one-hop lightpath to the neighboring nodes. This ring called a *point-to-point WDM ring* (PPWDM), uses the minimum number of wavelengths but is the most expensive in terms of electronic processing cost. On the other extreme, a *fully-optical ring* has no electronic cost since all the traffic streams are directly connected between nodes through connecting lightpaths. However, it requires the maximum number of wavelengths. A *hub ring* is one which has a node designated as a hub. The hub is the only node to contain a DCS and has lightpaths directly connecting it to all other nodes. This ring is wide-sense nonblocking which implies that it can also support dynamic traffic. Although this ring has the least non-zero electronic cost, it still requires many wavelengths. A *double hub ring* has two hubs with lightpaths connecting them to all other nodes. Although this ring is rearrangeably nonblocking, it is reasonably efficient in the number of wavelengths and the electronic cost. A *hierarchical* ring is composed of two PPWDM subrings and performs as well as a PPWDM ring at the expense of a few extra wavelengths. Gerstel et al. [42] further analyzed traffic grooming issues in UPSR and BLSR WDM rings and established lower bounds on the number of ADMs in UPSR and BLSR WDM rings.

Chiu and Modiano in [43] develop algorithms to groom traffic in unidirectional SONET/WDM ring networks. It is shown that the traffic grooming problem is NP-complete by transforming the bin-packing problem (which is already known to be NP-complete) into the traffic groom-

ing problem in polynomial time. They first consider the traffic grooming problem for a ring with uniform, all-to-one node traffic. They also specify lower bounds on the number of ADMs required for uniform, all-to-all node traffic and provided heuristics which performed close to the lower bound. They also consider the distance-dependent traffic model here the amount of traffic between node pairs is inversely proportional to the distance separating them and provide lower bounds and heuristics for the minimum number of ADMs. They also consider a single-hub ring with a DCS at the hub and specified an optimal algorithm for the all-to-all uniform traffic case. Furthermore they prove that any solution not using a hub can be transformed into a solution with hub using fewer or same number of ADMs.

Zhang and Qiao in [44] consider the traffic grooming problem for both unidirectional and bidirectional SONET/WDM rings. They specify heuristics for uniform as well as non-uniform traffic. They split the problem into two phases. In the first phase, all the traffic demands are packed into as few circles as possible, where each circle has capacity equal to the tributary rate and contains nonoverlapping demands. In the second phase, multiple circles are groomed together so as to maximize the overlap of end nodes. An end node is a node that terminates a traffic connection in a circle. The maximization of the overlap of end nodes is reflected as a *minimization* in the number of SONET ADMs needed to satisfy the set of traffic demands. They specified an optimal circle construction algorithm for uniform traffic and heuristic for circle construction for non-uniform traffic. A generic circle grooming algorithm applicable to both uni-directional and bi-directional rings was also specified. A similar two-phase approach for grooming arbitrary traffic in BLSR rings was proposed by Wan et al. in [45]. In the first stage, they generate primitive rings from the traffic requests (which are denoted as arcs). The cost of each primitive ring is the number of nodes in it. The objective in this phase is to obtain a set of primitive rings such that the total cost of all primitive rings is minimum. In the next phase, the primitive rings are grouped together such that each group forms a logical SONET ring. The associated ADM cost of each group is the number of nodes contained in this group and the total ADM cost is the sum of all the groups' ADM costs. Since both these phases are NP-hard problems in themselves, heuristics are devised for the generation of primitive rings

and approximation algorithms are presented for optimal grooming of rings.

3.4.2 Dynamic Traffic Grooming

Most of the SONET traffic today is groomed and setup in a static scenario. It is provisioned once and remains in place for a long period of time. However, in the future, IP is likely to become the prevailing protocol over WDM and SONET ADMs may no longer be required to pack traffic onto the wavelengths. In this scenario, it is the responsibility of the IP layer to effectively multiplex traffic onto wavelengths. These IP-over-WDM networks are likely to be arranged in a mesh topology rather than a ring. More importantly, the traffic requirements of IP are bound to change much faster than the legacy traffic based on SONET. In such a scenario, it is important that dynamic traffic grooming is employed so that the networks are able to efficiently accommodate changes in traffic. Berry and Modiano in [46] focussed on minimizing equipment costs in such a dynamic traffic grooming scenario for SONET/WDM rings. They considered the traffic grooming problem for a class of traffic called *t-allowable traffic*. In such a traffic model, each node is capable of sourcing at most t bi-directional circuits at a given time. They established lower bounds on the number of ADMs needed to support such traffic and provide necessary and sufficient conditions that a network must satisfy to support such traffic. These conditions are used to specify algorithms for assigning ADMS to the nodes to accommodate any t-allowable traffic in a non-blocking way.

CHAPTER 4. Performance Analysis of Traffic Grooming in Optical Networks

4.1 Introduction

The focus of this chapter is to provide an analytical framework and obtain some insight on how traffic grooming affects the blocking performance in different network topologies. Specifically we study and compare the performance of constrained and sparse grooming networks. The first corresponds to the case where grooming is performed only at the OADMs. The second type of network corresponds to the case where, in addition to grooming at the OADMs, the crossconnects at some or all of the nodes are provided with traffic stream switching capability.

As described in the previous chapter, current research has focussed on minimizing electronic equipment costs and providing efficient network designs in WDM rings. However, analytical models and network blocking performance for WDM grooming networks has received very little attention in the literature thus far. On the other hand, a lot of work has been done in studying the call blocking performance of wavelength-routed networks using different routing and wavelength assignment schemes. It has been established that wavelength conversion, that is, the ability of a routing node to convert one wavelength to another, plays an important role in improving the blocking performance. Wavelength conversion for WDM networks was proposed by Lee and Li [28] and it was shown that wavelength converters reduce wavelength conflicts and improve the performance by reducing the blocking probability. Lower bounds on the blocking probability for an arbitrary network for any routing and wavelength assignment algorithm were derived by Ramaswami and Sivarajan [14]. It was further shown that use of wavelength converters resulted in a 10 to 40 percent increase in wavelength reuse. Birman [32] proposed a reduced load approximation scheme to calculate the blocking probabilities for their optical

network model for two routing schemes: fixed routing and least-loaded routing. However, their model did not consider the load correlation between links. Barry and Humblet [20] proposed analytical models of networks, using fixed routing and random wavelength assignment, taking wavelength correlation into account. They also studied the effects of path length, switch size and hop number on the blocking probability in networks with and without wavelength conversion.

Subramaniam et al. [33] studied sparse wavelength conversion and its effects on blocking performance. Their analytical model takes into account both wavelength correlation and the dynamic nature of the traffic. Sridharan and Sivarajan [47] presented a new analytical technique based on the inclusion-exclusion principle for networks with no wavelength conversion and random wavelength assignment. Their model improves on Birman's model in that it is independent of hop-length and scales only with the capacity of the link. While the above models concentrated on fixed routing, models based on Least Loaded Routing [48] and Alternate Routing [23] have also been studied. Analytical models [23],[17] for first-fit wavelength assignment scheme, based on overflow traffic model, have also been proposed. Karasan and Ayanoglu [19] provide a review of the various schemes and their associated analytical models.

There has also been considerable interest in studying the performance of networks which utilize both TDM and WDM. Sabry and Midwinter [49] proposed preliminary models for their multiwavelength TDM network in which time-slots on a wavelength could be dedicated to each source-destination pair. Yates [50] studied the performance improvements offered by wavelength converters and time-slot interchangers in shared-wavelength TDM networks and dedicated-wavelength TDM networks. However, the analysis was restricted to the case where all calls have uniform bandwidth requirements and occupied one time slot on a wavelength.

In this chapter, we provide an analytical framework using which the blocking performance of grooming networks can be studied. Our model takes into account the capacity distribution on a wavelength and the correlation on neighboring links given that incoming calls are of varying capacity. Previous research has concentrated on the case where the wavelength or a single time slot on a wavelength is considered as the basic unit of bandwidth. We address

the performance differences obtained when grooming is restricted at the OADMS and the case where traffic stream switching can be performed between wavelengths.

4.2 Analytical Models for Constrained Grooming Networks

In this section, we develop approximate analytical models with reasonable computational requirements for constrained grooming networks. The analytical models provide the blocking probabilities of calls for different capacities and can be applied to networks with arbitrary topologies. We use the network and traffic assumptions specified in Chapter 3, Sections 3.2 and 3.3. In addition, we restrict ourselves to the random wavelength assignment (RWA) strategy for our analytical model. In this strategy, the wavelength to be assigned to a call is chosen randomly from the set of available wavelengths on the path. Other algorithms such as First-Fit and Max-Sum provide better performance. However, they are considerably more difficult to analyze.

4.2.1 Analysis for a Single Wavelength Link

Consider a single link, single wavelength system with wavelength capacity, C and granularity g. Let $\lambda_l(j)$ be the link arrival rates of traffic streams of line-speed j (capacity jC/g). Let n_j be the number of traffic streams of line-speed j multiplexed into the wavelength. The wavelength can contain $(n_1, n_2, ..., n_j, ..., n_g)$ traffic streams of line-speeds from 1 to g provided:

$$0 \leq n_j \leq \lfloor \frac{g}{j} \rfloor \tag{4.1}$$

$$\sum_{j=1}^{g} j n_j \leq g \tag{4.2}$$

Let the call holding time be exponentially distributed with parameter μ. We can model the above system as a Markov chain with a state space given by $(n_1, n_2, ..., n_j, ..., n_g)$ where $n = \sum_{j=1}^{g} n_j$ is the total number of calls in the system and values of n_j satisfy constraints (4.1) and (4.2). The generator matrix Q^* of the Markov process governing the system can be formed according to the following rules. For a state transition:

1. From state $(n_1, n_2, ..., n_j, ..., n_g)$ to state $(n_1, n_2, ..., n_j + 1, ..., n_g)$, provided constraints (4.1) and (4.2) are satisfied. We denote the arrival of a call of line-speed j and the transition rate is given by $\lambda_l(j)$.

2. From state $(n_1, n_2, ..., n_j, ..., n_g)$ to state $(n_1, n_2, ..., n_j - 1, ..., n_g)$ provided $n_j > 0$. We denote the departure of a call of line-speed j. The transition rate is given by $n_j\mu$.

3. The diagonal elements of the matrix are negative such that the sum of all the elements of any row in the matrix equals zero. Specifically their value is given by $-\lambda_s - n\mu$ where λ_s is the sum of only those λ_j rates, with valid single-call arrivals so that constraints (4.1) and (4.2) would not be violated.

4. For all other state transitions, the transition rate is zero.

The stationary probability vector X at an arbitrary time for the generator Q^* is the unique solution to the equations:

$$XQ^* = 0, Xe = 1. \tag{4.3}$$

where e is a column vector of 1s. Hence the elements of vector X are $x(n_1, n_2, ..., n_j, ..., n_g)$ which correspondingly provide the probability that the system is in state $(n_1, n_2, ..., n_j, ..., n_g)$ Once we calculate the steady-state probability vector X, we obtain the blocking probability $Q(j)$ of class-j traffic stream by

$$Q(j) = 1 - \sum_{i=0}^{g-j} X_c(i) \tag{4.4}$$

where $X_c(i)$ is the sum of only those probability values $x(n_1, n_2, ..., n_j, ..., n_g)$ of X such that the corresponding state $(n_1, n_2, ..., n_j, ..., n_g)$ yields a capacity of i, i.e., $\sum_{k=1}^{g} kn_k = i$.

4.2.2 Analysis of Single Wavelength Two-Hop Path

Consider the two-hop, single wavelength system as shown in Figure 4.1. Let $\lambda_N(j)$ be the arrival rates of traffic streams of line-speed j using only link A, i.e., the traffic stream enters

at node 1 and leaves at node 2. We denote such traffic streams as type-N traffic streams. Let $\lambda_M(j)$ be the arrival rates of traffic streams of line-speed j using only link B,i.e., the traffic stream enters at node 2 and leaves at node 3. We denote such traffic streams as type-M traffic streams. Let $\lambda_L(j)$ be the arrival rates of traffic streams of line-speed j which use both links A and B, i.e. it denotes the arrival of traffic that enters at node 1, continues through node 2 and leaves at node 3. We denote such traffic streams as type-L traffic streams. Type-L traffic streams are not a part of type-N and type-M traffic streams.

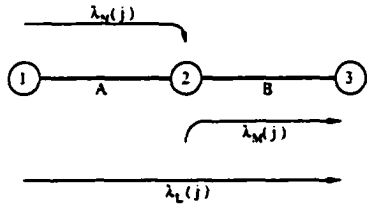

Figure 4.1 A two-hop single-wavelength system

Let n_j and m_j be the number of traffic streams of line-speed j multiplexed onto the wavelength at link A and B respectively. Let l_j correspond to the number of traffic streams of line speed j which continue on both links A and B. Hence the wavelength at link A contains $N = (n_1, n_2, ..., n_j, ..., n_g)$ and $L = (l_1, l_2, ..., l_j, ..., l_g)$ traffic streams and link B contains $M = (m_1, m_2, ..., m_j, ..., m_g)$ and $L = (l_1, l_2, ..., l_j, ..., l_g)$ traffic streams provided:

$$
\begin{aligned}
0 \leq n_j, m_j, l_j &\leq \lfloor \frac{g}{j} \rfloor \\
0 \leq \sum_{i=1}^{g} j.n_j + \sum_{k=1}^{g} k.l_k &\leq g \\
0 \leq \sum_{i=1}^{g} j.m_j + \sum_{k=1}^{g} k.l_k &\leq g
\end{aligned} \tag{4.5}
$$

Let the call holding time be exponentially distributed with parameter μ. We can model the above system as a Markov process with a state space given by $(n_1, n_2, ..., n_j, ..., n_{g-1}, n_g, m_1, m_2, ..., m_j, ...m_{g-1}, m_g, l_1, l_2, ..., l_j, ..., l_{g-1}, l_g)$. Let $n = \sum_{j=1}^{g} n_j$, $m = \sum_{j=1}^{g} m_j$ and $l = \sum_{j=1}^{g} l_j$ be the total number of traffic streams of type-N, type-M and type-L respectively with the state

space variables satisfying constraints in (4.5). The generator matrix Q^* of the Markov process governing the system can be formed according to the following rules. For a state transition:

1. From state $(n_1, n_2, ..., n_j, ..., n_g, M, L)$ to state $(n_1, n_2, ..., n_j + 1, ..., n_g, M, L)$ provided constraints in (4.5) are satisfied, we denote the arrival of a type-N call of line-speed j. The transition rate is given by $\lambda_N(j)$. Similar transition rates apply for type-M and type-L call arrivals.

2. From state $(n_1, n_2, ..., n_j, ..., n_g, M, L)$ to state $(n_1, n_2, ..., n_j - 1, ..., n_g, M, L)$ provided $n_j > 0$, we denote the departure of a type-N call of line-speed j. The transition rate is given by $n_j\mu$. Similar transition rates apply for type-M and type-L call departures.

3. The diagonal elements of the matrix are negative such that the sum of all the elements of any row in the matrix equals zero. Specifically their value is given by $-\lambda_s - (n+m+l)\mu$ where λ_s is the sum of only those λ_j rates for all type-N, M and L traffic streams, with valid single-call arrivals that will not violate constraints in (4.5).

4. For all other state transitions, the transition rate is zero.

The stationary probability vector for the two-hop path Y at an arbitrary time for the generator Q^* is the unique solution to the equations:

$$YQ^* = 0, Ye = 1. \tag{4.6}$$

The elements of vector Y, $y(n_1, n_2,..., n_j,..., ,n_g, m_1, m_2,..., m_j,...,, m_g, l_1, l_2,..., l_j, ...,,l_g)$ give the probability that the system is in the corresponding state specified in the parentheses. The blocking probabilities $Q_N(j)$, $Q_M(j)$ and $Q_L(j)$ of traffic streams of type-N, M and L respectively on the two-hop path can be obtained in a manner similar to (4.4).

4.2.3 Analysis for a Multi-Hop, Single Wavelength Path

In this subsection, we will specify two models to calculate the blocking probability on a multi-hop, single wavelength path (referred to as a wavelength-path). The first model based

on link independence, assumes the wavelength capacity distribution on the wavelength on a link is independent of that of neighboring links. In the second model, we consider wavelength capacity correlation between wavelengths on successive links of the path. We calculate the probability of blocking on a multi-hop single wavelength-path using the results for the two-hop single wavelength-path derived in the previous section.

4.2.3.1 Independence Model

In this model, we assume the load on the wavelengths of the link is independent of the loads of wavelengths on other links. The independence model has been shown to give valid estimates for densely connected network topologies or for networks with low end-to-end traffic loads. Consider a h hop wavelength-path $v_0, v_1, v_2, ..., v_{h-1}, v_h$ where $\lambda_l^{(i)}, 1 \leq i \leq h$, is the arrival rate at link (v_{i-1}, v_i). Using the procedure given in Section 4.2.1, we obtain the values of $Q_i(j)$ for the ith hop in the path. The end-to-end blocking probability $Q_{v_0 v_h}(j)$ that a class-j call is blocked on the path is simply given by the product form

$$Q_{v_0 v_h}(j) = 1 - (1 - Q_{v_0 v_1}(j))(1 - Q_{v_1 v_2}(j)) \\ ...(1 - Q_{v_{h-1} v_h}(j)) \tag{4.7}$$

However, the above model is inaccurate for sparse topologies and in case of high traffic on multihop calls. In this case, we go in for a wavelength correlation model.

4.2.3.2 Capacity Correlation Model

In this sub-section, we use a Markovian correlation model based on the wavelength capacity distribution to calculate the blocking probability. On this single wavelength-path, given the load of hop $1, 2, ..., i-1$, the load on hop i is dependent only the load on hop $i-1$. We consider a h hop path $v_0, v_1, v_2, ..., v_{h-1}, v_h$ from source v_0 to destination v_h. Let $\lambda_l^{(1)}, \lambda_l^{(2)}, ..., \lambda_l^{(h)}$ be the link arrival rates at hops $1, 2, ..., h$ respectively. Specifically, the calls corresponding to $\lambda_l^{(i)}$ at link i enter the path at node $i-1$ and leave at node i, where $1 \leq i \leq h$. Let $\lambda_s^{(1)}, \lambda_s^{(2)}, \lambda_s^{(3)}, ..., \lambda_s^{(h)}$ be the segment arrival rates at wavelength segments of length $1, 2, 3, ..., h$, respectively where each segment starts at the source node v_0. Specifically, calls corresponding to $\lambda_s^{(i)}$ for segment

i enter the path at the source node v_0 and leave the path at node i. It is to be noted, that $\lambda_s^{(1)}$, is the same as $\lambda_l^{(1)}$.

A call of line-speed j on this wavelength-path can be established if each link of the wavelength-path has adequate capacity to accommodate the call. Due to our correlation assumption, we can calculate the blocking probability of a call of line-speed j on the h-hop wavelength-path using the results from the two-hop path in the previous section. This is done as follows.

1. Divide the path into the following set of two hop paths,

$$\begin{aligned} &(v_0, v_1, v_2), (v_0, v_2, v_3), ..., \\ &(v_0, v_i, v_{i+1}), \quad 1 \leq i \leq h-1 \\ &..., (v_0, v_{h-2}, v_{h-1}), (v_0, v_{h-1}, d) \end{aligned} \tag{4.8}$$

2. For each two hop path, $(v_0, v_i, v_{i+1}), 1 \leq i \leq h-1$ in the above set, its associated arrival rates are $\lambda_N = \lambda_s^{(i)}$, $\lambda_M = \lambda_l^{(i+1)}$ and $\lambda_L = \lambda_s^{(i+1)}$.

3. Using the arrival rates, obtain the steady-state probability vector $X_i(N, M, L), 1 \leq i \leq (h-1)$ for each two-hop path (v_0, v_i, v_{i+1}), using the procedure described in the section 4.2.2.

4. For the given wavelength, now we calculate the end-to-end blocking probability $Q_{v_0 v_h}(j)$ of a call of line-speed j (or capacity jC/g) on the h-hop wavelength-path from v_0 to v_h as

$$\begin{aligned} Q_{v_0 v_h}(j) &= 1 - Pr\{\text{capacity } jC/g \text{ is available} \\ &\qquad \text{on the two hop path}(v_0, v_{h-1}, v_h)\} \\ &= 1 - Pr\{\text{cap. } jC/g \text{ is available on link } h| \\ &\text{cap. } jC/g \text{ is available on segment } (v_0, v_{h-1})\} \times \\ &Pr\{\text{cap. } jC/g \text{ is available on segment } (v_0, v_{h-1})\} \end{aligned}$$

The above formulation leads us to a recursive function by viewing the segment (v_0, v_{h-1}) as a two-hop path with the middle node as v_{h-2}. In general, a segment (v_0, v_{i+1}) can be viewed as a two-hop path with node v_i as the middle node. That is, we view the first i hops as the first hop and the $i+1$th hop as the second hop. Using the chain rule of probability, we have.

$$Pr\{jC/g \text{ is available on segment}(v_0, v_{i+1})\} =$$

$$\sum_{\forall valid\ N^i} \sum_{\forall valid\ L^i} \left\{ \sum_{\forall valid\ M^i} X^i(N^i, M^i, L^i) \times Pr\{\textit{capacity is available on segment } (s, v_i) | L^{i-1} = L^i \oplus N^i\} \right\} \tag{4.9}$$

$$\begin{aligned} 0 \le C_{N^i} + C_{L^i} \le g - c \\ 0 \le C_{M^i} + C_{L^i} \le g - c \\ 1 \le i \le (h-1) \end{aligned} \tag{4.10}$$

N^i, M^i and L^i are the set of N-type, M-type and L-type call vectors for the two-hop path of (v_0, v_i, v_{i+1}) respectively. For example, $X^i(N^i, M^i, L^i)$ gives the steady state probability values for the two hop system of (v_0, v_i, v_{i+1}) when the call combinations are N^i, M^i and L^i. The variables C_{N^i}, C_{M^i} and C_{L^i} in Eqn. 4.10 are the total capacity of N-type, M-type and L-type calls respectively on the two-hop path of (v_0, v_i, v_{i+1}). The *valid* vector combinations of N^i, M^i and L^i for Eqn. 4.9 are defined so that the inequalities in Eqn. 4.10. are satisfied.

The operation $L^{i-1} = L^i \oplus N^i$ is defined such that number of the calls, $l_j^{(i)}$, of capacity j, that use both the first and second links of the two hop path (v_0, v_i, v_{i+1}), and the number of calls, $n_j^{(i)}$, of capacity j that use only the first link of the two hop path (v_0, v_i, v_{i+1}), are added together, $l_j^{(i)} + n_j^{(i)}$, to yield $l_j^{(i-1)}$, which is the number of calls of capacity j, that use both the first and second links of the two hop path (v_0, v_{i-1}, v_i) on the channel.

4.2.4 Analysis for a Network

Thus far, we have calculated the end-to-end blocking probability for a single wavelength-path. To calculate the path blocking probability, we assume the wavelength independence model. This assumes that the distribution of capacity on a wavelength on a link is independent of the distribution of capacity on other wavelengths on the same link. From the blocking probability $Q_p(j)$ of line-speed j calls for a wavelength-path, we calculate the path blocking probability for path p with W wavelengths as

$$P_p(j) = (Q_p(j))^W \tag{4.11}$$

In this case, $Q_p(j)$ is calculated by using the procedure given in the previous sub-sections. The analyses in the previous sections assumes that the single wavelength arrival rates at the links and segments of the network are known. Hence, if $\lambda_{(l)}(j)$ is the arrival rate of line-speed j calls at the link. The arrival rate at the wavelength, $\lambda^w_{(l)}(j)$ can be estimated by

$$\lambda^w_{(l)}(j) = \frac{\lambda_{(l)}(j)}{W} \tag{4.12}$$

Typically, the traffic in a network is specified in terms of a traffic matrix A which specifies the offered load between pairs of stations. In our case, we will have j traffic matrices, with each traffic matrix A_j corresponding to traffic loads of line-speed j. Using the offered loads between node pairs, we have to estimate the load at the links and segments in our network. However, the offered load between node pairs is not entirely carried by the links as some of the calls are blocked. The extent of call blocking is in turn dependent on the offered load. This interdependence between the blocking probability and the offered load leads to a set of coupled non-linear equations called the Erlang map [18] and its solution is called the Erlang fixed point. Since, the holding time of all of our calls between the node pairs are exponentially distributed with unit mean, in our case, the offered loads at the links and nodes are equal to their respective arrival rates.

Hence if the probability of blocking of a line-speed j call on a link l on the path is $P_l(j)$, the probability of blocking of a line-speed j call on path p is $P_p(j)$, and the arrival rate of

line-speed j call on a path p is $\lambda_p(j)$, then a good approximation [18] for the arrival rate of a class-j call at the link l is given by

$$\lambda_l(j) = \sum_{\forall p | l \in p} \lambda_p(j) \frac{(1 - P_p(j))}{(1 - P_l(j))} \tag{4.13}$$

A similar formula also applies to determining the arrivals of class-j calls, $\lambda_s(j)$ at a segment s of a path,

$$\lambda_s(j) = \sum_{\forall p | s \in p} \lambda_p(j) \frac{(1 - P_p(j))}{(1 - P_s(j))} \tag{4.14}$$

Of course, $P_p(j)$ is in turn determined by the link and segment arrival rates and is calculated by using the procedure given in Sub-section 4.2.3.2 and using (4.11) and (4.12). The average blocking probability for a line-speed j call in the network is then given by

$$P_B(j) = \frac{\sum_{\forall p} \lambda_p(j) P_p(j)}{\sum_{\forall p} \lambda_p(j)} \tag{4.15}$$

Recall from (3.1), the probability that a call is of line-speed j is r_j hence, the blocking probability of a call, P_B irrespective of its line-speed is,

$$\sum_{j=1}^{g} P_B(j) r_j \tag{4.16}$$

But the expected capacity of a call is $E\{j\}C/g$ where $E\{j\}$ is as defined in (3.2). Therefore, we can obtain the average capacity lost, C_L, due to call blocking as,

$$C_L = P_B E\{j\}/g \tag{4.17}$$

This gives us a system of non-linear equations for the constrained grooming network. We use the following iterative procedure to solve for $P_B(j)$ for all paths. We define $\lambda_l^{(i)}(j)$, $\lambda_s^{(i)}(j)$, $Q_p^{(i)}(j)$, $P_p^{(i)}(j)$, $P_B^{(i)}(j)$, $P_l^{(i)}(j)$, $P_s^{(i)}(j)$ as the values obtained at the end of the ith iteration for the respective variables without the superscript (i). First we set $Q_p^{(0)}(j)$, $P_p^{(0)}(j)$, $P_B^{(0)}(j)$, $P_l^{(0)}(j)$, $P_s^{(0)}(j)$ to zero and i to 1 as part of the initial conditions. Then we follow the iterative method specified below:

1. Determine the link arrivals rates,$\lambda_l^{(i)}(j)$, from (4.13). If we consider wavelength capacity correlation then we determine the segment arrival rates,$\lambda_s^{(i)}(j)$, using (4.14). Obtain the respective wavelength arrival rates using (4.12).

2. If we consider wavelength correlation, we use the methods given in Sub-sections 4.2.2 and 4.2.3.2 to calculate $Q_p^{(i)}(j)$, $P_l^{(0)}(j)$ and $P_s^{(0)}(j)$. If we consider wavelength independence, we use the methods specified in Sub-sections 4.2.1 and 4.2.3.1 to calculate $Q_p^{(i)}(j)$, $P_l^{(0)}(j)$.

3. Calculate $P_p^{(i)}(j)$ using (4.11).

4. Calculate $P_B^{(i)}(j)$ using (4.15).

5. If absolute, percentage difference between $P_B^{(i)}(j)$ and $P_B^{(i-1)}(j)$ is smaller than a preselected threshold value, ϵ, (in our case, $\epsilon = 1e^{-3}$), then terminate. Otherwise, increment i and goto step 2.

It should be mentioned that the above iterative procedure does not always converge to a solution. In particular, we found that the procedure for the correlation model case is highly sensitive to input traffic data and is prone to fail to converge. Although there exists methods such as Newton's method that are guaranteed to converge, we resort to this method as it is computationally efficient and simpler, and converges within a few iterations for most cases.

4.3 Analysis for a Sparse Grooming Network

In this section, we consider the effect of adding WGXC nodes in the network. In a sparse grooming network, only some (say K) of the N nodes of the network are provided with full grooming capability. Instead of calculating the blocking performance of each of the $\binom{N}{K}$ placement combinations, we use the probabilistic approach similar to [33]. We assume that with probability q, a node is equipped with full grooming capability such that on an average there are $K = Nq$ WGXC nodes in the network. The probability q, which we will refer to as *grooming factor*, results in a binomial distribution of WGXC nodes in the network with mean Nq. So we consider a h-hop path $s, 1, 2, ..., i, ..., h-1, d$ and we wish to compute the blocking

probability of a call of line-speed j on the path. We use a recursion formula which uses the principle that node i on the path is the last WGXC node from s and there are no WGXC nodes after node i until node d. Therefore, a call of line-speed j is not blocked if $\{a\}$ it is not blocked on the first i hops of the path and $\{b\}$ capacity jC/g exists on the last $h-i$ hops of the path. If we assume that the wavelength occupancy on a link is independent of the wavelength occupancy of the other links on the paths, we can assume that two events $\{a\}$ and $\{b\}$ are independent. Now we can calculate the blocking probability of call of line-speed j on a h hop path as

$$\begin{aligned} P_p^{(h)}(j) = P(&\text{The call is blocked} \mid \\ &\text{no WGXC nodes are on the path}). \\ &P(\text{no WGXC nodes are on the path}) + \\ \sum_{i=1}^{h-1} &P(\text{Blocking} \mid \text{node } i \text{ is the last WGXC node} \\ &\text{on the path from } s) \times \\ &P(\text{node } i \text{ is the last WGXC node}) \end{aligned}$$

which is,

$$\begin{aligned} P_p^{(h)}(j) = (Q_{(sd)}^w(j))^W (1-q)^{h-1} + \\ \sum_{i=1}^{h-1} [1 - (1 - P_p^{(i)}(j)). \\ (1 - (Q_{(id)}^w(j))^W)] q (1-q)^{h-i-1}. \end{aligned} \tag{4.18}$$

We calculate $Q_{(ik)}^w(j)$, where i, k are nodes on the path p, using the single hop wavelength link model specified in subsection 4.2.1. Note that we cannot apply the correlation model directly here as the event of blocking on the last $h-i$ hops will not be independent of the event of blocking on the first i hops. To obtain the overall blocking in an arbitrary network, we use the iterative procedure in the previous section, where we replace line 3 of the procedure as:

3. Calculate $P_p^{(h)}(j)$ using (4.18).

4.4 Numerical Results

In this section, we use the results of the analysis in the previous section and calculate blocking probabilities for two network topologies, a 16-node mesh-torus and a 8-node ring, under constrained and sparse grooming conditions. To verify the accuracy of the proposed analytical models, we performed a simulation study for the cases and compared the results. In addition, we also performed a simulation study for a 6-node network based on a nonblocking centralized switch configured as a WGXC and WSXC. Simulations were run in batches of 10^6 calls each, until the blocking values between successive call batches differed by less than 0.1 percent. Similarly, the iterative procedure for analysis was stopped when the performance values between successive iterative steps differed by less than 0.1 percent.

In the case of 16 node mesh-torus under constrained (with all WSXC nodes) and sparse grooming (with all WGXC nodes) conditions, the independence model provides reasonable estimates for the blocking probability at different line-speeds as shown in Figures 4.2 and 4.3. For the constrained grooming case in Figure 4.2, the correlation model provides more accurate estimates than the independence model. For the case of the ring, shown in Figures 4.4 and 4.5., the correlation model provided more accurate estimates than the independence model for high line-speed connections. In both models, accuracy of the estimates decreased as the line-speed of the call decreased. We find that the large differences in magnitude between the blocking for high and low line-speed connections, makes it more difficult for the models to accurately predict the blocking at both high and low magnitudes. In fact, this effect is more pronounced in the case of the ring network due to the high load correlation of links

Compared to constrained grooming, sparse grooming offers an order of magnitude decrease in blocking probability for high line-speed connections and multiple orders of magnitude decrease in blocking for low line-speed connections. The reason for this is in part due to the fact that smaller connections groom better and switch easier into wavelengths and also in part due to our assumption of random wavelength assignment for traffic streams. This shows that sparse grooming offers significant improvement in blocking performance even for random wavelength assignment and we can expect better performance for other wavelength assignment schemes

which perform better than random wavelength assignment.

In Figures 4.6 and 4.7, we observe the effect of sparse grooming and granularity on the capacity loss, C_L, due to blocking of calls in the mesh-torus and the ring under low link loads (0.01 for the ring and 0.05 for the mesh). Here, the offered load at the nodes in terms of wavelength capacity is maintained constant over different g. As is obvious, in both networks, C_L decreases as q is increased. Here the case for $q = 0$ corresponds to a constrained grooming network and that for $q = 1$ corresponds to a sparse grooming network with all WGXC nodes. However, it is interesting to note that the rate of decrease in C_L for the ring is more than that of the mesh. We also observe an increase in C_L with increase in granularity(g). This increase in C_L is more due to the ineffective packing of traffic streams by the random wavelength assignment algorithm can possibly be improved by using a better wavelength assignment scheme. Finally, we consider the effect of g on a non-blocking centralized switch network connected to six access stations in both constrained and sparse grooming conditions. Studying such a network can provide the lower bound on the blocking performance as blocking occurs only at the links leading to the access stations. Here we find the interesting case that as the g is increased, the capacity loss due to blocking of a WSXC node increases while that of a WGXC node decreases. This suggests that in some cases, increasing the granularity might be beneficial for a sparse grooming network.

4.5 Conclusions

In this chapter, we proposed analytical models for WDM networks with traffic grooming capabilities based on the wavelength capacity distribution and its correlation on neighboring links. The results of the analytical models were compared with simulation studies and they were shown to provide close estimates for well connected networks. The correlation model was shown to perform better than the independence model. Both of the models were accurate in providing estimates for high line-speeds. However, they did not exhibit the same level of accuracy for low line-speeds in sparse networks. We studied and compared the performance of constrained and sparse grooming networks. Compared to constrained grooming, sparse

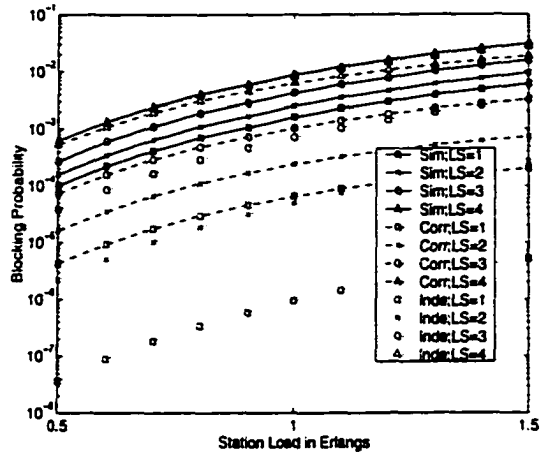

Figure 4.2 Blocking probability vs. load per station in Erlangs for a Constrained Grooming 4×4 mesh-torus network with $W = 5$ and $g = 4$. (LS: Line-Speed, Sim: Simulation, Corr: Correlation Model, Inde: Independence Model)

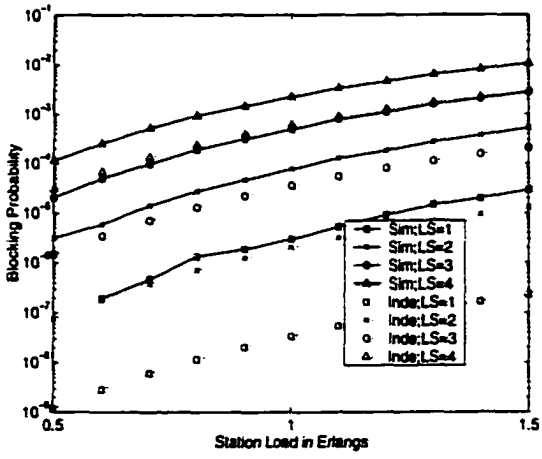

Figure 4.3 Blocking Probability vs. load per station in Erlangs for a Sparse Grooming 4×4 mesh-torus network with $W = 5$ and $g = 4$. (LS: Line-Speed, Sim: Simulation, Inde: Independence Model)

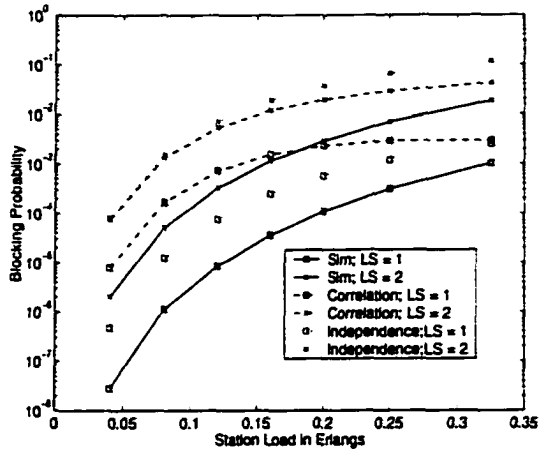

Figure 4.4 Blocking Probability vs load per station in Erlangs for a Constrained Grooming 8-node ring network with $w = 5$ and $g = 2$. (LS: Line-Speed, Sim: Simulation, Corr: Correlation Model, Inde: Independence Model)

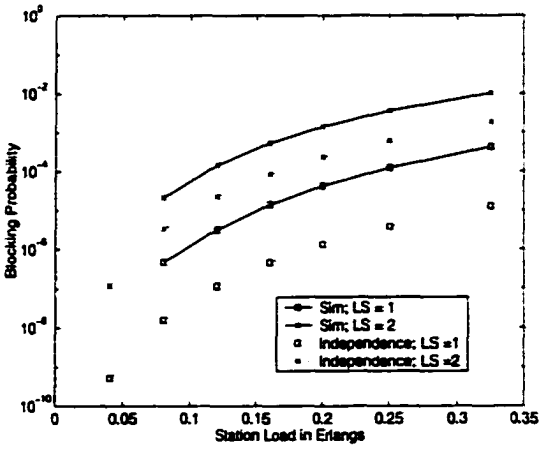

Figure 4.5 Blocking Probability vs load per station in Erlangs for a Sparse Grooming 8-node ring network with $W = 5$ and $g = 2$. (LS: Line-Speed, Sim: Simulation, Inde: Independence Model)

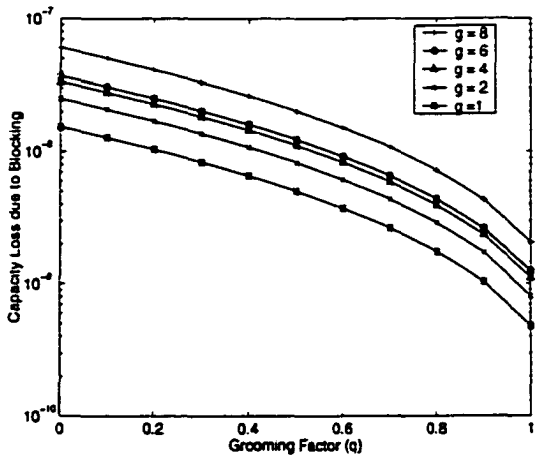

Figure 4.6 Capacity Loss due to Blocking vs. Grooming Factor,q for a 4×4 mesh-torus network with $W = 5$ for different g.

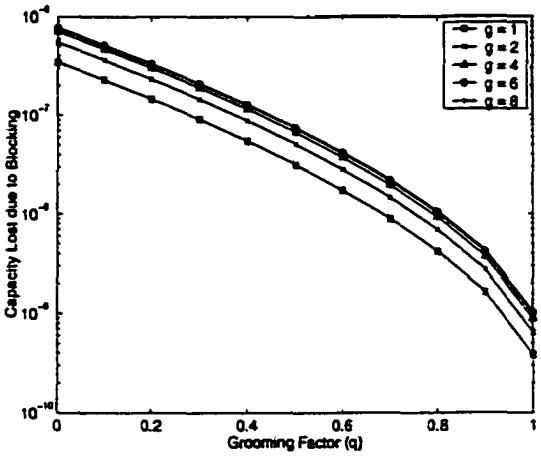

Figure 4.7 Capacity Loss due to Blocking vs. Grooming Factor q for a 8 node ring network with $W = 5$ for different g.

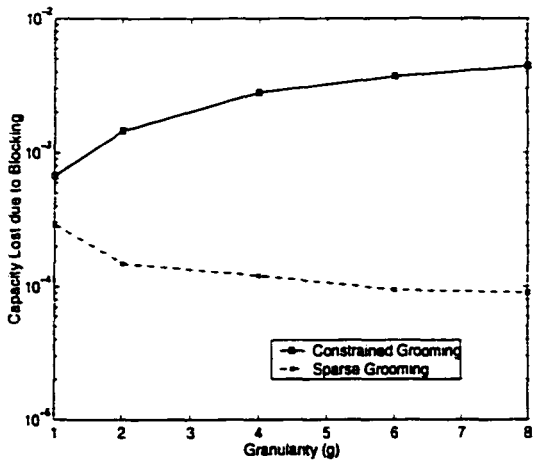

Figure 4.8 Capacity Loss due to Blocking vs granularity g for a non-blocking centralized switch with Constrained and Sparse Grooming and attached to 6 access station nodes. $W = 5$

grooming offers at least an order of magnitude decrease in blocking probability for high line-speed connections and multiple orders of magnitude decrease in blocking for low line-speed connections. The performance improvement is not equal for traffic of different line-speeds. At low link loads in a network, increasing the granularity of traffic on a lightpath results in an increase in capacity loss due to blocking for constrained grooming networks but results in a improvement in some cases for sparse grooming networks.

CHAPTER 5. Capacity Fairness of WDM Grooming Networks

5.1 Introduction

In the previous chapter, we studied the characteristics of traffic grooming WDM networks with arbitrary topologies from the perspective of blocking performance. It was shown that the blocking performance is not only affected by the link traffic and the routing and wavelength assignment strategy, it is also affected by the arrival rates of different low-rate traffic streams, their respective holding times and more importantly, the capacity distribution of the wavelengths on the links. A link-correlation model was also presented which took into account the capacity distribution of wavelengths and the correlation on neighboring links to calculate the blocking performance. In such networks, call requests arrive randomly and can ask for a low-rate traffic connection to be established between the source and destination. Under dynamic traffic conditions, call requests that ask for capacity nearer to that of the full wavelength experience higher probability of blocking than those that ask for a smaller fraction. In fact, the difference in blocking performance between the high and low capacity traffic streams becomes more significant as the traffic stream switching capability of the network increases. This difference in blocking performance for different capacities is directly affected by the routing and wavelength assignment policy that is used to route the call request. Hence, it is important that a call request is provided service in a *fair* manner commensurate with the capacity it requests. This *capacity fairness* is different from the fairness measure based on hop count that has traditionally been addressed in the literature [51] [23].

Birman and Kershenbaum [51] proposed two techniques for fairness improvement with respect to hop length. In the first method called Reservation technique, they reserve wavelengths exclusively for longer-hop paths on every link. However, the longer-hop paths can also compete

with the shorter-hop paths for other wavelengths. In their second method called Protecting Threshold technique, the traffic on long paths is protected from the traffic on short paths by admitting the short path traffic only when the link utilization is below a given threshold. This leads to fairness in blocking. Harai et al. [23] proposed a limited alternate routing method to improve fairness. In this method, long paths have a larger number of alternate paths than short paths. By limiting the number of alternate connections in short paths, we can accommodate more long path connections. These methods introduce fairness by regulating the admission of connection requests based on the path length at the expense of increase in overall blocking probability. They can be grouped into the general category of algorithms called *connection admission control* algorithms.

In optical networks without wavelength conversion, a lightpath should use the same wavelength throughout the route on all links of the path. This requirement is called the wavelength continuity constraint and contributes to the increase in probability of a call request being blocked. As the path length from source to destination increases, the blocking probability of the corresponding call request increases. Hence in a network with no wavelength conversion, long paths have higher blocking probability than short paths. Wavelength conversion can be employed at the network nodes to reduce the blocking of longer-hop connections. Wavelength conversion for WDM networks was studied in [28], [14], [33], [20]. It was shown that wavelength converters reduce wavelength conflicts and improve the performance by reducing the blocking probability. On the other hand, an increase in the network's wavelength conversion capability results in the network admitting longer-hop paths, which consumes more network resources. This increases the blocking probability of shorter-hop paths, compared to their performance in networks with no wavelength conversion.

Usually, the common metric in evaluating the performance of D-RWA algorithms is the blocking probability. However, a good D-RWA algorithm for traffic grooming networks should treat all call requests in a "fair" manner while ensuring efficient utilization of the network. Usually, the problem of D-RWA is separated into the subproblems of routing and wavelength assignment and solved independently. Current Dynamic Wavelength Assignment (D-WA) al-

gorithms, such as first-fit (FF)[15], random assignment (R)[19], most-used (MU)[17] and Max-Sum (MS)[16], were designed in a network scenario where the full wavelength was the basic unit of bandwidth. However, in WDM networks capable of traffic grooming, the basic unit of bandwidth is a traffic stream whose capacity can be less than that of a wavelength. The blocking and fairness performance of these algorithms in such a traffic grooming scenario is not known.

In this chapter, we study the fairness performance of traditional D-WA algorithms in terms of capacity, in a traffic grooming WDM network. We find that these algorithms do not treat call requests of different capacities in a fair manner. This motivates the need for a good mechanism to provide capacity fairness. We propose a new connection admission control scheme which can be used along with existing wavelength assignment algorithms to attain fairness in capacity. Our proposed algorithm achieves fairness in capacity while not over-penalizing the network blocking performance. For our simulation study, we assume dynamic traffic model conditions and use the network and traffic assumptions specified in Chapter 3, Sections 3.2 and 3.3. Additionally, we define a traffic stream of line-speed j as a *Class* j traffic stream. A call that requests a *Class* j traffic stream is referred to as a *Class* j call request.

5.2 Capacity Fairness

In a network, where every user pays for the bandwidth he requests and consumes, it is important that every user get the same type of services as any other. The network system that offers the service must be fair and should not have any inherent bias against a particular subset of users. Although this concept of fairness is simple to understand, the exact definition of fairness however, is extremely case-dependent upon the networking issues involved. In addition, it is usually the case that any efforts by a control mechanism to ensure fairness on an issue results in the degradation of performance in other qualities of the network.

We define *capacity fairness* based on the following. In our network, call requests arrive randomly at a node pair. As explained previously, we have assumed the traffic model such that each class of traffic streams generates the same combined capacity worth of calls. However,

calls of high capacity are blocked more often than those of small capacity. In fact, as the number of WGXC nodes i.e. the traffic stream switching capability in the network increases, there is more than an order of magnitude difference in blocking probability between calls of highest capacity and lowest capacity. A user who has knowledge of this unfairness can request his total required capacity in smaller traffic streams rather than as a whole. This is unfair to those users who are either ignorant of the unfairness and/or cannot request their total capacity in splittable flows. To prevent this i.e. to achieve capacity fairness, the blocking probability of a high capacity, say of line-speed m, call should equal the combined blocking performance of m calls of line-speed 1. Hence, we formally state the definition below:

Capacity fairness is achieved, when the blocking performance of m calls of line-speed n is equal to the blocking performance of n calls of line-speed m

At this point, we will assume that a user who requests capacity in terms of smaller number of calls will relinquish all his accepted calls immediately, even if one of them is blocked.[1] Therefore, if p_m is the blocking probability of a class-m call and p_n is the blocking probability of a class-n call, then to achieve capacity fairness:

$$1-(1-p_m)^n = 1-(1-p_n)^m \ \forall 1 \leq m,n \leq g. \tag{5.1}$$

In addition, an algorithm should achieve capacity fairness while keeping the overall blocking probability to an acceptable level. The overall blocking performance of the network can be defined in terms of the blocking probability per unit line-speed of the call requests. When capacity fairness is achieved, according to Eqn. 5.1, the blocking probability, p_j, of a class j call is the same as the blocking performance value, of j class-1 calls whose blocking probability is p_1 i.e.

$$p_j = 1-(1-p_1)^j \tag{5.2}$$

or

[1] We do not consider the scenarios, where the user can request a set of calls and accept or reject a subset of the accepted set.

$$p_1 = 1 - \sqrt[j]{1 - p_j}. \tag{5.3}$$

Hence, using Eqn. 5.3 we can obtain an estimate of p_1 from p_j, We will refer to this estimate, $\hat{p_j}$, as the blocking probability per unit line-speed of a class j call. Now the overall network blocking probability per unit line-speed, $\hat{P}$, is given by

$$\hat{P} = \frac{\sum_{j=1}^{g} \hat{p_j}}{j}. \tag{5.4}$$

Recall from Chapter 3, Section 3.3, Equation 3.3 that $\hat{\lambda_{sd}}$ should be the equivalent arrival rate of calls at s-d pairs in the network if all call requests are of the lowest granularity, i.e. of class-1. For a given physical topology, if we assume that all incoming call requests are of class-1 and their arrival rate per node pair is $\hat{\lambda_{sd}}$, then the corresponding network blocking performance Q obtained is the best estimate for $\hat{P}$ when capacity fairness is achieved.

It is usually the case that the unfairness in an algorithm affects calls of the highest or the lowest capacity more than the calls of intermediate capacity. Keeping this in mind, we can give a good estimate of fairness using just the blocking performance of the highest and lowest capacity calls. Hence we can define the *fairness ratio* F_r for an algorithm running a network as the ratio of blocking probability per unit line-speed of the call with the highest line-speed (g), $\hat{p_g}$ to the blocking probability per unit line-speed of the call with the lowest line-speed (1), $\hat{p_1}$, or

$$F_r = \frac{\hat{p_g}}{\hat{p_1}}. \tag{5.5}$$

If the value of F_r is greater than 1, then the algorithm is said to favor high capacity call requests over low capacity call requests and vice versa. Therefore, if F_r for an algorithm is close to 1, then we can reasonably assume that the algorithm is also fair to calls of *all* capacities. Therefore a good admission control algorithm should ensure that $\hat{P}$ is close to Q and at the same time ensure capacity fairness using Equation 5.1 and have a fairness ratio close to 1.

5.3 Connection Admission Control for Capacity Fairness

In this section, we specify an algorithm that works along with any routing and wavelength assignment algorithm and introduces capacity fairness by exercising connection admission control using run-time blocking performance information. *Connection admission control* (CAC) is simply defined as the set of actions that are to be taken upon a call arrival in order to establish whether to accept or reject the connection request. Connection admission control relies on two factors.The first is that incoming call requests can specify their network requirements and the second is on the system's ability to measure, monitor and update the global state of the network, which in this case is the blocking performance of calls of various capacities at the nodes. Since the algorithm makes its decision to accept or reject a call based only on the current blocking values, the CAC algorithm is effective only after the network has been up and running for quite some time. This is because initially the blocking performance of the network may be inaccurate or may not be known. Due to the dependence of the algorithm on such a "warm-up" period, the algorithm should not be relied upon to provide capacity fairness during this period before attaining accurate and stable the run-time blocking probability attain accurate and stable values. Hence we assume that the CAC procedure is carried out when the network is in a state where there are previously established traffic streams and wavelengths are already assigned to those traffic streams in the network. Therefore the CAC algorithm uses the run-time blocking probabilities p_j of calls of class j in the network. The CAC algorithm is independent of the routing and wavelength assignment scheme and can work along with any routing and wavelength assignment scheme. The procedure for the CAC algorithm is as follows.

Assume a new call arrives for a node pair (s, d) and requests a capacity of j to be established from s to d:

1. Check if a traffic stream of capacity j can be established on the path i.e., enough capacity on wavelengths exist to carry the traffic stream. If the path cannot be established, reject the call.

2. Obtain an estimate of overall network blocking probability per unit line-speed, $\hat{P}$ from Eqn. 5.4 and the blocking probability per unit line-speed of the class j calls, $\hat{p_j}$, from Eqn. 5.3.

3. if $(\hat{p_j} \geq \hat{P})$ then accept the call and go to step 6.

4. let $q_m = (\hat{P} - \hat{p_j})/\hat{P}$.

5. Reject the call with probability q_m.

6. If the call is not rejected, start the wavelength assignment algorithm for the set of available wavelengths on the path to establish the connection. Update the blocking performance parameters.

We will refer to q_m as the *mean ratio*. Essentially, q_m is the rejection probability for the call. We can also obtain another estimation for rejection probability using the standard deviation D of blocking probability per unit line-speed values, $\hat{p_j}, 1 \leq j \leq g$. In this case q_D is given by

$$q_D = (\hat{P} - \hat{p_j})/(D) \tag{5.6}$$

We refer to q_D as the *deviation ratio*. q_D can be substituted for q_m in the algorithm. The fairness performance for the two cases of the algorithm will be shown in the next section. As the network services the calls that arrive, due to changes in network topology or traffic, it might happen that the current blocking of the network might differ significantly from the average blocking performance calculated over the lifetime of the network for the algorithm. To ensure accuracy in the estimation of blocking, we can use a rolling window of the most recent set of call arrivals and estimate the blocking performance using only those call arrivals rather than considering the complete set of calls since the network started operation.

5.4 Numerical Results on 6X6 Mesh-Torus

We performed a simulation study of the call blocking performance in a 6×6 bi-directional mesh-torus network to study the capacity fairness property of various wavelength assignment

algorithms and to evaluate the performance of our admission control scheme. Apart from the wavelength assignment schemes of Random (R) wavelength assignment, First-Fit(FF), Most-Used (MU) and MaxSum (MS), we have also considered a wavelength assignment scheme called Best-Fit (BF) that is unique to grooming networks. In Best-Fit wavelength assignment, among the available wavelengths for the traffic request, the traffic stream is assigned to that wavelength which has the least free capacity remaining when the incoming traffic stream is accommodated. We selected the mesh-torus network over other topologies like ring, hypercube, etc. because compared to the ring the mesh-torus has more connectivity which can help generate a good amount of traffic switching at the nodes. Also, compared to the hypercube, the average hop length is larger, which also gives rise to a good amount of load correlation between the links. For all the cases, we assumed the number of wavelengths (W) per fiber to be 5. We assumed the granularity (g) of the wavelength to be 4. This means that a traffic stream can ask for a minimum of one-fourth the capacity of the wavelength. We will illustrate some interesting results of the simulation study. In Fig. 5.1, we have plotted the fairness ratio versus the node load in Erlangs. We observe that for low node loads, the fairness ratio is high indicating that high capacity calls are favored more than low capacity calls. But as the node load is increased, the network traffic as a whole is increased. This increases the blocking probability of both low capacity and high capacity connections. Hence all calls irrespective of whether they are high or low capacity start to experience blocking. We find that the Best-Fit does the best with respect to fairness and provides the fairness ratio that is closest to 1. On the other hand, the MaxSum algorithm, which provides the least overall network blocking than other wavelength assignment algorithms we have considered, has the highest fairness ratio at low loads in the network.

Next, we observe how the fairness ratio increases as the number of grooming nodes i.e., WGXC nodes, in the network is increased, in Fig. 5.2. We find that initially when no WGXC nodes are present in the network, the connections of high capacity have less blocking probability per unit line-speed than those with low capacity. But as the grooming capability of the network is increased,we find a reversal and connections of high capacity have higher blocking probability

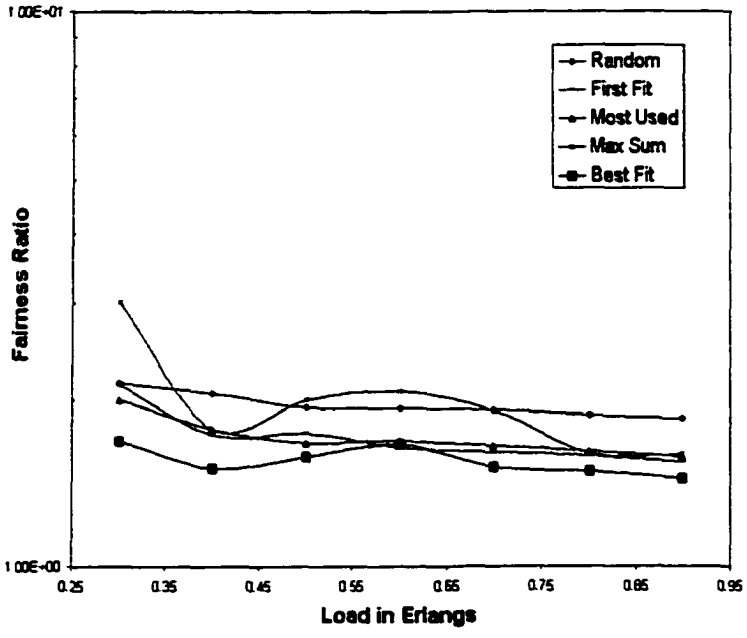

Figure 5.1 The fairness ratio versus node load in Erlangs for a bidirectional 6×6 mesh-torus with $g = 4$ and $W = 5$.

per unit line-speed than low capacity connections. The reason for this is that low line-speed connections groom better and fit easier into wavelengths than high line-speed connections. It is interesting to note that when the number of grooming nodes are around 10 to 15, the fairness ratio is close to 1. The MaxSum algorithm also has the highest fairness ratio when the grooming nodes are high, and the lowest fairness ratio (away from one) when there are no grooming nodes in the network. This motivates the need for effective schemes to achieve capacity fairness.

Next we will study the performance of our connection admission control (CAC) scheme. We will compare the performance when the CAC algorithm is used along with the first-fit (FF) wavelength assignment scheme, and when the FF scheme is used without the CAC scheme. We assume the network scenario when there are no grooming nodes in the network. In the fairness ratio graph shown in Fig. 5.3, we find that both of the CAC schemes, *mean ratio* and *deviation ratio* achieve excellent fairness where the fairness ratio is equal to 1 when compared to First Fit which has a fairness ratio is less than one. This confirms that the CAC algorithm

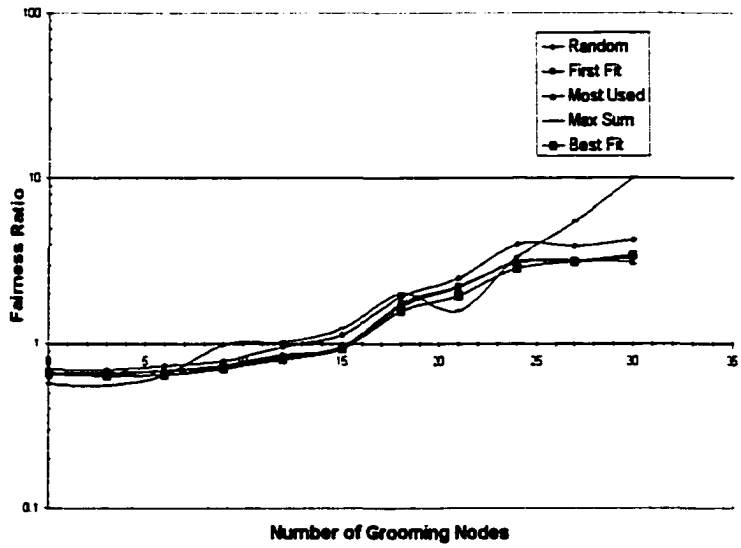

Figure 5.2 The fairness ratio versus number of WGXC nodes for a bidirectional 6×6 mesh-torus with $g = 4$ and $W = 5$.

works very well under high loads to the network.

Now we would like to see the increase in overall network blocking probability per unit line-speed that is required to achieve the fairness. This graph is shown in Fig. 5.4. We find there is a relatively small and consistent increase in blocking performance of the CAC-FF scheme when compare to just the FF scheme. This shows that our scheme can achieve capacity fairness with little increase in overall network blocking probability per unit line-speed.

5.5 Conclusion

We have addressed the concept of capacity fairness in WDM networks with grooming capabilities. Such a network can consist of OADMs, optical crossconnect and traffic grooming equipment capable of switching traffic streams from one wavelength to another. In such networks, a call can request a low-rate traffic connection to be established between the source and destination. In this scenario of supporting low-rate circuit-switched traffic streams, the call request that asks for a high-capacity for its connection will encounter a higher probability of blocking than those which ask for a smaller fraction. We provided a qualitative and quan-

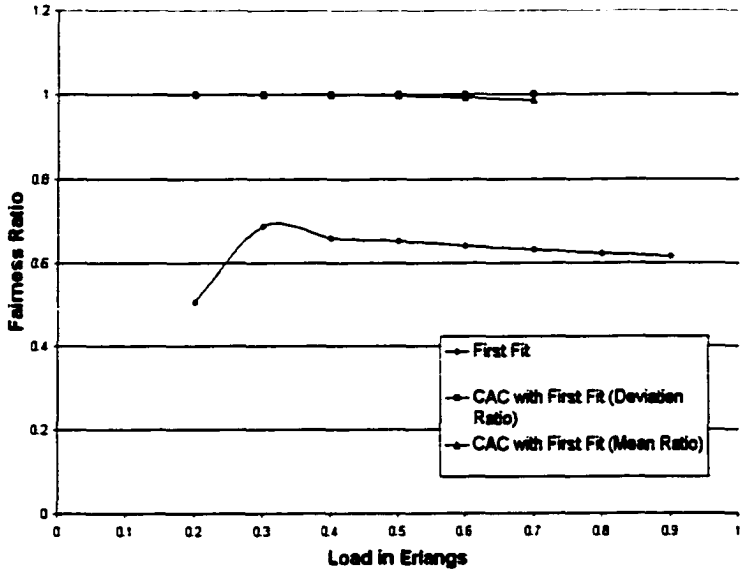

Figure 5.3 The fairness ratio versus node load in Erlangs for a bidirectional 6×6 mesh-torus with $g = 4$ and $W = 5$.

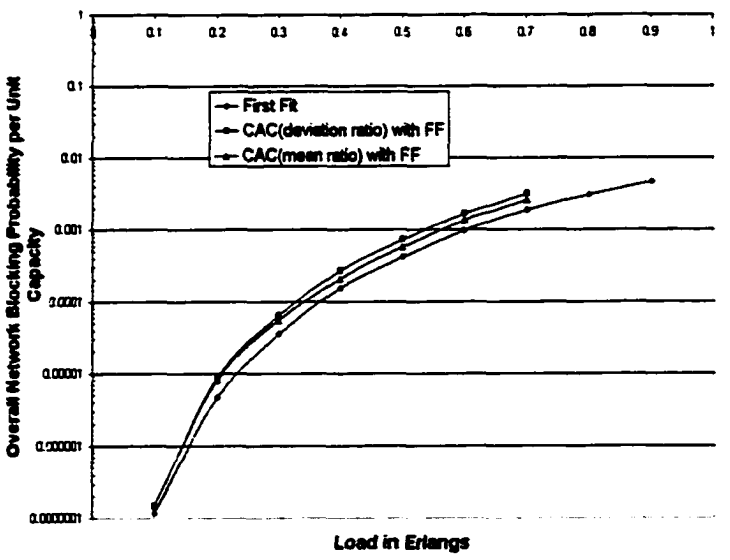

Figure 5.4 The overall network blocking probability per unit line-speed versus node load in Erlangs for a bidirectional 6×6 mesh-torus with $g = 4$ and $W = 5$.

titative definition of capacity fairness. Current dynamic routing and wavelength assignment techniques were designed for conventional wavelength routing networks where the wavelength was the basic unit of bandwidth. These algorithms are not good at achieving capacity fairness. Therefore additional mechanisms such as connection admission control are required to achieve fairness in capacity. A good connection admission control scheme should provide capacity fairness while at the same time ensure that the increase in overall network blocking probability per unit line-speed is minimal. We proposed such a connection admission control scheme that ensures capacity fairness while at the same time ensures a small increase in blocking performance. We have studied the performance of the algorithm under limited conditions such as the mesh-torus topology. Although the connection admission control method is a viable scheme to ensure capacity fairness, we need to study its performance under high and low loads, on other network topologies such as ring and arbitrary mesh networks, and using dynamic-routing methods.

CHAPTER 6. Traffic Grooming for WDM Mesh Survivable Networks

6.1 Introduction

In constrained grooming networks, due to the high bandwidths involved, any link failure in the form of a fiber cut will have catastrophic results unless protection and restoration schemes for the interrupted services form an integral part of the network design and operation strategies. Although network survivability can be implemented in the higher layers above the optical network layer (eg. self-healing in SONET rings and the ATM virtual path layer, fast rerouting in MPLS and changing routes using dynamic routing protocols in the IP layer), it is advantageous to go in for optical WDM survivability mechanisms since they offer a common survivability platform for services to the higher layers. A variety of optical path protection schemes can be designed using concepts such as disjoint dedicated backup paths, shared backup-multiplexing, and joint primary/backup routing and wavelength assignment. Lighpath restoration schemes, on the other hand, do not rely on pre-routed backup channels but instead dynamically recompute new routes to effectively reroute the affected traffic after link failure. Although this saves bandwidth, the timescale for restoration can be difficult to specify and can be on the order of hundreds of milliseconds. Hence in a dynamic scenario, path protection schemes are likely to be more useful and practical than path restoration schemes.

In this chapter, we deal with lightpath protection schemes for WDM networks with grooming capabilities when the traffic demand is dynamic and consists of low-rate traffic streams. Specifically, we provide protection against any *single-link failure* at the optical network layer using (1:1) optical path protection. Every physical link is assumed to have a fixed number of wavelengths and the blocking probability of traffic stream connections is considered the primary performance metric. Calls for a source-destination pair arrive randomly and can request

a low-rate dependable traffic connection to be established between the node pair for the duration of the call. The call request is served by first establishing a primary (working) *traffic stream path* (TSP) and then establishing a link-disjoint backup (protection) TSP. If either the backup or the primary TSP cannot be set up, then the traffic stream request is assumed to be blocked. Indeed, the backup TSP does not carry any information but takes over the primary's role in case of a link failure on the primary TSP. Hence the backup path can be used to carry preemptable low-priority traffic which will be interrupted when the primary path fails. Both the primary and the backup TSPs can traverse intermediate WSXC and WGXC nodes between the source and destination. A TSP can traverse more than one lightpath on its path from the source to the destination. The wavelength assignment on the lightpath is governed by the primary requirement that the same wavelength must be used on all the links along the path. This requirement is called the wavelength continuity constraint. In this manner, each lightpath typically carries many multiplexed lower-speed traffic streams, each of which can be either a primary TSP or a backup TSP. In addition, to reduce the overhead of backup traffic streams, we use the bandwidth sharing technique, called *backup multiplexing* [52]. In this technique, only a small fraction of link-resources, i.e. a fraction of the wavelength, is reserved for all the backup traffic streams going through the link. The basic idea is that two backup TSPs can share part of the wavelength capacity if their corresponding primary (working) TSPs do not fail simultaneously. This happens when their paths are link disjoint, for a single link failure model.

6.1.1 Background

Various routing and wavelength assignment methods have been proposed to provide protection and restoration in WDM networks [6]. The work in [53] proposed design protection schemes to protect against component failures. [54] presented an ILP formulation for WDM self-healing rings employing 1:N line protection mechanisms. [55] developed ILP formulations for the RWA problem and wavelength utilization for a static traffic demand for different link and path protection schemes. Miyao and Saito in [56] formulated integer programming-based

design problem to optimally select combinations of working and restoration paths, number of fibers and number of OXCs at each node so that fast restoration is achieved. The above work considered the RWA problem under static traffic demand. RWA methods for dynamic traffic with protection have also been proposed in [57], [58] and [59]. [57] considered backup multiplexing-based lightpath routing techniques to provide dependable connections in WDM networks with dynamic traffic demand. The work in [58] considered the problem of dynamically establishing dependable connections with specified failure restoration guarantees. They developed algorithms for scenarios where a dependable connection is established at the time of connection setup, but the backup lightpath may not be available to the connection throughout its existence. The availability of the backup path is dependent upon the failure guarantee prespecified during connection setup. [59] proposed a dynamic strategy to re-arrange protection paths so that the capacity is increased and newer requests can be accommodated.

In this chapter, we consider the dynamic establishment of primary and backup traffic streams and study how they can be groomed onto the WDM network. Specifically, we address the following questions: How can we optimally multiplex the primary and backup traffic streams onto a wavelength on a link? How can this multiplexing be extended to traffic stream paths in the network? In such a case, is it better to multiplex the primary and backup streams together onto the same wavelength or is it better to segregate them to different wavelengths? What is the effect of such a grooming policy on the blocking performance? How does the topology, and the RWA algorithm affect our choice of grooming? To the best of our knowledge, there has been no prior research done to study the performance of dynamic grooming policies for establishing low-rate dependable connections in traffic grooming WDM networks. We conduct extensive simulation experiments to evaluate the effectiveness of the grooming policies on different topologies with different RWA algorithms.

6.2 Traffic Stream Multiplexing on a Single Wavelength Link

Consider a wavelength w on a fiber link l with capacity C. Typically, many traffic stream paths (TSPs) of varying capacity can be groomed onto the wavelength. These TSPs can be

either primary or backup traffic streams. Let C_P denote the total capacity required for all primary TSPs on the link. Let C_B denote the total capacity required for all backup TSPs on the link. The free (unused) capacity, C_F, is then given by $C_F = C - C_B - C_P$. Primary TSPs are distinctly multiplexed on the wavelength so that they occupy their individual capacities on the wavelength. Hence, if $P = \{p_1, p_2, p_3, ..., p_n\}$, with respective capacities $\{c_1^p, c_2^p, c_3^p, ..., c_n^p\}$, is the set of primary TSPs that traverse the link, then $C_P = c_1^p + c_2^p + c_3^p + ... + c_n^p$. On the other hand, backup TSPs share the capacity using the resource sharing technique of *backup multiplexing* [52]. Let $B = \{b_1, b_2, b_3, ..., b_n\}$ denote the set of backup TSPs traversing the wavelength w on link l. Let their respective capacities be $\{c_1^b, c_2^b, c_3^b, ..., c_n^b\}$ and their respective primary TSPs be denoted by the set $Q = \{q_1, q_2, q_3, ..., q_n\}$. Hence a primary TSP q_i with capacity c_i^b has a corresponding backup TSP b_i. Under the single link failure model, we can now calculate the exact total backup capacity C_B needed to handle all possible cases of single-link failures. The algorithm to calculate C_B is given in Figure 6.1(a).

The algorithm can be modified to serve the dynamic case where we already have a pre-computed backup capacity, C_{prev}, serving the set of backup paths, B. Let a new backup traffic stream request, b_{sd} for a capacity c_{sd} arrives at the wavelength channel. Assume that its primary traffic stream path p_{sd} can been established in the network. In this case, we only need to calculate the spare capacity for each link, j of the primary path p_{sd} where $j \in p_{sd}$. The new backup capacity C_{new} is $max\{C_{prev}, s_j\}$ where s_j are the spare capacities obtained for each link j of the primary path p_{sd}. If $C_{new} \leq C_{prev}$, then no extra capacity on the channel need be reserved as backup capacity and the backup traffic stream is established over the wavelength. Otherwise, the backup path can be established if the free capacity C_F is at least $C_{new} - C_{prev}$. The algorithm for the dynamic case is shown in Figure 6.1(b). It is to be noted that to allocate a primary path, say p_{sd} of capacity c_{sd}, we simply need to ensure we have c_{sd} capacity free on the wavelength. When a traffic stream connection leaves the network, the primary and backup traffic stream path are released. The capacity of the primary channel needs to be released and is added to C_F. For the backup path, we simply remove the traffic stream from the channel and run the algorithm in Figure 6.1(a) for the link to obtain the new backup capacity.

1: For each link $i, i \in L, i \neq l$
2: $SpareCapacity(i) = 0$
3: For each primary TSP, $q_j \in Q$
4: If q_j contains link i then
5: $SpareCapacity(i) = SpareCapacity(i) + c_i^b$
6: EndIf
7: EndFor
8: EndFor
9: $C_B = Max\{SpareCapacity(i)\}, \forall i \neq l$

(a) Algorithm to calculate C_B for wavelength w for link l with capacity C

1: For each link $i, i \in p_{sd}, i \neq l$
2: $SpareCapacity(i) = c_{sd}$
3: For each primary TSP, $q_j \in Q$
4: If q_j contains link i then
5: $SpareCapacity(i) = SpareCapacity(i) + c_i^b$
6: EndIf
7: EndFor
8: EndFor
9: $C_B^{new} = Max\{C_B^{prev}, SpareCapacity(i)\}, \forall i \neq l$

(a) Dynamic Algorithm to calculate C_B^{new} for wavelength w for link l with current backup capacity C_B^{prev} and a new arrival of backup TSP b_{sd}, where $l \in b_{sd}$, with capacity c_{sd} and primary TSP can be set up on p_{sd}.

Figure 6.1 Optimal Multiplexing of Backup Traffic Stream Paths on a wavelength-link

6.3 Grooming traffic streams on the network

Traffic stream paths in the network can be either primary or backup traffic streams. Such traffic streams can be groomed onto the wavelengths in two ways: (a) Both primary and backup TSPs can be groomed onto the same wavelength. This is referred to as *Mixed Primary-Backup Grooming Policy (MGP)*. (b) The wavelength can consist of either primary or backup traffic streams but not both. This is referred to as *Segregated Primary-Backup Grooming Policy (SGP)*. Figure 6.2 shows an example of MGP and SGP on a link with three wavelengths. The capacity on the wavelength can essentially be grouped into three types, capacity used by the primary TSPs or Primary Capacity(PC), capacity used by the backup TSPs or Backup Capacity(BC) and the unused or free capacity (FC).

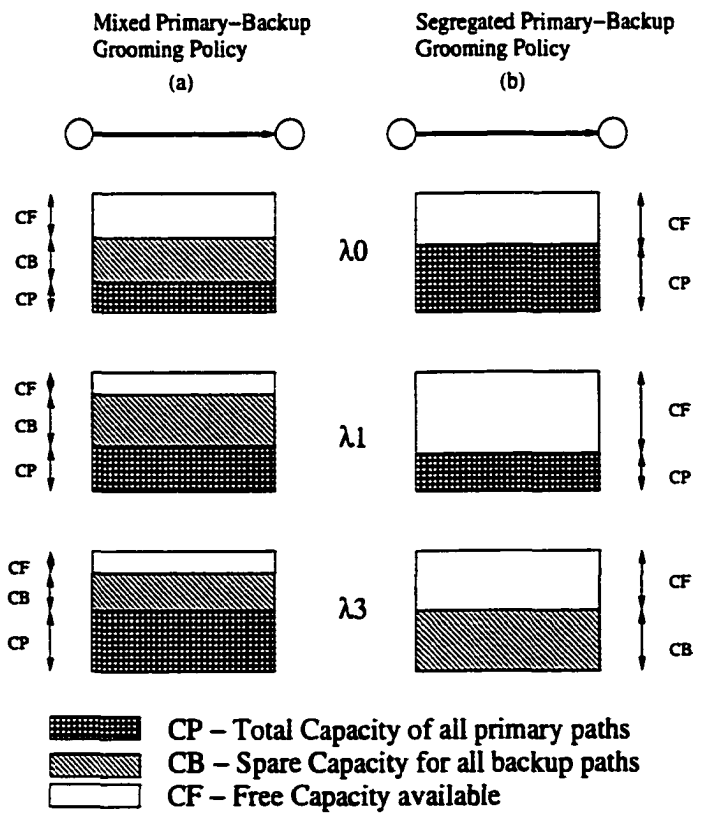

Figure 6.2 Traffic Stream Grooming Policies in a link

In order to use the channels efficiently, we make use of the backup multiplexing technique.

In this technique, if two primary TSPs are link-disjoint then their corresponding backup TSPs can share the capacity on a wavelength on a link. This process of grooming primary and backup TSPs on to the WDM network is illustrated through a simple example. Consider the eight node network as shown in Figure 6.3. Each edge consists of bidirectional fiber links with two wavelengths per fiber link in each direction. The example network shown in the Figure 6.3 is represented as a layered graph with two wavelength layers λ_0 and λ_1. The figure shows the allocation of wavelengths and paths to four pairs of primary and backup TSPs, $< p_i, b_i >, 1 \leq i \leq 4$, where b_i is the backup TSP for primary TSP p_i. We assume that the four traffic stream requests each of capacity $0.5C$, arrive in order and each request is set up before the next traffic stream request arrives. Assume the network uses MGP to assign traffic stream paths to wavelengths. Assume that the channel capacity is C.

The first request, for a dependable connection from node 2 to node 4, can be established as shown on λ_0. The primary TSP is established on the link $2-4$ on λ_0 and the backup TSP is established through links $2-3-7-4$ on the same wavelength. To establish the second request from node 1 to node 8, we can establish the primary TSP on λ_1 through links $1-3-5-7-8$ and the backup TSP on λ_0 through links $1-2-4-6-8$. The primary TSP cannot be established on λ_0 on the same path even if there is capacity available. This is due to the crossconnect constraints at nodes 3 and 7. Specifically, if p_2 were established on λ_0 through links $1-3-5-7-8$, then the backup TSP b_1 would be disturbed. However, the wavelength channel on λ_0 on link $2-4$ carries both a primary and backup TSP.

When the third request for a dependable connection from node 4 to node 7 arrives, the primary TSP can be established on link $4-7$ on λ_1. However, this primary TSP is link-disjoint with primary TSP p_2. Hence, the backup TSP b_3 can be backup-multiplexed with b_2 that is, they can share the same capacity on links $4-6$ and $6-8$. On the contrary, the backup TSP b_4 between node 3 to node 4 cannot be backup multiplexed with b_1 since primary TSP p_1 is not link disjoint with primary TSP p_4. Hence, even if they can be groomed on to the same wavelength, λ_0, they cannot share the capacity on the wavelength. If we assume that the network uses Segregated Grooming Policy, then we cannot groom the primary TSP p_1 and

backup TSP $b-2$ on to the same wavelength λ_0.

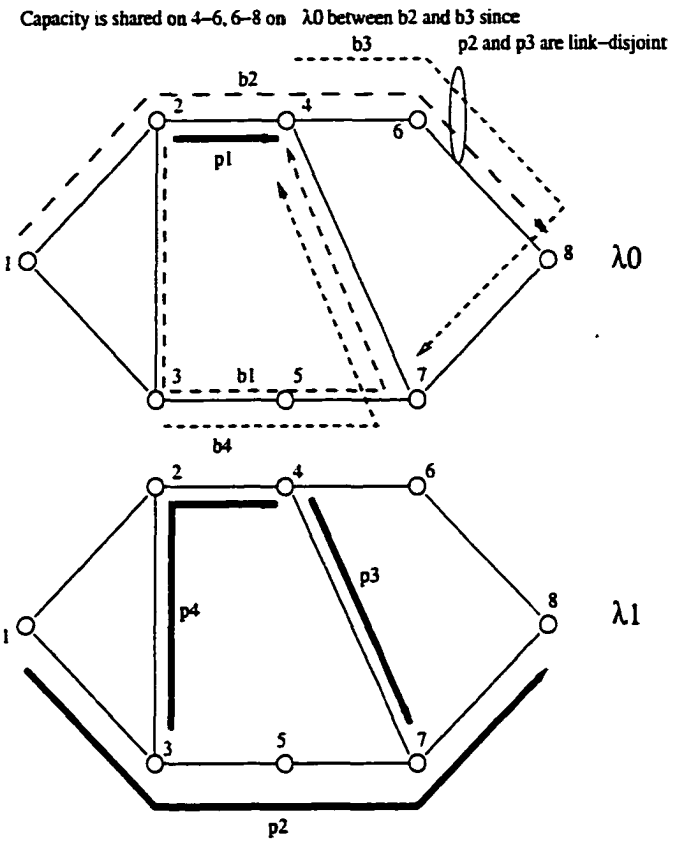

Figure 6.3 Grooming Traffic Streams on a WDM Network with two wavelengths

6.4 Routing and Wavelength Assignment

6.4.1 Routing Strategy

In this subsection, we describe the dynamic routing and wavelength assignment strategies which we use to set up the traffic stream path (TSP) in the network. We basically use the adaptive routing approach of *fixed alternate-path routing*, to select the primary and backup traffic stream paths in the network. In this scheme, a fixed set of pre-determined routes, say k is maintained for each source-destination pair. These routes are chosen to be link-disjoint and are ordered in the non-decreasing order of their hop-length. When a request arrives for a

dependable traffic stream connection for a capacity c between a source-destination pair (s, d), we select the two shortest paths out of the k disjoint paths on which the primary and the backup TSP can be established. The primary path can be established if the free capacity on at least one wavelength on each the links of the path is greater than or equal to the required capacity. The backup path can be established if the sum of the free capacity and the shareable backup capacity available through backup multiplexing on at least one wavelength on the links of the path is greater than or equal to the required capacity. In addition, it should be ensured that the traffic streams can be groomed on to the wavelengths without disturbing the existing traffic streams. The traffic request is assumed to be blocked if it is not possible to establish either the primary or the backup on any of the k predetermined paths. Another approach to adaptive routing is fully-adaptive routing, in which the route is determined dynamically at the time of the connection request. Although this can give better performance, we restrict ourselves to fixed alternate-routing strategy as we are more interested in studying the effect of traffic grooming policies on the blocking performance.

Note that it is possible to establish a backup TSP on a path on which the corresponding primary TSP might be blocked. This is due to the fact that the backup TSP can be established by sharing its capacity with the existing backup capacity on the wavelengths even if free capacity is not available. On the other hand, the primary needs free capacity greater than or equal to the required capacity on the wavelengths of the links to establish the connection.

6.4.2 Wavelength Assignment of traffic streams

The wavelength assignment problem is unique to optical networks. In this subsection, we will study how the wavelength assignment of primary and backup traffic streams can be made when the grooming policy used in the network is either *mixed* or *segregated*. If SGP is used in the network, each wavelength is classified as either PRIMARY, BACKUP or FREE. A FREE wavelength is one which has no traffic streams multiplexed in it. A PRIMARY (BACKUP) wavelength is one which is composed of one or more primary (backup) traffic streams multiplexed onto it. On the other hand, such a classification is not necessary when

MGP is used in the network, as both primary and backup traffic streams are multiplexed onto the wavelengths. Before applying the wavelength assignment algorithm, the set of available wavelengths on the primary and backup path needs to be obtained. The procedure in Section 6.2 is used for each wavelength on each link, to obtain the set of wavelengths on the primary (or backup) path which can accommodate the primary (or backup) traffic stream. In addition, if SGP is used in the network, the set of wavelengths for the primary path is restricted to those wavelengths which are either PRIMARY or FREE. A similar restriction applies to the set of wavelengths for the backup path. There is, however, no such restriction if MGP is used in the network.

If no wavelengths are available for either the primary or backup path, then an alternate route is selected according to the procedure given in the previous subsection. In the following, we will use three simple wavelength assignment heuristics to route the primary and backup traffic streams and study how they can applied to the cases of MGP and SGP. Although more complex algorithms such as MaxSum and RCL can also be applied and can give better performance, we restrict our study to the following simple cases, as our objective is to compare the performance of the grooming policy. In addition, since we are considering 1:1 path protection, we can assume that the wavelengths of the primary and the backup can be different and their assignments are made independent of each other. In the case of a failure, the source and destination tune to the backup wavelength and switch to the backup path. In addition, the crossconnects at the intermediate nodes of the backup path need to be appropriately configure to activate the backup path.

In the case of a failure, the source and destination tune to the backup wavelength and switch to the backup path. If SGP is used, the crossconnects at the intermediate nodes of the backup path need to be appropriately configured to setup the lightpaths that activate the backup path. However, if MGP is used in the network, the lighpaths are already configured and the backup traffic stream path is ready for use.

1. First Fit (FF): In this case, the first-fit wavelength assignment strategy is used for both primary and backup paths and the wavelength chosen for the traffic stream connection

has the smallest index among the set of available wavelengths along the path.

2. First Fit - Last Fit (FF-LF): In this case, we use first-fit wavelength assignment strategy for the primary path. However, to assign the wavelengths for the backup traffic stream path, we choose the wavelength with the largest index among the set of available wavelengths along the path. The basic idea here is to reduce the conflict between the primary and backup traffic streams.

3. Best Fit (BF): We use the Best-Fit wavelength assignment for each of the primary and backup traffic stream paths. In the case of the primary traffic stream path, among the available wavelengths in the set, the traffic stream is assigned to that wavelength which has the least free capacity remaining after the traffic stream is accommodated. For wavelength assignment of the backup traffic stream, we select the wavelength that minimizes the total *additional* backup capacity that we need to set up the backup traffic stream on the links of the path.

6.5 Numerical Results

To compare the performance of the two grooming policies with the wavelength assignment algorithms, we performed a simulation study for the cases and compared the results. Simulations were run in batches of 10^6 calls each, until the blocking values between successive call batches differed by less than 0.1 percent. Three topologies were used: a 16-node mesh-torus, a 8-node ring and the 14-node NSFnet. For our simulation study, we assume dynamic traffic conditions and use the network and traffic assumptions specified in Chapter 3, Section 3.3. In addition, as explained in Section 6.4, we assume fixed alternate path routing and the call is assumed to be blocked if either the primary or the backup cannot be established on the set of pre-specified paths in the network. The overall network blocking performance will be used as the metric for comparing the effect of wavelength assignment, topology, alternate path routing and granularity on the grooming policy used in the network.

6.5.1 Effect of wavelength assignment and topology

In Figures 6.4, 6.5 and 6.6 we plot the blocking probability of various wavelength assignment algorithms for MGP and SGP against the offered load for a 4×4 mesh-torus, NSFNET and a 8 node ring respectively. All the figures illustrate the important role played by the grooming policy in determining the blocking performance. In the case of the mesh-torus network and the NSFNET, for high loads, we observe that the Last Fit algorithm offers the best performance when the grooming policy is SGP but offers the worst performance in the case of MGP. In the case of the ring, the First-fit algorithm offers the best performance when the grooming policy is MGP and the worst performance in the case of SGP. Overall, for both the mesh-torus and the NSFNET, we observe that SGP offers better performance (more than an order of magnitude decrease in blocking probability for the NSFNET). However, in the case of the 8 node ring, it is interesting to note that MGP performs better. The reason for this reversal in performance is as follows. As explained before, using SGP allows us to run the backup traffic streams over the wavelengths without configuring the crossconnects. Mixed grooming, on the other hand requires us to configure the crossconnects if the wavelengths carry primary traffic along with the backup traffic. Therefore, although MGP offers the inherent advantage of being able to mix primary and backup streams in the wavelengths, it restricts the amount of sharing of backup traffic stream paths that can potentially be done in the network. The mesh-torus network has more connectivity than the ring. This helps it generate a good amount of traffic switching and mixing at the nodes. This traffic switching and mixing translates to more sharing of backup streams for the SGP. Therefore SGP provides better performance for the mesh-torus. On the other hand, in the case of the ring, due to the limited number of paths between the nodes and the high load correlation, most of the traffic is just pass-through and there is very little mixing and traffic switching between wavelengths and the potential for backup traffic stream sharing is low. Hence in this case, MGP provides better performance than SGP.

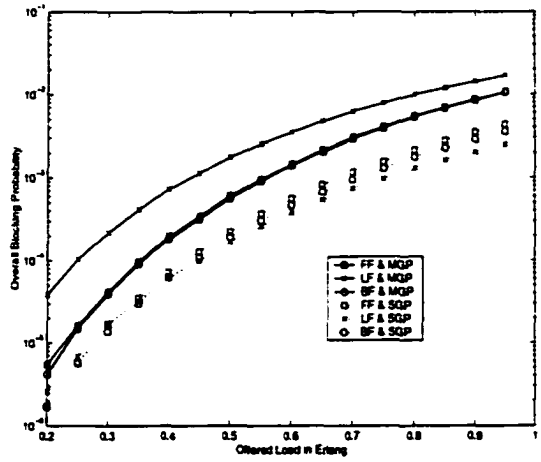

Figure 6.4 Overall Blocking Probability vs. Offered Load per station in Erlangs for 4×4 mesh-torus network with $W = 5$ and $g = 4$ for different wavelength assignment and grooming policies (FF : First Fit, LF : Last Fit, BF : Best Fit, MGP : Mixed Grooming Policy, SGP : Segregated Grooming Policy

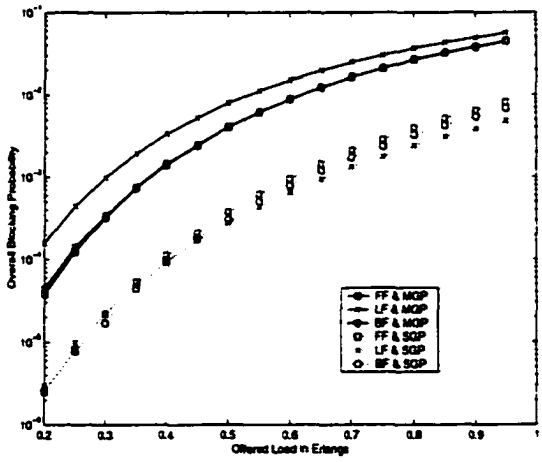

Figure 6.5 Overall Blocking Probability vs. Offered Load per station in Erlangs for 14 node NSFNET network with $W = 5$ and $g = 4$ for different wavelength assignment and grooming policies (FF : First Fit, LF : Last Fit, BF : Best Fit, MGP : Mixed Grooming Policy, SGP : Segregated Grooming Policy

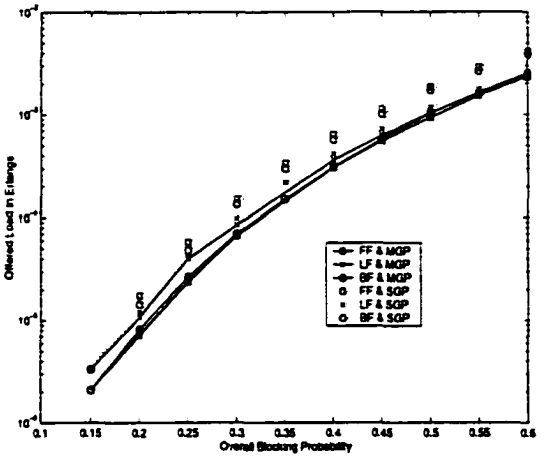

Figure 6.6 Overall Blocking Probability vs. Offered Load per station in Erlangs for 8 node ring network with $W = 5$ and $g = 4$ for different wavelength assignment and grooming policies (FF : First Fit, LF : Last Fit, BF : Best Fit, MGP : Mixed Grooming Policy, SGP : Segregated Grooming Policy

6.5.2 Effect of grooming granularity

In Figures 6.8 and 6.7, we plot the blocking probability for different granularities for both cases of MGP and SGP, against the offered load. In the case of both the mesh-torus and the ring, we can observe that as we increase the granularity, the blocking probability decreases. In addition, we find that we can increase the granularity for a mesh-torus network with MGP (or SGP in the case of a ring) and make it perform better than a mesh-torus network with SGP of lower granularity (or correspondingly a ring network with MGP of lower granularity). We can also observe a small increase in the difference in blocking probabilities for MGP and SGP when the granularity is increased for both the ring and the mesh-torus.

6.5.3 Effect of number of alternate paths

In Figure 6.9, we consider the effect of changing the number of alternate paths for the primary and backup traffic streams in a 4×4 mesh-torus. We can readily observe that we can obtain multiple orders of magnitude decrease in blocking with even a small increase in the number of alternate paths. Although, the number of alternate paths which a node pair

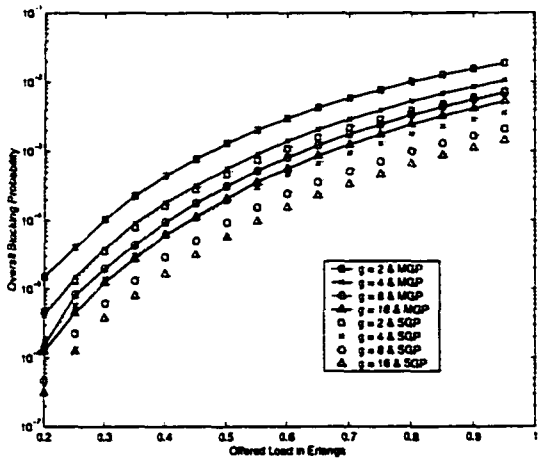

Figure 6.7 Overall Blocking Probability vs. Offered Load per station in Erlangs for 4×4 mesh-torus network with $W = 5$ and for different granularities (g) and grooming policies(g = granularity, MGP : Mixed Grooming Policy, SGP : Segregated Grooming Policy

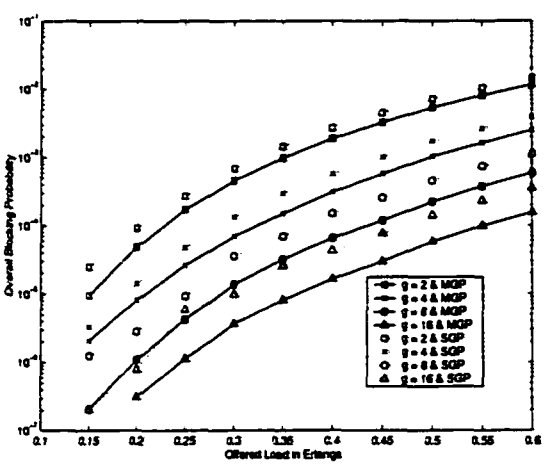

Figure 6.8 Overall Blocking Probability vs. Offered Load per station in Erlangs for 8 node ring network with $W = 5$ and for different granularities (g) and grooming policies(g = granularity, MGP : Mixed Grooming Policy, SGP : Segregated Grooming Policy

can have is limited by its topology. In addition, we can also observe that with an increase in number of alternate paths, the difference in blocking performance between MGP and SGP increases.

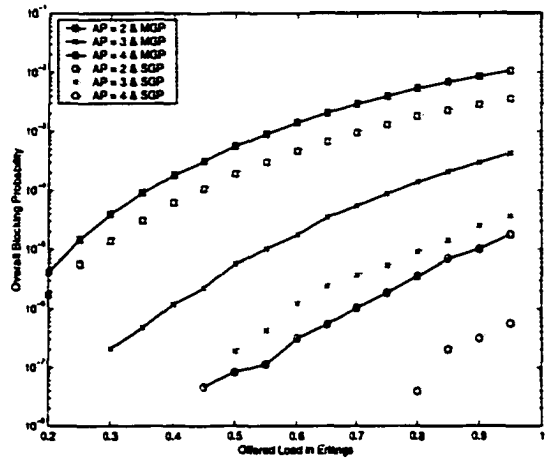

Figure 6.9 Overall Blocking Probability vs. Offered Load per station in Erlangs for 4×4 mesh-torus network with $W = 5$ and $g = 4$ for different number of alternate paths and grooming policies(AP = number of alternate paths available for a s-d pair, MGP : Mixed Grooming Policy, SGP : Segregated Grooming Policy

6.6 Conclusion

WDM networks of the future have to offer dynamic, heterogeneous sub-wavelength services and must be able to pack these services efficiently onto the wavelengths. In addition, for networks of practical size, the number of available wavelengths is lower than the number of users by a few orders of magnitude. Efficient grooming of traffic can help resolve these issues. In such networks, due to the high bandwidths involved, it is advantageous to implement survivability mechanisms to protect against link failures in the form of a fiber cut. In this chapter, we studied the performance of dynamic grooming policies for establishing low-rate dependable connections in WDM mesh networks. Specifically, we dealt with lightpath protection schemes when the traffic demand is dynamic and consists of low-rate traffic streams. We first presented methods to optimally multiplex primary and backup traffic streams onto a wavelength on a

link. Next we proposed two schemes for grooming traffic streams onto a wavelength: Mixed Primary-Backup Grooming and Segregated Primary-Backup Grooming. We illustrated with an example, of how the traffic streams can be setup in the network using SGP or MGP. We next showed how the routing and wavelength assignment of traffic streams can be done and presented three simple wavelength assignment algorithms. The two schemes of SGP and MGP were compared for various topologies, for different granularities and for different number of alternate paths. It was shown that using SGP provided better performance for the mesh-torus and the NSFNET, while using MGP provided better performance for the ring. In this respect, it was confirmed that SGP is useful for topologies with good connectivity and good amount of traffic switching and mixing at the nodes. On the other hand, MGP is useful for topologies such as ring, with high load correlation and low connectivity. It was also shown that the performance improvement of SGP over MGP in the mesh-torus is increased as the number of alternate paths for the primary and backup traffic streams is increased.

CHAPTER 7. Summary and Future Work

WDM technology has ushered in a new era in communications by enabling us to use the huge capacity available in optical fiber. Recent advances in WDM component technology has bought the wavelength-routed all-optical network closer to reality. All-optical networks (AONs) offer advantages such as digital transparency, functional simplicity and help overcome the electronic bottleneck by establishing lightpaths between the non-neighboring nodes. In such networks, wavelength converters play an important role in improving the utilization of the wavelengths in the fiber links and help in reducing the blocking rate by decreasing the effect of the wavelength continuity constraint. In chapter 2, we presented an algorithm for optimally placing a given number of converters in AONs with arbitrary mesh topologies. Our algorithm is independent of the method used to compute the blocking probability. We detailed the procedure for obtaining the blocking performance for all converter placement combinations by calculating the blocking performance of only some converter placement combinations. We used the principle that placing a converter at the outer nodes does not affect the blocking probability. Hence all converter placement combinations that differed only in the outer nodes can be assigned the same blocking performance value. The algorithm works better than the exhaustive method of converter placement (offering efficiencies of more than 95 percent). In particular, it works very well in networks with high connectivity or when the number of converters to be placed is about half that of the number of nodes in the network. We also presented four heuristics to compute a solution close to the optimal solution. The heuristics are more useful for quickly eliminating bad placement choices and can be used along with the optimal algorithm to further reduce the computation time for obtaining the optimal solution. In addition, the heuristics can also be used based on the network information available. Sometimes, the full information

about the topology, the routing or the traffic matrix is not available. For example, if only the traffic/number of paths passing through a node is known, we can apply the Path-based Index heuristic. Similarly, the Inner Node heuristic can be used if the network topology is known and the traffic characteristic of the network is not known.

As the networking infrastructure of the world moves to the two-layer model of IP-over-WDM, the WDM layer is likely to gradually evolve to a hybrid network with both electronic switching and wavelength-routing technologies. Although wavelength capacities have been increasing in bandwidth, the user traffic requirements are in the range of STS-1 up to the full wavelength capacity. Hence to avoid inefficiencies in filling up of wavelength capacity in the network and its associated cost increases, there is a need for WDM networks to offer sub-wavelength services and be able to groom these traffic services efficiently onto the wavelength. In chapters 3 to 6, we dealt with issues in network design and operation of WDM grooming networks.

We introduced the concept of constrained and sparse grooming networks. We showed how traffic streams are groomed onto a lightpath in a mesh network and explained with an example the lighpath establishment procedure in WDM grooming networks. We proposed a capacity correlation model to study the blocking performance of constrained grooming networks. The model takes into account the load correlation on neighboring links and the capacity distribution on the wavelength to compute the blocking performance. We also considered the effect of WGXC nodes in the network and specified an analytical model for sparse grooming networks. The results from the analytical model was found to be close to simulation results. Sparse grooming offers at least an order of magnitude decrease in blocking and multiple order of magnitude decrease in blocking over constrained grooming. From this we can conclude that sparse grooming can offer significant performance improvement in terms of blocking performance and capacity loss for both the ring and mesh-torus networks. However, this performance improvement is not equal across the set of traffic streams of different line-speeds. Several extensions to the above work are possible. As such the state space size of the model is limited by the granularity. Hence we need to improve upon and come up with newer analytical models that

will be less affected by the granularity. In addition, we also need to come up with analytical models for other wavelength assignment algorithms such as first-fit, most-used, etc.

We next addressed the concept of capacity fairness in WDM networks with grooming capabilities. We provided a qualitative and quantitative definition of capacity fairness. Current dynamic routing and wavelength assignment (RWA) algorithms were studied under the purview of capacity fairness and it was observed that these algorithms are not good at achieving capacity fairness. We proposed a connection admission control scheme which could be used along with any RWA algorithm to achieve capacity fairness. The algorithm provided good capacity fairness while at the same time does not over-penalize the overall blocking performance. Although the connection admission control scheme is a viable scheme to ensure capacity fairness, we need to come up with integrated routing and wavelength assignment algorithms which ensure capacity fairness and at the same time, reduce the blocking probability.

Finally we considered the problem of dynamically establishing dependable low-rate traffic stream connections in WDM grooming networks. We specified a dynamic algorithm for obtaining the optimal spare capacity of a wavelength on a link when a number of backup traffic streams are multiplexed onto it. We identified two schemes for grooming primary and backup traffic: Mixed Primary-Backup Grooming Policy (MGP) and Segregated Primary-Backup Grooming Policy (SGP). These schemes can be applied in a WDM mesh network scenario along with any routing and wavelength assignment algorithm. From the simulation results, we can infer that SGP is useful in network topologies, such as mesh-torus, characterized by good connectivity and a good amount of traffic switching and mixing at the nodes. On the other hand, MGP is useful in network topologies such as the ring, characterized by low connectivity and high load correlation. Although a lot of research has been done in minimizing the electronic equipment in WDM grooming rings, the problem of efficient traffic grooming in arbitrary mesh networks so as to minimize network cost also needs to be addressed.

BIBLIOGRAPHY

[1] "High-performance Parallel Interface," American National Standards Institure, X3T9.3, rev. 6.9, November 1989.

[2] B. Albert and A. P. Jayasuma, *FDDI and FDDI-II - Architecture, protocols and performance*, Artech-House, 1994.

[3] Walter Goralski, *SONET*, Second Edition, McGraw-Hill, 2000.

[4] "Lucent Technologies," http://www.lucent.com.

[5] "CorWave LR," http://www.corvis.com/products/LR.htm.

[6] R. Ramaswami and K. Sivarajan, *Optical Networks: A Practical Perspective*, Morgan Kaufmann, 1998.

[7] M. S. Goodman, H. Kobrinski, M. Vecchi, R. M. Bulley, and J. M. Gimlett, "The LAMBDANET multiwavelength network: architecture, applications, and demonstrations," *IEEE J. on Sel. Areas in Communications*, vol. 8, no. 6, pp. 995-1004, August 1990.

[8] K. Nosu, H. Toba, K. Inoue, and K. Oda, "100 channel optical FDM technology and its applications to optical FDM channel-based networks," *IEEE/OSA J. on Lightwave Technology*, vol. 11, pp. 764-776, May/June 1993.

[9] E. Hall, J. Kravitz, R. Ramaswami, M. Halvorson, S. Tenbrink, and R. Thomsen, "The Rainbow-II gigabit optical network," *IEEE J. on Sel. Areas in Communications*, vol. 14, no. 5, pp. 814-823, June 1996.

[10] W. T. Anderson et al., "The MONET project-a final report," *IEEE J. on Lightwave Technology*, vol. 18, no. 12, pp. 1988-2009, December 2000.

[11] C. Guillemot et al., "Transparent optical packet switching: The European ACTS KEOPS project approach," *IEEE J. on Lightwave Technology*, vol. 16, no. 12, pp. 2117-2134, December 1998.

[12] C. R. Giles, "Lightwave applications of Fiber Bragg Gratings," *IEEE J. on Lightwave Technology*, vol. 15, pp. 1391-1404, 1997.

[13] K. A. McGreer, "Arrayed Waveguide Gratings for Wavelength Routing," *IEEE Communications Magazine*, vol. 36, no. 12, pp. 62-68, 1998.

[14] R. Ramaswami and K. N. Sivarajan, "Routing and wavelength assignment in all-optical networks," *IEEE/ACM Trans. Networking*, vol. 3, no. 5, pp. 489-500, October 1995.

[15] I. Chlamtac, A. Ganz, G. Karmi, "Lightpath Communications: An approach to high bandwidth optical WANs," *IEEE Trans. Communications*, vol. 40, pp. 1171-1182, July 1992.

[16] S. Subramaniam and R. A. Barry, "Wavelength Assignment in Fixed Routing WDM Networks," *Proc. IEEE Intl. Conf. Communications*, Montreal, Canada, pp. 406-410, November 1997.

[17] A. Mokhtar and M. Azizoglu, "Adaptive Wavelength Routing in All-Optical Networks," *IEEE/ACM Trans. on Networking*, vol. 6, no. 2, pp. 197-206, April 1998.

[18] A. Girard, *Routing and Dimensioning in Circuit-Switched Networks*, Addison-Wesley, 1990.

[19] E. Karasan and E. Ayanoglu, "Performance of WDM Transport Networks," *IEEE Journal on Selected Areas in Communications*, vol. 16, pp.1081-1096, September 1996.

[20] R. A. Barry and P. A. Humblet, "Models of blocking probability in all-optical networks with and without wavelength changers," *IEEE Journal on Selected Areas in Communications*, vol. 14, no. 5, pp. 858-867, June 1996.

[21] J. Jue and G. Xiao, "An Adaptive Routing Algorithm for Wavelength-Routed Optical Networks with a Distributed Control Scheme," *Proc. 9th Intl. Conf. on Comp. Comm. and Networks*, pp. 192-197, 2000.

[22] L. Li and A. K. Somani, "Dynamic Wavelength Routing using Congestion and Neighborhood Information," *IEEE/ACM Trans. on Networking*, vol. 7, no. 5, pp. 779-786, October 1999.

[23] H. Harai, M. Murata, and H. Miyahara. "Performance of Alternate Routing Methods in All-Optical Switching Networks," *Proc. IEEE INFOCOM'97*, pp. 516-524, April 1997.

[24] L. Li and A. K. Somani, "Fiber Requirement in Multifiber WDM Networks with Alternate-Path Routing," *Proc. 8th Intl. Conf. on Comp. Comm. and Networks*, 1999.

[25] X. Zhang and C. Qiao, "Wavelength Assignment for Dynamic Traffic in Multi-Fiber WDM Networks," *Proc. 7th Intl. Conf. on Comp. Comm. and Networks*, 1998.

[26] H. Zhang, J. P. Jue, and B. Mukherjee, "A Review of Routing and Wavelength Assignment Approaches for Wavelength-Routed Optical WDM Networks," *Optical Networks Magazine*, vol. 1, no. 1, pp. 47-60, January 2000.

[27] R. Ramaswami and G. H. Sasaki. "Multiwavelength optical networks with limited wavelength conversion," in *Proc. IEEE INFOCOM '97*, pp. 489-498, April 1997.

[28] K. C. Lee and O. K. Li, "A wavelength-convertible optical network," *IEEE Journal on Lightwave Technology*, vol. 11, pp. 962-970, May/June, 1993.

[29] J. Yates, J. Lacey, D. Everitt and M. Summerfield, "Limited-Range Wavelength Translation in All-Optical Networks," *Proc. IEEE INFOCOM'96*, vol. 3, pp. 954-961, March 1996.

[30] V. Sharma and E. A. Varvarigos, "Limited Wavelength Translation in All-Optical WDM Mesh Networks," *Proc. IEEE INFOCOM'98*, vol. 2, pp. 893-901, March 1998.

[31] T. Tripathi and K. Sivarajan, "Computing Approximate Blocking Probabilities in Wavelength-Routed All-Optical Networks with Limited Range Wavelength Conversion," *Proc. IEEE INFOCOM'99*, vol. 1, pp. 321-328, March 1999.

[32] A. Birman, "Computing Approximate Blocking Probabilities for a Class of All-Optical Networks," *IEEE Journal on Selected Areas in Communications*, vol 14, no. 5, pp.852-857, June 1996.

[33] S. Subramaniam, M. Azizoğlu, and A. K. Somani. "All-optical networks with sparse wavelength conversion," *IEEE/ACM Transactions on Networking*, vol. 4, no. 4, pp. 544-557, August 1996.

[34] S. Subramaniam, A. K. Somani M. Azizoglu, and R. A. Barry, "A performance model for wavelength conversion with non-Poisson traffic," *Proc. IEEE INFOCOM'97*, pp. 499-506, April, 1997.

[35] S. Subramaniam, M. Azizoglu, and A. K. Somani, "On the optimal converter placement in wavelength-routed networks," *IEEE/ACM Transactions on Networking*, vol. 7, no. 5, pp. 754-766, OCtober 1999.

[36] B. Mukherjee, *Optical Communication Networks*, McGraw-Hill Series on Computer Communications, 1997.

[37] L. Li and A. K. Somani, "Efficient Algorithms for the Wavelength Converter Placement on All-Optical Networks," *Proc. Conference on Information Sciences and Systems*, Maryland, March 1999.

[38] K. R. Venugopal, M. Shivakumar and P. Sreenivasa Kumar, "A Heuristic for Placement of Limited Range Wavelength Converters in All-Optical Networks," in *Proc. IEEE INFOCOM'99*, vol. 2, pp. 908-915, March 1999.

[39] Y. Zhou, G. Rouskas and H. Perros, "Blocking in Wavelength-routing Networks: Part I: The single path case," in *Proc. IEEE INFOCOM'99*, vol. 1, pp. 321-328, March 1999.

[40] G. Xiao and Y. W. Leung, "Algorithms for Allocating Wavelength Converters in All-Optical Networks," *IEEE/ACM Trans. on Networking*, vol. 7, no. 4, pp.545-557, August 1999.

[41] O. Gerstel, R. Ramaswami, and G. Sasaki, "Cost-Effective Traffic Grooming in WDM Rings," *IEEE/ACM Trans. Networking*, vol. 8, no. 5, pp. 618-630, October 2000.

[42] O. Gerstel, P. Lin, and G. Sasaki, "Combined WDM and SONET Design," *Proc. IEEE INFOCOM'99*, pp. 734-743, March 1999.

[43] A. L. Chiu and E. H. Modiano, "Traffic Grooming Algorithms for Reducing Electronic Multiplexing Costs in WDM Ring Networks," *J. of Lightwave Technology*, vol. 18, no. 1, pp. 2-12, January 2000.

[44] X. Zhang and C. Qiao, "An Effective and Comprehensive Approach for Traffic Grooming and Wavelength Assignment in SONET/WDM Rings," *IEEE/ACM Trans. Networking*, vol. 8, no. 5, October 2000.

[45] P. J. Wan, G. Calinescu, L. Liu, and O. Frieder, "Grooming of Arbitrary Traffic in SONET/WDM BLSRs," *IEEE J. on Selected Areas in Communications*, vol. 18, no. 10, pp. 1995-2003, October 2000.

[46] R. Berry and E. Modiano, "Reducing Electronic Multiplexing Costs in SONET/WDM Rings with Dynamically Changing Traffic," *IEEE J. on Selected Areas in Communications*, vol. 18, no. 10, pp.1961-1971, October 2000.

[47] A. Sridharan and K. N. Sivarajan, "Blocking in All-Optical Networks," *IEEE INFOCOM 2000*, March 2000.

[48] K. Chan and T. P. Yun, "Analysis of Least Congested Path Routing in WDM Lightwave Networks," *Proc. IEEE INFOCOM'94*, pp. 962-969, 1994.

[49] M. Sabry and J. Midwinter, "Towards an Optical Ether." *IEE Proc. Journal*, vol. 141, no.5, pp. 327-335, October 1994.

[50] J. Yates, "Performance Analysis of Dynamically-Reconfigurable Wavelength-Division Multiplexed Networks," *Ph.D thesis*, The University of Melbourne, Australia, 1997.

[51] A. Birman and A. Kershenbaum. "Routing and Wavelength Assignment Methods in Single-Hop All-Optical Networks with Blocking," *Proc. IEEE INFOCOM'95*, pp. 431-438, April 1995.

[52] S. Han and K. G. Shin, "Efficient Spare-Resource Allocation for Fast Restoration of Real-Time Channels from Network Component Failures," *Proc. 18th IEEE Real-Time Systems Symposium*, pp. 99-108, 1997.

[53] J. Armitage, O. Crochat and J. Y. Le Boudec, "Design of a Survivable WDM Photonic Network," *Proc. IEEE INFOCOM'97*, pp. 244-252, April 1997.

[54] A. Fumagalli et al., "Survivable Networks Based on Optimal Routing and WDM Self-Healing Rings," *Proc. IEEE INFOCOM'99*, pp. 726-733, March 1999.

[55] S. Ramamurthy and Biswanath Mukherjee, "Survivable WDM Mesh Networks, Part I - Protection," *Proc. IEEE INFOCOM'99*, pp. 744-751, March 1999.

[56] Y. Miyao and H. Sitao, "Optimal Design and Evaluation of Survivable WDM Transport Networks," *IEEE Journal on Selected Areas in Communications*, vol. 16, no. 7, pp. 1190-1198, Sept 1998.

[57] G. Mohan and C. Siva Ram Murthy, "Routing and wavelength assignment for establishing dependable connections in WDM networks," *29th Annual International Symposium on Fault-Tolerant Computing, 1999* , pp. 94-101, 1999.

[58] G. Mohan and A. K. Somani, "Routing Dependable Connections with Specified Failure Restoration Guarantees in WDM Networks," *Proc. IEEE INFOCOM'00*, vol. 3, pp. 1761-1770, March 1999.

[59] V. Anand and C. Qiao, "Dynamic Establishment of Protection Paths in WDM Networks," *Proc. ICCCN'00*, pp. 198-204, 2000.

[60] T. Cinkler, D. Marx, C. P. Larsen, and D. Fogaras, "Heuristic Algorithms for Joint Configuration of the Optical and Electrical Layer in Multi-Hop Wavelength Routing Networks," *Proc. IEEE INFOCOM 2000*, pp. 1000-1009, March 2000.

[61] E. Karasan and E. Ayanoglu, "Effects of Wavelength Routing and Selection Algorithms on Wavelength Conversion Gain in WDM Optical Networks," *IEEE/ACM Trans. on Networking*, vol. 6, no. 2, pp. 186-196, April 1998.

[62] S. Thiagarajan and A. K. Somani, "Capacity Fairness of WDM Networks with Grooming Capabilities," *Optical Networks Magazine*, vol. 2, no. 3, pp. 1-9, May/June 2001.

[63] S. Thiagarajan and A. K. Somani, "Performance Analysis of WDM Optical Networks with Grooming Capabilities," *Proc. SPIE Intl. Symp. on Voice, Video, and Data Comm.-Terabit Optical Networking:Arch., Control, and Management*, pp. 253-262, Boston, USA, November 2000.

[64] S. Thiagarajan and A. K. Somani, "An Efficient Algorithm for Optimal Wavelength Converter Placement on Wavelength-Routed Networks with Arbitrary Topologies," in *Proc. IEEE INFOCOM'99*, March 1999.

[65] S. Thiagarajan and A. K. Somani, "A Capacity Correlation Model for WDM Networks with Constrained Grooming Capabilities," *IEEE Intl. Conf. Communications*, Helsinki, Finland, June 2001.

[66] S. Thiagarajan and A. K. Somani, "Traffic Grooming for Survivable WDM Mesh Networks," *to appear in Opticomm 2001*, Denver, USA, August 2001.

ACKNOWLEDGEMENTS

First and foremost, I would like to thank Prof. Arun Somani for introducing me to the field of optical networking and being my mentor during my study at Iowa State University. His knowledge, support, hard work and teaching have set an example I hope to match some day. Special thanks to Prof. Manimaran Govindarasu for his helpful advice in matters technical and beyond. I would like to thank my thesis committee members, Prof. Robert Weber, Prof. Ahmed Kamal and Prof. Soma Chaudhuri for their valuable technical feedback and comments. I would also like to thank Prof. Mani Mina for his advice and the technical discussions I had with him.

Over the four years of my study, I would like to thank some of my fellow graduate students: Ling Li, Srinivasan Ramasubramanian, Murari Sridharan, Deepali Deshpande, Jing Fang, and Nagapratima Kunapareddy. Each of them in their own way helped make my time in my PhD program interesting and enjoyable.

Support in part by the National Science Foundation grants NCR-9628165, NCR-9796318, ANI-9973102 and by Defense Advanced Research Projects Agency under Contract N66001-0-1-8949 is gratefully acknowledged.

Finally, I thank my parents and my brother Ravi for their invaluable support and constant encouragement during my doctoral studies.